THE GREEN ALGA *CHLAMYDOMONAS REINHARDTII:* A NEW MODEL SYSTEM TO UNRAVEL THE ASSEMBLY PROCESS OF RESPIRATORY COMPLEXES

DISSERTATION

Presented in Partial Fulfillment of the Requirements for the Degree Doctor of Philosophy in the Graduate School of The Ohio State University

By

María del Rosario Barbieri

Graduate Program in Plant Cellular and Molecular Biology

The Ohio State University

2010

Dissertation Committee

Professor Patrice P. Hamel, Adviser

Professor Iris Meier

Professor Erich Grotewold

Professor Juan D. Alfonzo

ABSTRACT

The general purpose of this research is to contribute to a better understanding of the mitochondrial NADH: ubiquinone oxidoreductase (Complex I) and to illustrate the current view of its assembly process. I propose to use the green alga *Chlamydomonas reinhardtii* as a novel model system to carry out the molecular dissection of Complex I assembly. The main objective is to discover novel genes controlling the assembly process of this multimeric enzyme.

Several reasons including patient death at young age, strict regulations, and ethical concerns make the study of Complex I on humans highly difficult. Although traditionally well established model systems such as the fungi *Yarrowia lipolytica* and *Neurospora crassa* and human cell lines have proven useful to understand the role of specific subunits in the assembly process, forward genetic approaches leading to discovery of novel assembly factors have been limited by the lack of straightforward screening methodologies (REMACLE *et al.* 2008). The process of plant Complex I assembly is largely obscure at present, despite the progress achieved in recent years. In plants, similarly to other eukaryotes, there is no simple strategy to approach the issue of assembly. Thus, the development of a model system where both mitochondrial and nuclear genomes can be manipulated is highly desirable for the study of Complex I.

Chapter 2 shows the use of *Chlamydomonas reinhardtii* as a forward genetics tool to screen for Complex I deficiency mutants and the finding of six new loci that result in defects of assembly. Based on large level of conservation of Complex I subunits in eukaryotes as well as the presence of homologs of currently proposed assembly factors, this work follows the hypothesis that the assembly process is also conserved among eukaryotes. Chapter 3 refers to the molecular identification of one of these genes as the Complex I subunit NUOB10, homolog of the bovine PSDW subunit. Also, a molecular mapping approach for another mutant suggests that the mutation does not affect a structural subunit of Complex I and that the final identification of this gene will lead to the discovery of a novel assembly factor. Finally, Chapter 4 provides an initial evaluation for the overall functional conservation of two known assembly factors: CIA30 and OXA1, both of which have a ortholog gene in *Chlamydomonas*.

To my love

ACKNOWDLEGMENTS

I could not have done this work without the help and guidance of my adviser, Dr. Patrice P. Hamel. I am always grateful to him. He has been the most wonderful scientific mentor and friend through these years. In the most enduring times he has shown me the attitude to celebrate everyday achievements and overcome the obstacles of research. I would not have arrived here without his sharing of scientific thoughts with a warm cup of tea (I should also extend my gratitude to Birgit Alber, our scientific tea chat sponsor).

Yet I would not be here without the support of my committee members, Dr. Iris Meier, Dr. Eric Grotewold and Dr. Juan Alfonzo. I would like to thank them for their continuous encouragement and advice. Not in my committee but an advisor nonetheless, Dr. Claire Remacle from the University of Liege, Belgium, thank you for providing your insights to my research.

Two past labmates have specially contributed to this project Cécile Nouet and Véronique Larosa and deserve a special note for their technical, intellectual and spiritual contributions to this project. Thanks to my labmates through these years, Nitya, Sara Cline, Mohamed Karamoko, Stéphane Gabilly, Darren Murrey and Vincent Corvest, for their encouragement and help.

I am especially thankful to my fifth-floor Aronoff friends, especially Srilakshmi Makkena, Sowmya Venkatakrishnan, Nitya again and Sachin Teotia. They have been just wonderful, encouraging, helpful and supportive. Also, thanks to all the staff members of our department, with especial thanks to Rene Madsen, for making my life easier every day.

To my friends in science, in life and in poetry, you've been here with me all these years, day and night, next block or next hemisphere, I am indebted to you. My dearest Fernando "Mordi", we have not yet written our last verse. Susana, Vanessa, Tom, Elisa, Cécile, Niro, thanks for being my family in Columbus, and for the laughs and the dinners and the encouragement in the difficult times. Meye, Verónica, and Carla, you have built a piece of home far from home. Mariana L., Silvita, LauKa, Ceci O., Claudio and Kari, Flavia, you confirmed to me that we can make distance a meaningless word.

My last and most special thanks are to my love, Pierre whose unconditional support and company have given me the necessary strength for this journey. To my mom, my sister Mili and brother Salva, my nephews Luli and Rodri, who understood and accepted that I needed to look for my own path.

VITA

1974 .....Born-Buenos Aires, Argentina

2001 .....Licenciado en Ciencias Biologicas, University of Buenos Aires-Argentina

2003 to present .....Graduate Teaching and Research Associate, The Ohio State University

PUBLICATIONS

Research Publication

1. C. Remacle, S. Cline, L. Boutaffala, S. Gabilly, V. Larosa, M.R. Barbieri, N. Coosemans, P.P. Hamel (2009). The ARG9 gene encodes the plastid re*sid*ent *n-1 acetyl ornithine aminotransferase 2* in the green alga *Chlamydomonas reinhardtii*. Eukaryotic Cell, 8 (9): 1460-1463.
2. C. Remacle, M. R. Barbieri, P. Cardol and P.P. Hamel (2008). Eukaryotic complex I: functional diversity and experimental systems to unravel the assembly process. Mol Genet Genomics, 280 (2): 93-110.
3. C. Tami, A. Peralta, R. Barbieri, A. Berinstein, E. Carrillo, O. Taboga (2004). Immunological properties of FMDV-gP64 fusion proteins expressed on SF9 cell and baculovirus surfaces. Vaccine, 23: 840-845.

4. M.R.Barbieri, N.L. Kerber, N.L. Pucheu, M.H. Tadros, A.F. Garcia (2002). Effect of Light and oxygen and adaptation to changing light conditions in a photosynthetic mutant in which the LHI complex of *Rhv. sulfidophilum* was heterologously expressed in a strain of *Rb. capsulatus* whose *puc* operon was deleted. Current Microbiology, 45: 209-216.

FIELDS OF STUDY

Major Field: Plant Cellular and Molecular Biology

TABLE OF CONTENTS

Page

LIST OF TABLES

LIST OF FIGURES

CHAPTER 1

INTRODUCTION

1.1. Mitochondrial respiratory chain

From bacteria to eukaryotic cells, efficient energy production systems rely on the oxidation of high energy molecules and sequential transfer of electrons through a series of multi-enzymatic membrane-associated complexes to reduce a final electron acceptor of lower energy. The energy released in the process accumulates as a proton electrochemical balance across the given membrane and is used to drive energy-requiring cell functions, mainly ATP synthesis. The canonical mitochondrial oxidative phosphorylation system, also known as the respiratory chain, consists of an electron transfer chain and a proton pump. The electron transfer chain consists of four main multi-protein enzymatic complexes located at the mitochondrial inner membrane and two mobile components that transfer electrons between the complexes (GREEN and TZAGOLOFF 1966; LENAZ and GENOVA 2009) (Figure 1.1). Namely, the four complexes are NADH: ubiquinone oxidoreductase (Complex I), succinate: ubiquinone oxidoreductase (Complex II), ubiquinone: cytochrome *c* oxidoreductase (Complex III) and cytochrome *c* oxidase (Complex IV). The mobile component ubiquinone or Coenzyme Q (CoQ) is a lipophilic

molecule that diffuses in the membrane bilayer while the heme protein cytochrome *c* sits on the external side (intermembrane space) (HATEFI 1985). These four complexes cooperate in the generation of the electrochemical proton gradient across the mitochondrial inner membrane. Indeed, complexes I, III and IV couple electron transfer to proton translocation by a fifth complex: ATP synthase.

Additional components contribute electrons to the respiratory chain or act as alternative electron acceptors. Quinone can accept electrons from a series of donors and in turn, it can donate electrons to more than one acceptor in the mitochondrial inner membrane. Therefore, respiratory chain components are also classified as members reducing to the quinone pool and those oxidizing it. In this sense, Complexes I, II and alternative NADH dehydrogenases (ND) in plants and fungi, constitute the first group while Complex III+IV and alternative oxidases (AOX) belong to the second group. Only complexes I, III and IV couple electron transfer to proton translocation and thus, they are called phosphorylating complexes.

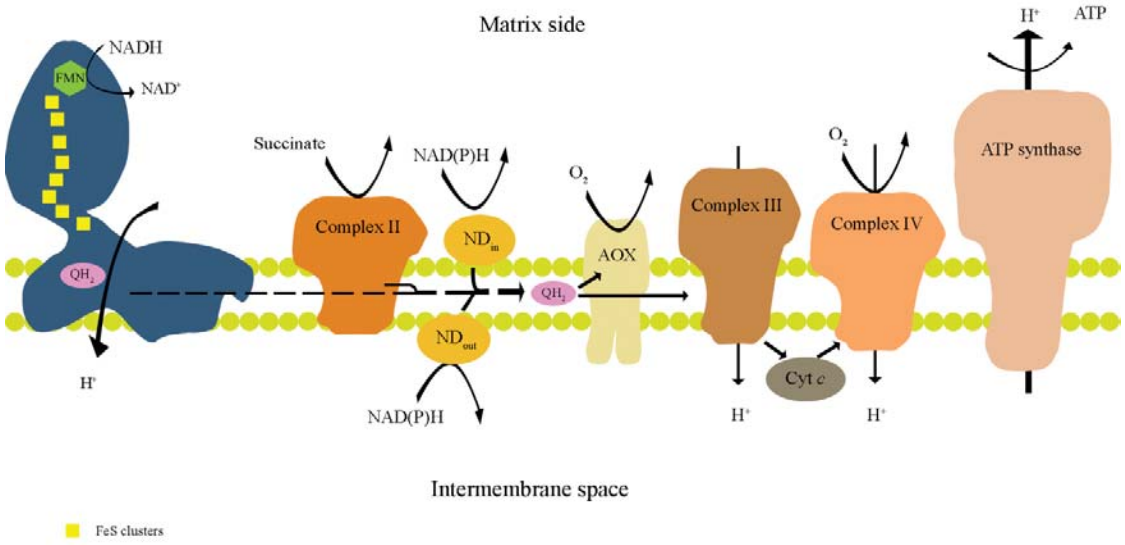

Figure 1.1 General organization of the plant and fungal mitochondrial respiratory chain.

Complex I is highlighted on the left and decorated to show the presence of eight iron-sulphur clusters (yellow) and the flavin mononucleotide (FMN) group. Other enzymatic complexes are shown with their relevant substrates. Note the presence of Type II NADH dehydrogenases (ND) on both sides of the mitochondrial inner membrane and alternative oxidase (AOX), both absent from mammals. Source: (REMACLE *et al.* 2008).

.

1.2. Mitochondrial Complex I

With a mass of around 950 kDa, eukaryotic Complex I has much more complexity than its 550-kDa bacterial counterpart. The holoenzyme is composed of over 40 nuclear- and mitochondrial-encoded protein subunits, a non-covalently bound flavin mono-nucleotide (FMN) and eight Fe-S clusters[1] (ABDRAKHMANOVA *et al.* 2004; CARDOL *et al.* 2004; FEARNLEY *et al.* 2007; HEAZLEWOOD *et al.* 2003; HIRST *et al.* 2003; MEYER *et al.* 2008; REMACLE *et al.* 2001b; VIDEIRA and DUARTE 2002). Of these protein subunits, 33 are common to all eukaryotes and only 14 have a homolog in the bacterial type-I NADH dehydrogenase (CARDOL *et al.* 2004). Therefore, the bacterial homolog subunits are considered to be *core* subunits of the complex (Table 1.1) and it has been proposed that the other eukaryotic *accessory*[2] subunits participate either in assembling, maintaining the stability and/or regulating the complex's activity. In mammals and fungi, the seven most hydrophobic core subunits (ND1-6 and ND4L) are encoded by the mitochondrial genome (Table 1.1), while the remaining core genes have been transferred to the nucleus. In *Chlamydomonas reinhardtii*, the genes encoding subunits ND6 and ND4L have also been transferred to the nucleus. As expected from from their eukaryotic origin, all accessory subunits are nuclear encoded.

[1] A ninth cluster, which is not evolutionary conserved, has been identified in some prokaryotes. See section 1.2.1.

[2] Accessory subunits are also usually known as *supernumerary* subunits. Both terms are used as synonyms in this work.

E. coli	*C. reinhardtii*	*A .thaliana*	*H. sapiens*	*B. taurus*
NuoA	Nuo3	ND3^{m}	ND3	Nd3^{m}
NuoB	Nuo10	PSST	NDUFS7	PSST
NuoC*	Nuo9	ND9^{m}	NDUFS3	30 kDa
NuoD*	Nuo7	ND7^{m}	NDUFS2	49 kDa
NuoE	Nuo5	28.3 kDa	NDUFV2	24 kDa
NuoF	Nuo6	53.5 kDa	NDUFV1	51 kDa
NuoG	NuoS1	75 kDa	NDUFS1	81.5 kDa
NuoH	ND1^{m}	ND1^{m}	ND1	Nd1^{m}
NuoI	Nuo8	TYKY	NDUFS8	TYKY
NuoJ	ND6^{m}	ND6^{m}	ND6	Nd6^{m}
NuoK	Nuo4L	ND4L^{m}	ND4L	Nd4L^{m}
NuoL	ND5^{m}	ND5^{m}	ND5	Nd5^{m}
NuoM	ND4^{m}	ND4^{m}	ND4	Nd4^{m}
NuoN	ND2^{m}	ND2^{m}	ND2	Nd2^{m}

Table 1.1. Nomenclature of the 14 core subunits of Complex I in different organisms.

*: NuoC and NuoD are fused in one single subunit in *E. coli*. ^{m}: encoded in the mitochondrial genome.

1.2.1. Complex I structure and mechanism

NADH: ubiquinone oxidoreductase (Complex I; EC1.6.5.3) is the largest and least understood of the respiratory complexes in terms of structure. Usually considered the point of entry of electrons into the respiratory chain, it catalyzes the reduction of quinone by NADH coupled to the translocation of protons across the membrane as schematized in the following reaction (GALKIN *et al.* 2006):

$$NADH + Q + H^{+} + 4\vec{H}^{+}_{i} \rightarrow NAD^{+} + QH_2 + 4\ \vec{H}^{+}_{o}$$

where Q is quinone, QH_2 is the quinone reduced form or ubiquinone (UQ), $\vec{H}^+$ are vectorial protons or protons pumped across the membrane, from the matrix side (i, in) to the intermembrane space (o, out). In addition to $\vec{H}^+$, a scalar proton is consumed for each NADH molecule that is oxidized. A scalar proton is one that is transferred to the positive side of the membrane together with electrons and therefore, does not contribute to electrochemical potential. Although the complexity of this enzyme is largely augmented in eukaryotes compared to the relative simple 14-subunit prokaryotic form, the biochemical mechanism for NADH oxidation/quinone reduction and proton transfer are believed to be conserved.

Recently, the structures of NADH occupied and non-occupied Complex I peripheral arm have been solved, providing new insights on the mechanisms of NADH oxidation and ubiquinone reduction (BERRISFORD and SAZANOV 2009). The region connecting the soluble arm to the membrane arm harbors the remaining 4Fe-4S clusters and forms the quinone binding pocket (SAZANOV 2007). Subunit NuoB (PSST) contains the 4Fe-4S N2 cluster, which transfers electrons to quinone. The linear arrangement and atomic distances of the iron-sulfur clusters from the FMN cofactor to the quinone binding site suggests that electron transfer occurs as shown in Figure 1.3.

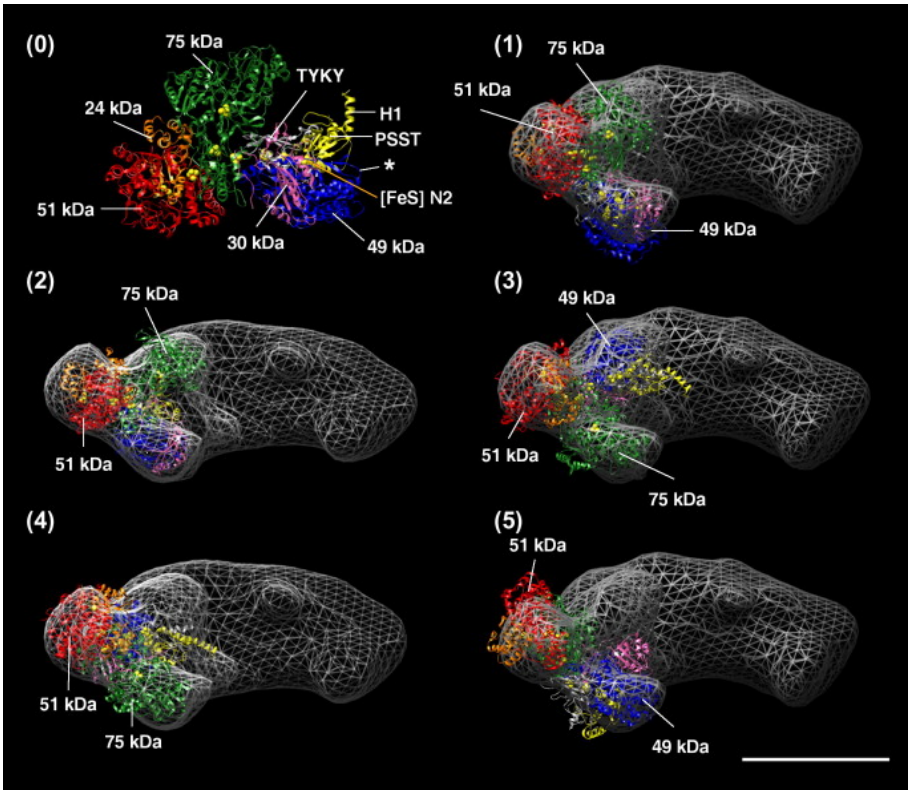

Figure 1.2. Top view of the fitted structure of Complex I.

Superimposition of 3D reconstructions from EM data and the X-Ray crystallographic data from the peripheral arm. Subunits are colored as follows: 51 kDa, *red*, 24 kDa, *orange*, 75 kDa, *green*, 30 kDa, *magenta*, PSST, *yellow*, TYKY, *grey*. * indicates the 49-kDa domain recognized in (ZICKERMANN *et al.* 2003). H1 indicates the PSST helix that reaches into the membrane arm. Numbers indicate: 0: X-Ray model from Sazanov *et al.* (2007); 1-5: fits of the X-ray model into the EM structure. Source: (CLASON *et al.* 2007).

In vivo values for Complex I reaction indicate a k_{cat} of approximately 500 s^{-1} (FATO *et al.* 1996). Binding of NADH to the Complex is not rate limiting as it has a time constant (τ) of approximately 0.2 μs (VERKHOVSKAYA *et al.* 2008). The simultaneous transfer of two electrons and one H^+ from NADH to FMN (hydride transfer) is followed immediately by the sequential transfer of the two electrons of the reduced FMN ($FMNH_2$) to N3 and N1a (SAZANOV 2007). Iron sulphur clusters can accept only one electron at a time, but only cluster N3 and not N1a has an E_m value high enough to oxidize $FMNH_2$ so it has been suggested that the second electron available from the now flavinsemiquinone (FSQ) reduces transiently and reversibly cluster N1a avoiding accumulation of the FSQ intermediate (SAZANOV 2007) (Figure 1.3). Clusters N3 to N6b have similar redox midpoint potentials (~ -250 mV) and electron transfer towards cluster N2 is not rate-limiting. N1a is reoxidized fast via FSQ/FMN upon re-oxidation of N2 which has a higher potential (~ -100 mV) and donates the two electrons, sequentially, to ubiquinone (UQ). Overall, electron transfer from NADH to cluster N2 site has a time constant of 90 μs and the release of the oxidized NAD^+ molecule from its binding pocket was proposed as the rate limiting step (VERKHOVSKAYA *et al.* 2008).

The use of electron paramagnetic resonance (EPR) to study Complex I provided the first clues on the mechanism of reduction of ubiquinone (E_m ~ 110 mV) by cluster N2 (OHNISHI 1998). Detection of two different forms of semiquinone (SQ) signals by EPR with differences in relaxation behavior, rotenone sensitivity and pH sensitivity allowed the modeling of the reduction mechanism (YANO *et al.* 2000). It was suggested that the transfer of the first electron to UQ is pH-dependent based on SQ EPR signal sensitivity

and the dependence of N2 E_m on pH (Bohr effect)(OHNISHI and SALERNO 2005; YANO *et al.* 2005; YANO *et al.* 2000). Transfer of the second electron to the SQ species to form ubiquinol (QH_2) was proposed as the source of energy for proton translocation (BRANDT 2006).

The membrane subunits ND2, ND3, ND4, ND4L, ND5 and ND6 have been proposed to form a gated proton channel based on their resemblance to Na+/K+ antiporters (VOGEL *et al.* 2007c). However, direct evidence assigning a function for each of these subunits is still missing. Most importantly, because electron transfer occurs on the soluble arm, it is unclear how the stepwise released energy from NADH oxidation is coupled to the transfer of protons through these "channels". A redox-linked (direct coupling) mechanism could explain the pumping of one proton at the interface between NuoN (49-kDa) and NuoB (PSST), which define the Q binding site. To explain the pumping of the other three protons, an indirect mechanism involving conformational changes of subunits Nuo L (ND4), NuoM (ND5) and NuoN (ND2) has been proposed. These subunits display similarity to monovalent cation/proton antiporters and have been proposed to be involved in proton translocation (SAZANOV 2007) A conformational change has been reported upon reduction of NADH. Comparisons of the SQ EPR signals in submitochondrial particles treated with the rotenone and stigmatellin were used to assign the point of action of these inhibitors within Complex I as well as their connection to the formation of reactive oxygen species (ROS) (FATO *et al.* 2009). The authors proposed a switch mechanism between two different states probably driven by a conformational change. Similar conclusions were driven from the analyses of reduced

and oxidized crystal forms of the soluble arm in *T. thermophilus* (BERRISFORD and SAZANOV 2009), which led to a mixed mechanism for proton transfer in which the redox state of clusters N6b and N2 would be the main contributors for a conformational driven proton translocation.

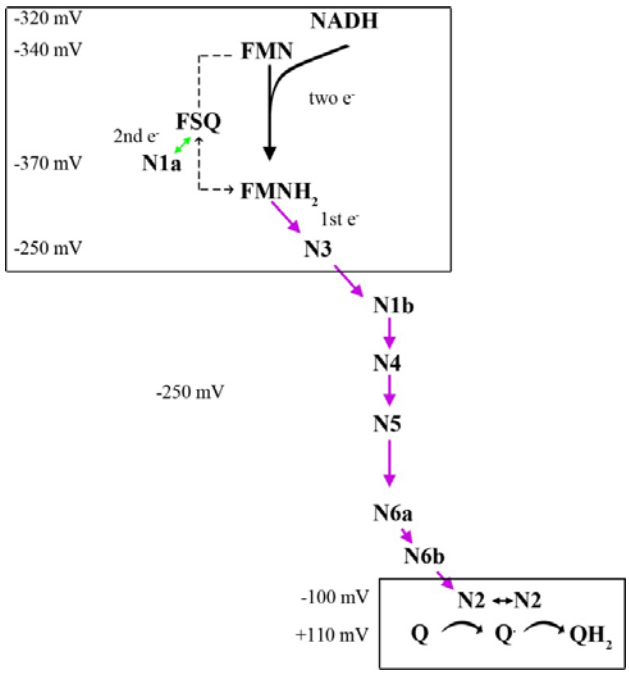

Figure 1.3. Mechanism of electron transfer from NADH to quinone through the iron-sulfur clusters

The two-electron midpoint potentials (E_m) of NADH and FMN, and the one-electron E_m of the iron-sulphur (Fe-S) clusters and quinone are indicated on the left. Fe-S clusters N3 to N6b have similar E_m (~ -250 mV) values. $FMNH_2$ transfers one electron to cluster N3 resulting in the formation of flavosemiquinone (FSQ) (dashed line), which is transiently stabilized as FMN (dashed line) by temporarily donating an electron to cluster N1a (green line). At the N2 cluster site, the first electron reduces ubiquinone (Q) to semiubiquinone (Q·) which is fully reduced to ubiquinol (QH_2) with the arrival of the second electron to cluster N2. See text for more details.

1.2.2. The assembly of Complex I

Mitochondrial dysfunction has been associated to several myopathies and neurodegenerative diseases (for instance cardiomyopathies and Parkinson's disease). Deficiencies in the functioning of the respiratory chain in humans have a minimum birth prevalence of 13.1/100,000 (THORBURN 2004). Among these, dysfunction of Complex I alone accounts for approximately 30% of the cases, and multiple complex dysfunctions – involving Complex I deficiency- for another 25% (SCAGLIA *et al.* 2004). Although mutations in mitochondrial and nuclear Complex I subunit genes explain many Complex I-associated deficiency cases in humans. Surprisingly there is still no molecular explanation for approximately 60 % of the Complex I defects. For this group of patients no mutations can be found in mitochondrial and nuclear Complex I structural genes, indicating that other genes involved in the regulation of assembly and/or stability of Complex I still have to be identified (TRIEPELS *et al.* 2000).

Based on the structural conservation of eukaryotic Complex I and its cofactors, it has been proposed that the assembly process is also conserved. Models for assembly have been built on evolutionary, biochemical and genetic studies using in mammal, fungi, bacteria and plants (LAZAROU *et al.* 2009; REMACLE *et al.* 2008; VOGEL *et al.* 2007a). This section does not intend to be comprehensive and the reader is referred to those reviews for more in depth understanding.

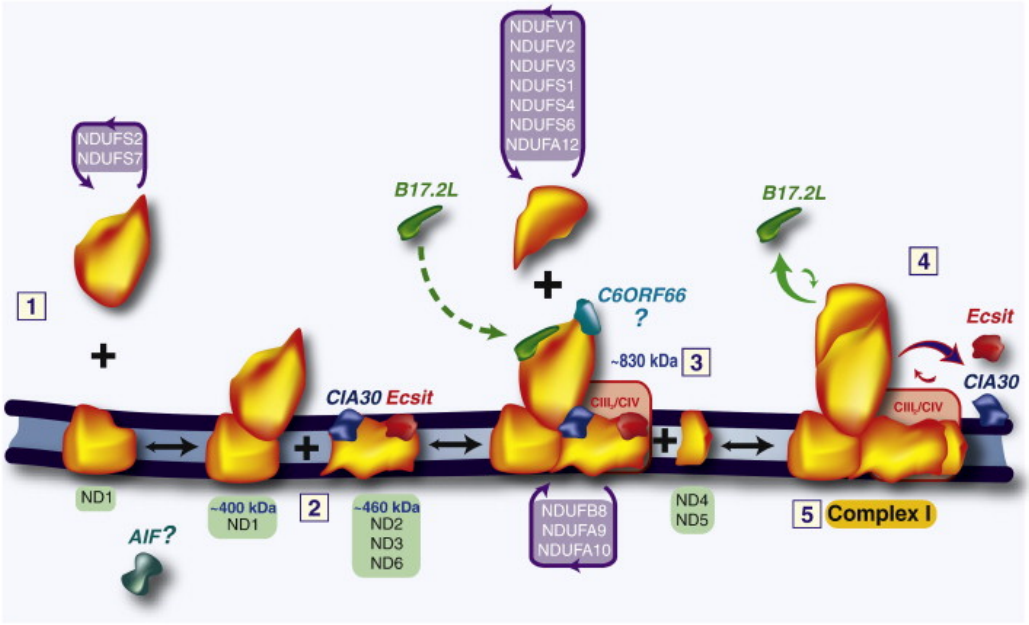

Figure 1.4. Model of Complex I modular assembly process in eukaryotes.

Assembly factors are required for the association of earlier modules or subcomplexes into later ones. CIA30, Ecsit, B17.2L and C6ORF66 are indicated here. The step of incorporation of some subunits is highlighted as well. $CIII_2$/CIV indicates the supra level organization of Complex I and late assembly intermediates into respirasomes. Source: (LAZAROU *et al.* 2009)

Three functional modules have been defined for Complex I (LAZAROU *et al.* 2009; VOGEL *et al.* 2004): a hydrophilic module facing the mitochondrial matrix and containing the NADH dehydrogenase subunits and the FMN group; a connecting module and a membrane module. Several biochemical and genetic studies suggest that the assembly process of Complex I occurs as the sequential addition of hydrophilic and hydrophobic modules (LAZAROU *et al.* 2009) both in bacteria and eukaryotes (Figure 1.4). Dissociation with the chaotrophic detergent lauryldimethylamine oxide (LDAO) followed by ion-exchange chromatography allowed the purification of two subcomplexes representing a) the membrane arm (Iβ), and b) a membrane-associated subcomplex (Iα) that could be further dissociated to purify a smaller subcomplex (Iλ) containing the soluble subunits in the peripheral arm (HIRST *et al.* 2003), although some subunits were present in more than one subcomplex (Figure 1.5).

1.2.2.1.Core subunit mutation effects on Complex I activity and assembly

The 14 core subunits are highly conserved in all organisms containing Complex I. Therefore, their mutation is expected to severely affect the complex's activity but also its assembly. Extensive research has been done on the understanding of these defects in humans and was recently reviewed (LAZAROU *et al.* 2009). Although not exhaustive, the following examples will help illustrate the evidence that mutations in different subunits result in the disruption of assembly at different stages. In *Neurospora crassa*, *Δnuo21*, lacking the homolog of bovine TYKY subunit, which coordinates iron-sulphur clusters N6a and N6b, results in the lack of a fully assembled Complex I and instead accumulates two soluble assembly intermediates of 100 and 350 kDa (NEHLS *et al.* 1992).

Null, knockdown and point mutations affecting the gene encoding the ND3 membrane subunit result in the lack of formation of a membrane arm in *Neurospora* (ALVES and VIDEIRA 1998), humans (SARZI *et al.* 2007) and *Chlamydomonas* (CARDOL *et al.* 2006). Mutations in subunits ND4 and ND5 in *Chlamydomonas* abolish the formation of a mature complex but yields the formation of an intermediate assembly of 700 kDa that has lost the ability to reduce quinone[3] (CARDOL *et al.* 2008), although this subcomplex is still anchored to the membrane.

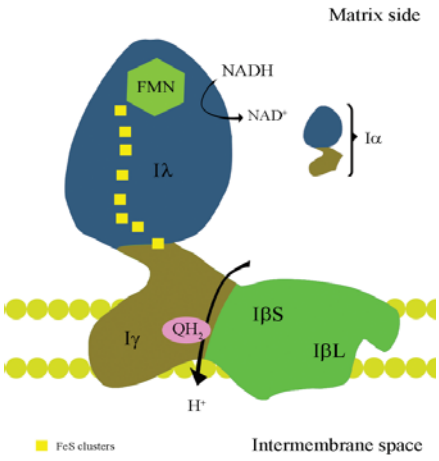

Figure 1.5. Modular organization of Complex I.

Source: (REMACLE *et al.* 2008)

[3] The quinone binding site is located at the interface of subunits PSST, 49-kDa and the membrane arm. (Sazanov *et al.* 2006).

1.2.2.2.Role of the accessory subunits in Complex I assembly

Although they do not form part of the electron transfer pathway, accessory subunits play a role in assembly and stabilization of eukaryotic Complex I. In some cases, disruption of these subunits may result in conformational changes in the arrangement on the core subunits that impact the catalytic activity as well. Complex I activity is impaired in the *nuemΔ* (NUEM, 39-kDa subunit) null mutant strain in *Yarrowia lipolytica* and the 900 kDa Complex I lacks the 51-kDa subunit as well but still incorporates the 49-kDa subunit (ABDRAKHMANOVA *et al.* 2006). In the mutant, a 700 kDa subcomplex was detected using an antibody against the NESM (ESSS) subunit while both 49- and 51-kDa subunits accumulated in two subcomplexes of 400 and 200 kDa. Point mutations in the NUEM subunit affected the binding of its own NAD(P)H but still yielded an assembled and functional Complex I, although unstable. A similar role in assembly has been proposed for supernumerary subunits of other respiratory complexes. For instance, deletion of the Cox7p supernumerary subunit of Complex IV in yeast results in lack of cytochrome oxidase activity and assembly, based on the disappearance of cytochrome aa_3 spectrophotometric peak (AGGELER and CAPALDI 1990). Similarly, null mutants of accessory subunits of yeast bc_1 complex (Complex III) result in impaired assembly/stability of this complex (LEE *et al.* 2001; MALANEY *et al.* 1997; ZARA *et al.* 2004).

1.2.2.3.Complex I assembly factors

De novo assembly of such a large Complex requires the aid of several chaperones or "assembly factors", many of them still wait to be discovered. Even if overall the assembly process is conserved across organisms, some underlying differences remain, probably reflecting some species-specific variations in subunit composition (VOGEL *et al.* 2007c). The use of mutants in different subunits that result in the formation of assembly intermediates as well as pulse chase experiments and GFP labeling (VOGEL *et al.* 2007a) provided an idea of the sequence of events that lead to the formation of a mature complex.

Assembly factors are generally defined as required for the process of assembly but not present in the mature complex. The two first discovered assembly factors for Complex I, CIA30 and CIA84, were identified in *N. crassa* (SCHULTE 2001) as they copurified with an intermediate assembly accumulating in a mutant of the 21 kDa subunit (KUFFNER *et al.* 1998) and Chapter 3). The assembly function of CIA30 was extended to humans (VOGEL *et al.* 2005) and its mutation has been shown to cause Complex I deficiency in humans (DUNNING *et al.* 2007). Since then, using candidate gene approaches, several assembly factors have been identified (Table 1.2). If the hypothesis of assembly conservation is valid, it is likely that at least some of the already identified assembly factors in other systems are also conserved in the plant kingdom. Orthologs for several confirmed and candidate assembly factors exist in plants and algae (Table 1.2).

Assembly of Complex I requires proper incorporation of the eight iron-sulphur clusters into the subunits. In a search for mitochondrial Fe-S assembly factors, Ind1, a

protein involved in the assembly of Complex I Fe-S clusters, was identified in *Yarrowia lipolytica* and seems to be specific for Complex I (BYCH *et al.* 2008). In the Δ*ind1* mutant the electron paramagnetic resonance (EPR) signals for clusters N1 and N2 were strongly reduced. However, *IND1* deletion only causes a partial reduction in Complex I amounts, suggesting that other proteins partially compensate for Ind1 dysfunction. An RNAi knockdown for the human homolog of Ind1, HuInd1, however, seems to accumulate a small subcomplex, indicating that assembly of Fe-S into the subunits is necessary for the formation of early-intermediate subcomplexes (SHEFTEL *et al.* 2009). Patients with Friedrich's ataxia carry mutations in the gene encoding frataxin, a mitochondrial protein involved in iron homeostasis and assembly of Fe-S proteins. Complex I activity is severely reduced in patients carrying a mutation in this gene, in addition to Complex II/III and aconitase (BRADLEY *et al.* 2000). *Arabidopsis atfh-1* mutants are partially depleted of frataxin (BUSI *et al.* 2006). The activity of tricarboxylic acid cycle and Complex II were also highly reduced in these mutants and that the mRNA levels for these enzymes and Fe-S cluster-containing Complex I subunits were increased. Complex I activity was reduced about 30% in these mutants (Dr. Diego Gonzalez-Casati, personal communication).

So far, most assembly factors are conserved. However, similarly to the species-specific subunits, some assembly factors seem to be exclusive to a particular phylogenetic group.

Assembly factors specific to the animal kingdom: The factor B17.2L (OGILVIE *et al.* 2005) associates with an 830 kDa subcomplex and its disruption also results in

reduced accumulation of Complex I and disease. The lack of association with smaller subcomplexes suggests that B17.2L is involved in the late stages of assembly. B17.2L is specific to animals, as no homologs have been found in other eukaryotes. Another example is C6ORF66, a 20.2 kDa oncoprotein identified by patient homozygosity mapping (SAADA *et al.* 2008). A Leu69Pro substitution in C6ORF66 results in accumulation of two subcomplexes and a strong reduction of Complex I activity. In a search for CIA30-interacting proteins, the cytosolic protein Ecsit was identified as another animal-specific assembly factor (VOGEL *et al.* 2007b) with mitochondrial localization. Ecsit co-migrates with CIA30 in three subcomplexes (830, 600 and 500 kDa), which are reduced in RNAi knockdowns. Ecsit depletion also results in a change in NDUFS3 and ND1 subunits association with Complex I and subcomplexes, shifting towards lower molecular weight assembly intermediates. Because Ecsit depletion results in down accumulation of CIA30, a role in CIA30 stabilization was proposed.

Assembly factors specific to the green lineage: In contrast to humans and fungi, almost no assembly factors have been identified in plants. L-galactono-1,4-lactone dehydrogenase (GLDH), an enzyme involved in ascorbate biosynthesis, is the only example of a plant-specific assembly factor (PINEAU *et al.* 2008). GLDH is found in association with an 800 kDa subcomplex in the *Nicotiana sylvestris* NMS1 mutant, while absent from the mature Complex (1000 kDa). *Arabidopsis gldh* mutants lack an assembled Complex I. It was suggested that GLDH is displaced by ND5 in the final steps towards Complex I maturation However, the mechanism by which GLDH controls Complex I assembly is still unclear.

Human	*Arabidopsis*	*Chlamydomonas*	Description
NDUFAF1[1] (CIA30)	At1g74420/At1g17350	au5g.8340(28% I)	NADH dehydrogenase (ubiquinone) 1 alpha subcomplex, assembly factor 1 precursor (Homo sapiens), Auxin-induced-related / indole-3-acetic acid induced-related
C20orf7[2,3]	At1g22800 (45.8 I)	au5g.4754 (43% I)	probable methyltransferase
C8orf38[4]	At1g62730 (41.2% I)	au5.g11030 (39% I)	putative phytoene synthase
HuInd1[5] (NUBPL)	At4g19540 (INDL, 60.2%)	au5.g192 (49% I)	nucleotide binding protein-like, Mrp-like iron sulphur protein

Continued

Table 1.2. Assembly factor conservation in plants and humans.

Except for AtGLDH, the human proteins were used to identify homologs in *Arabidopsis thaliana*, using the HomoloGene tool at the National Center for Bioinformatics Information (NCBI). When not appearing in the HomoloGene results, similar sequences were found in *Arabidopsis* and *Chlamydomonas reinhardtii* with a BLAST protein search. Percent of identity (%I) with the human (or *Arabidopsis*) homolog is highlighted between parentheses. "*" indicates candidate assembly factors as proposed in (PAGLIARINI *et al.* 2008); [1] (DUNNING *et al.* 2007); [2,3] (GERARDS *et al.* 2009; SUGIANA *et al.* 2008); [4] (PAGLIARINI *et al.* 2008); [5] (SHEFTEL *et al.* 2009); [6] (SAADA *et al.* 2009); [7] (VOGEL *et al.* 2007b); [8,9] (BRADLEY *et al.* 2000; HEIDARI *et al.* 2009); [10] (BUSI *et al.* 2006); [11] (PINEAU *et al.* 2008).

Table 1.2 continued

Human	*Arabidopsis*	*Chlamydomonas*	Description
NDUFAF3[6] (C3orf60)	At3g60150 (30% I)	au5g.3009 (34% I)	NADH dehydrogenase (ubiquinone) 1 alpha subcom;plex, assembly factor 3 isoform a
Ecsit[7]	not present	not present	evolutionary conserved signaling intermediate in Toll pathway isoform 1. CIA30-interacting factor
C2orf56 *	At3g28700 (42% I)	au5g.8728 (40% I)	hypothetical protein
Frataxin[8,9]	At4g03240 (FH[10] , 37.6% I)	au5g.3831 (FTX1, 51% I)	iron chaperone, involved in Fe-S cluster assembly
not present	At3g47930 (AtGLDH)[11]	au.g4408 (32% I)	mitochondrial L-Galactono-1,4-Lactone dehydrogenase, associated with Complex I
PhyH*	At2g01490 (46.3% I)	au5g.2269 (48% I)	phytanoyl-CoA 2-hydroxylase

Continued

Table 1.2 continued

Human	***Arabidopsis***	***Chlamydomonas***	**Description**
C10orf65 (NLP2)*	AT2G45440 (26% I)	au5g.8946 (28% I)	N-acetylneuraminate pyruvate lyase 2 (putative), dihydropiconilate synthase (DPS1)
OXCT1*	not present	not present	3-oxoacid CoA transferase 1
GPAM*	not present	not present	mitochondrial glycerol 3-phosphate acyltransferase
LACTB*	not present	not present	mitochondrial ribosomal protein L56; mitochondrial 39S ribosomal protein L56; serine beta lactamase-like protein LACTB

1.3. Complex I function in plants

The subunit composition of plant Complex I differs slightly from that of mammals. Proteomic studies and genome comparisons suggest that twelve subunits (NDUFS1, NDUFB1, NDUFB2, NDUFA3, NDUFA4, NDUFV3, NDUFA7, NDUFB2, NDUFB5, NDUFB6, NDUFA10 and NDUFB8[4]) are absent from both vascular plants and *Chlamydomonas reinhardtii* (CARDOL *et al.* 2005; CARDOL *et al.* 2004). On the other hand, additional subunits -NUOP1 (At4g20150, ND9), NUOP3 (At3g07480) and at least three carbonic anhydrase-like proteins are present in both algae and higher plants (CARDOL *et al.* 2005; CARDOL *et al.* 2004). Subunits NDH11 and NDH16 have been only identified by proteomic analyses in rice and *Arabidopsis* (CARDOL *et al.* 2004; HEAZLEWOOD *et al.* 2003) while three other proteins where only identified in *Chlamydomonas*: NUOP4, NUOP5, NUOP6 (CARDOL *et al.* 2004). It is of interest to determine whether these twelve proteins, individually or as a group, have equivalent roles in Complex I function or if they provide specialized functions of Complex I in each organism. Except for the carbonic anhydrases there is no genetic evidence to validate the role of these specific subunits as *bona fide* constituents of Complex I and, although unlikely, the possibility that they may constitute artifacts of the biochemical preparations cannot be disregarded.

[4] Subunit names follow the nomenclature for humans.

1.3.1. Carbonic anhydrases in plant Complex I

One of the most distinguished features of plant and algal Complex I is the presence of a number of carbonic anhydrases, a ubiquitous group of enzymes catalyzing the reversible conversion of HCO_3^- to CO_2 (bicarbonate dehydration). The presence of carbonic anhydrases as Complex I components seems to be exclusive to the green lineage. These subunits, were first identified by N-terminal sequencing in proteomic analyses of purified Complex I in potato (HERZ *et al.* 1994) and broad bean (LETERME and BOUTRY 1993). By mass spectrometry analysis four similar enzymes were identified in *Arabidopsis* -At5g63510 (γCAL1), At3g48680 (γCAL2), At1g47260 (CA2), At5g66510 (γCA3)- and two in rice -BAB39954, BAC16488-(HEAZLEWOOD *et al.* 2003). A fifth enzyme, At1g19580 (γCA1), was recently identified (MEYER *et al.* 2008). Similar analyses in *Chlamydomonas* showed that the algal complex also contains three associated γCAs: FBP1, FBP2 and CAH9 (CARDOL *et al.* 2004). A T-DNA insertional mutation in *Arabidopsis γCA2* results in a drastic reduction of Complex I activity (20% of wildtype levels) and Complex I accumulation (PERALES *et al.* 2005). The remaining activity may be in part due to partial redundancy by the other anhydrases. This idea is supported by yeast-two hybrid experiments in which γCAL1 and γCA3 interact with γCAL2 (PERALES *et al.* 2004).

Partial solubilization with digitonin and 2D-PAGE in *Arabidopsis* showed that γCAs are associated to the membrane arm (SUNDERHAUS *et al.* 2006). In addition, single particle electron microscopy (SPEM) analyses in a *Chlamydomonas* close relative, *Polytomella*, led to the suggestion that the algal γCAs protrude from the central part of

the membrane arm towards the matrix (SUNDERHAUS *et al.* 2006), similarly to the extra domain previously found in SPEM of *Arabidopsis* purified Complex I (DUDKINA *et al.* 2005). However, SPEM analysis using purified Complex I obtained from the γ*ca2* mutant showed that the extra domain and its appearance remained unaffected (SUNDERHAUS *et al.* 2006). Because γ*ca2* is a complete knockout, the authors suggested that in the remaining Complex I other γCAs could maintain the subunit arrangement of the domain. Again, total accumulation of Complex I is reduced in the γ*ca2* mutant. Decoration of single particles with antibodies against the specific γCAs is necessary to understand how these subunits are arranged in the membrane arm.

Phylogenetic analyses of *Arabidopsis* Complex I-associated γCAs grouped them within the γ-subfamily (PARISI *et al.* 2004), a separated group of CAs initially described in the archea *Methanosacina thermophila* (ALBER and FERRY 1994) and exclusive to the green lineage within eukaryotes (PARISI *et al.* 2004). Although most of the functional aminoacids are conserved in plants, until now there was no functional evidence for plant γCA activity. In a very recent study, a soluble form of *At*γCA2 was expressed in *Escherichia coli* and *in vitro* assays of the purified protein showed that it can form stable homotrimers (MARTIN *et al.* 2009). In addition to bicarbonate dehydration some carbonic anhydrases also catalyze ester hydrolysis. The recombinant enzyme was unable to catalyze either of the two activities. However, the enzyme was able to bind inorganic carbon during *in vivo* labeling experiments. The function of γCAs in Complex I is so far speculative and a role in recycling mitochondrial CO_2 produced during photorespiration to make it more available for RubisCO in combination with other mitochondrial CAs was

proposed (MARTIN *et al.* 2009). In this context, γCAs would help to hydrate CO_2 and facilitate its transport from the matrix to the intermembrane space. However, the data presented in the study do not provide sufficient information to account for this proposed function. The photorespiratory pathways regenerates CO_2 in the mitochondrial matrix via the glycine decarboxylase complex (GDC, reviewed in (DOUCE *et al.* 2001). In addition, NADH derived from glycine decarboxylation is the preferred substrate for mitochondrial electron transport in plants (DAY 1985). A functional association of GDC with Complex I could simultaneously provide NADH and CO_2 for Complex I-dependent injection of electrons into the respiratory chain and Complex I-associated CO_2 shuttling across the inner membrane. Additionally, CO_2 generated by decarboxylating reactions in the trycarboxylic acid cycle (TCA) could also serve as a source of CO_2 for the γCAs in Complex I.

1.3.2. Metabolic aspects of Complex I activity defects

Short term effects of Complex I deficiency have been evaluated in *Arabidopsis* protoplasts treated with the Complex I inhibitor rotenone (GARMIER *et al.* 2008). In addition to a decrease in dry weight, rotenone-treated protoplasts specifically induced alternative NDs and AOX, but no other respiratory complexes. Inhibition of Complex I by rotenone also induced a decrease in mitochondrial protein expression, as reflected by the diminished abundance of the mitochondrial matrix processing peptidase (MPP) and the elongation factor Tu (GARMIER *et al.* 2008; LISTER *et al.* 2004). Import capacity was also reduced when measured *in vitro* using mitochondria from treated and non-treated cells (LISTER *et al.* 2004). Analysis of proteins in the mitochondrial fraction showed a

reduction in the abundance of cytosolic enzymes involved in glycolysis and cytosolic carbon metabolism (e.g. glyceraldehyde-3-P dehydrogenase) upon rotenone treatment (GARMIER *et al.* 2008). However, abundance of the corresponding transcripts and enzymatic activities from whole cells increased significantly in rotenone treated cells, suggesting that these proteins, normally associated with the mitochondrial outer membrane, change their cellular distribution as a functional adjustment. Similarly, changes in metabolite abundance were observed at different time points since rotenone inhibition, indicating a slowdown of the tricarboxylic acid cycle and increase of the glycolytic pathway, eventually leading to lactate accumulation (GARMIER *et al.* 2008).

Contrary to humans, plants tolerate Complex I deficiency fairly well during vegetative growth, although several of them show a slower growth rate and smaller vegetative and floral organs than wildtype plants (GUTIERRES *et al.* 1997). Deficiency in the NADH to quinone electron transfer by Complex I can be compensated by the presence of alternative NADH dehydrogenases (GUTIERRES *et al.* 1997; MELO *et al.* 1996; SABAR *et al.* 2000) (Figure 1.1). Particularly, an increase in the respiratory activity was observed in *Nicotiana sylvestris* CMS and NMS mutants when NADH was used as a substrate, and this activity was insensitive to rotenone treatment. When glycine was used as a substrate, the respiratory rate was highly reduced (GUTIERRES *et al.* 1997; SABAR *et al.* 2000). Consistently, in these mutants, the *in vivo* dark respiration rates are elevated with respect to the wildtype (DUTILLEUL *et al.* 2003). The CMSII mutant also displayed elevated levels of amines and most aminoacids, and decreased amounts of carbohydrates, suggesting a mitochondrial control over nitrogen assimilation (DUTILLEUL *et al.* 2005).

From transcriptome analyses it was proposed that the tricarboxylic acid (TCA) cycle has a modified response to the nitrogen status in Complex I mutants (PELLNY *et al.* 2008), assigning a direct role to Complex I in nitrogen metabolism signaling. The metabolic profiles of the *Arabidopsis ndufs4* mutant show that the impact of Complex I mutations is more significant at night times (MEYER *et al.* 2009) and an accumulation of organic acids and aminoacids that are substrates for respiration was observed. Transcripts of the electron transfer flavoprotein (EFP) pathway that feeds electrons from branched aminoacids to the respiratory chain bypassing Complex I were more abundant in the *ndufs4* and *ndufa1* (At3g08610, MWFE subunit) mutants (MEYER *et al.* 2009). Thus, it was concluded that the observed metabolic effects could be extrapolated to the absence of Complex I in general rather than a singular effect from the particular mutation.

The availability of respiratory mutants in plants allowed the analysis of mitochondrial role in photosynthesis. In the CMSII mutant, photosynthetic capacity, measured as Rubisco activity was similar to the wildtype (DUTILLEUL *et al.* 2003) although photosynthesis (measured as CO_2 uptake) was significantly reduced (DUTILLEUL *et al.* 2003; SABAR *et al.* 2000). However, under physiological conditions, the mutants showed a decrease in CO_2 uptake, probably because of a higher demand of extra-mitochondrial sinks to sustain the recycling of NADH. This redistribution in redox equivalents would result in inhibiton of photosynthesis (DUTILLEUL *et al.* 2003). Studies on the effect of Complex I on light acclimation of carbon assimilation in the CMSII mutant (PRIAULT *et al.* 2006a) showed that at high light the mutant is impaired when compaired to the wildtype. Also, this mutant seems to have an increase in

photorespiratory activity caused by a decrease in CO_2 mesophyll conductance (PRIAULT *et al.* 2006b) but in the absence of Complex I, the excess NADH from glycine decarboxylation is rebalanced by a metabolic shift towards cytoplasmic metabolic sinks and engagement of alternative dehydrogenases (DUTILLEUL *et al.* 2003; SABAR *et al.* 2000). Complex I impairment in green algae has been studied using *Chlamydomonas reinhardtii*. Mutation of *Chlamydomonas* mitochondria encoded subunits also leads to a slow growth phenotype in the dark (*sid*) (CARDOL *et al.* 2008; CARDOL *et al.* 2004; REMACLE *et al.* 2001a), and is accompanied by a delayed growth under mixotrophic conditions, again indicating that mitochondria still contribute energy equivalents in photosynthetic organisms (REMACLE *et al.* 2001b).

The term "state transition" refers to the short-term adaptation or change in the organization of photosynthetic electron flow that rebalances light excitation between photosystem I and II as a response to the reduction status of the plastoquinone pool (for an excellent review, see (WOLLMAN 2001). Briefly, when in state I, most of the light-harvesting complexes (LHCII) are associated to photosystem II (PSII), promoting plastoquinone reduction and formation of NADPH. Under high light conditions, or when the plastoquinone pool is highly reduced, a LHCII kinase associated to cytochrome b_6f is activated and phosphorylation of LHCII promotes its association with photosystem I (PSI) or, in other words, transition to state II. In addition to antenna relocalization, cytochrome b_6f also increases its colocalization with PSI during state II (VALLON *et al.* 1991). In the dark, state II transitions were already shown in *Chlamydomonas* mitochondrial Complex III mutant cells (*dum1*) depleted from ATP (BULTÉ *et al.* 1990).

Similarly, transition from linear (state I) to cyclic photosynthetic electron flow (state II) was found in Complex I, III and IV mutants in the light, together with an increase in non-photochemical plastoquinone reduction and lower O_2 evolution (CARDOL *et al.* 2003). ATP contents were lower in Complex III and IV but not in Complex I mutants; therefore, it was proposed that the shift to cyclic electron flow was sufficient to compensate for the lower ATP production in Complex I mutants (CARDOL *et al.* 2003). It has been suggested that mitochondria export larger amounts of ATP to the cytosol than chloroplasts (HOEFNAGEL *et al.* 1998) via highly active ATP/ADP transporters. Consistently, mitochondrial respiratory mutants lacking Complex I and Complex III activities and impaired in the transition from state I to state II, *dum22 stt7-9*, are unable to sustain photoautorophic growth under low light conditions , whereas single respiratory (*dum22*) or photosynthetic (*stt7-9*) mutations alone are able to produce enough ATP for carbon fixation, and therefore, sustain biomass production (CARDOL *et al.* 2009).

The metabolite changes and photosynthetic data agree with a model where respiratory mutations produce a reduction of mitochondrial contribution to cytosolic ATP formation, which results in an increase of glycolysis. Increased glycolysis would result in more cytosolic NADH import to the chloroplast and activation of the chlororespiratory pathway, which causes non-photochemical plastoquinone reduction and thus, induces transition to state II (CARDOL *et al.* 2009; CARDOL *et al.* 2003; GARMIER *et al.* 2008; WOLLMAN 2001). In this context it has been suggested that mitochondria contribute to an otherwise insufficient ATP pool necessary for the Calvin-Benson cycle and other chloroplast functions. In tobacco CMSII mutants, the non-photochemical quenching

response is delayed at the onset of light, and this delay correlates with an extended period of photosynthetic cyclic electron flow, an increase in the pool of reduced electron carriers that function as PSI electron acceptors (CARDOL *et al.* 2010). Under steady state conditions, the mutant and the wildtype do not show significant differences and transition to linear electron flow. However, ATP levels in CMSII and wildtype plants are also similar (CARDOL *et al.* 2010), probably because of the compensatory increase of the mitochondrial cytochrome electron flow.

1.3.3. Complex I defects and effects in fertility

The original link between respiratory activity and fertility was suggested from the fact that several cytoplasmic male sterile (CMS) mutants carry mitochondrial genomic rearrangements that result in the aberrant expression or deletion of respiratory subunits (GUTIERRES *et al.* 1997). Overall, reproductive effects of genes affecting mitochondrial function can be classified in those affecting sexual organ maturation, gametogenesis, embryogenesis and seed germination.

Tobacco CMS mutant plants generally show leaf variegation, dwarfism and abnormal pollen development (DE PAEPE *et al.* 1990), as it was observed in mutants with deletions in the mitochondrial *nad7* (CMSI) and *nad1* (CMSII) genes (LELANDAIS *et al.* 1998; PLA *et al.* 1995; SABAR *et al.* 2000) and the nuclear male sterile (NMS) mutant, defective in splicing of the mitochondrial transcript of *nad4* (BRANGEON *et al.* 2000). A similar phenotype was observed in the maize mitochondrial mutant, NCS2, which has a modest deficiency in Complex I (MARIENFELD and NEWTON 1994; SHUMWAY and BAUMAN 1967). Constitutive overexpression of *Arabidopsis CA2* (AtCA2) under the

control of Ca35S promoter results in male gametophytic sterility (VILLARREAL *et al.* 2009). Rotenone-sensitive (Complex I) respiration was absent from AtCA2 overexpressing plants and ROS accumulation in anthers was almost absent (VILLARREAL *et al.* 2009). The lack of ROS correlated with the absence of secondary lignin deposits in the endothecium, necessary for anther dehiscence and pollen release. The authors speculated that lack of ROS in the mutant prevented anther dehiscence and therefore blocked the viable pollen from leaving the anther.

The reproductive phenotype is not restricted to Complex I deficiency however, as mitochondrial and nuclear mutants affected in the function of other respiratory complexes show similar effects in pollen and embryo development and growth (LAUER *et al.* 1990; NEWTON *et al.* 1990). In the case of maize mitochondrial mutants homoplasmicity is hardly achieved, with the exception of maize NCS2 and NCS5 (cytochrome oxidase mutant), in which normally abortive embryos can be rescued from the kernel and propagated by tissue culture (GU *et al.* 1994; YAMATO and NEWTON 1999). A requirement of respiratory complexes for gametophytic development was demonstrated using an *Arabidopsis* mutant in the SDH1-1 (flavoprotein) subunit of Complex II (LEON *et al.* 2007). No homozygous progeny could be obtained from these mutants and the heterozygous plants had normal growth. However, seed set was reduced in the heterozygous plants as a result of an effect in both male and female gametophytes, in particularly *sdh1-1* pollen grains were aborted. *Arabidopsis* contains three isoforms of the *SDH2* (iron sulfur) gene, *SDH2-3* is highly expressed during late seed maturation but not in vegetative tissues and its mRNA decreases during germination (ELORZA *et al.* 2006).

However, germination is delayed in *sdh2-3* mutants (ROSCHZTTARDTZ *et al.* 2009), suggesting that SDH2-3 accumulation during dormancy is required for immediate activation of mitochondrial metabolism during germination.

Frataxin is a conserved chaperone involved in the assembly of mitochondrial iron-sulfur proteins, and its deficiency affects several mitochondrial proteins and decreases the activities of several respiratory complexes. *Arabidopsis* frataxin null mutants are embryo lethal and knock down mutants show a decrease in seed set (BUSI *et al.* 2006). Reproductive defects in respiratory mutants, in particular Complex I mutants, have been also observed in other organisms, such as *Neurospora crassa* (DUARTE *et al.* 1998; DUARTE and VIDEIRA 2000), *Drosophila melanogaster* (RAGONE *et al.* 1999) and *Caenoharbditis elegans* (TSANG *et al.* 2001), but a direct link between plant respiratory deficiency and fertility has not been established.

On the other hand, in several cases, male sterility is associated to the expression of apparently aberrant proteins in the mitochondrial inner membrane; these proteins are not necessary related to respiratory subunits, and therefore, a direct link between respiratory activity cannot be assured (reviewed in (HANSON and BENTOLILA 2004). Many of these non-respiratory proteins contain are associated to the inner mitochondrial membrane, and thus, as in the case of URF13, may open pores that disrupt the mitochondrial potential, rather than having a direct effect in a particular respiratory complex or enzyme. Recently, rapeseed CMS ORF138, was shown to associate in a high molecular weight complex (DUROC *et al.* 2009). In these mutants, none of the respiratory complexes assembly or activity was affected in whole plants, but no determination of the

specific respiratory complexes was conducted in anthers. Total oxygen consumption was elevated in anthers from sterile plants, suggesting a rearrangement of the respiratory chain in that developmental stage.

In addition, not all Complex I mutants described in plants are male sterile. *Arabidopsis frostbite (fro1)* is a *NDUFS4* null mutant (At5g67590, 18 kDa subunit), which has delayed development and altered response to cold stress (LEE *et al.* 2002). Although seeds from this mutant germinate late, germination rates were not affected. These observations were confirmed by another mutant in the same gene, *ndusf4*, which produces a similar phenotype and results in absence of Complex I activity (MEYER *et al.* 2009). *Arabidopsis ndufs4* delayed germination appears to be the result of a hormone imbalance rather than lack of stored nutrients or aborted embryos, as mutant seeds were able to germinate on time by addition of giberellic acid (GA) (MEYER *et al.* 2009).

In *Arabidopsis,* a knockout mutant in the L-galactono-1,4-lactone dehydrogenase gene (*Atgldh*), involved in the ascorbate biosynthesis pathway, results in absence of Complex I assembly (PINEAU *et al.* 2008). Otherwise lethal seedlings can be rescued in ascorbate supplemented media, indicating that the cause of lethality in this mutant is not due to Complex I deficiency. Moreover, seed set and germination rates in *Arabidopsis ca2* and *ca3* mutants, which only accumulate 20% of wildtype Complex I levels, are not affected (PERALES *et al.* 2005), suggesting that lack of Complex I activity *per se* does not cause infertility.

Two mechanisms are suggested to explain CMS (BUDAR *et al.* 2003): impaired ATP production resulting from the loss of function of mitochondrial genes; and an

undefined “gain of function” mechanism by which mitochondrial mutations result in the exclusive alteration of male gametophytic development. Complex I deficiency alone does not seem to be a cause for lack of fertility, because null mutations in nuclear genes encoding subunits are not associated with sterility (LEE *et al.* 2002; MEYER *et al.* 2009; PERALES *et al.* 2005). However, deletion of *nad7* in the tobacco CMSII mutant (GUTIERRES *et al.* 1997) as well as a nuclear encoded intron II splicing factor in the NMS (BRANGEON *et al.* 2000) both result in male sterility. Conversely, increased expression of respiratory subunits (VILLARREAL *et al.* 2009), or accumulation of chimeric proteins - related or not to respiratory subunits- (BONHOMME *et al.* 1992; LAUER *et al.* 1990; MARIENFELD and NEWTON 1994) at the mitochondrial inner membrane seems to consistently alter fertility. A standing hypothesis suggests that these proteins may disrupt the mitochondrial inner membrane and thus, cause cell-specific stress with sterility as the outcome. Anthers from ORF138 CMS plants have an increased oxygen consumption relative to fertile plants (DUROC *et al.* 2009). These results are consistent with the formation of a pore in the inner membrane by ORF138, which was shown to oligomerize (DUROC *et al.* 2005), similar to pore formation in the mitochondrial inner membrane of maize T-URF13 CMS plants (RHOADS *et al.* 1995). In this context, the energy hypothesis can be incorporated into the gain of function idea if the permeabilization of the membrane results in dissipation of the electrochemical potential and thus, deficient energy production and change in ROS accumulation/distribution.

CHAPTER 2

DISSECTION OF COMPLEX I ASSEMBLY IN THE GREEN ALGA *CHLAMYDOMONAS REINHARDTII*

2.1. Introduction

Defects in the respiratory chain have a birth prevalence of around 1/5,000-7,000 births (SKLADAL *et al.* 2003; SMEITINK *et al.* 2001), 55 % of which involve a deficiency in NADH: ubiquinone oxidoreductase (Complex I, EC1.6.5.3) activity alone or together with alterations in other respiratory complexes (LOEFFEN *et al.* 2000; THORBURN 2004). Complex I is an L-shaped multimeric enzyme consisting of a hydrophilic peripheral arm protruding into the mitochondrial matrix and a membrane arm that undergo modular assembly reviewed in (LAZAROU *et al.* 2009). It is well recognized that the assembly of multimeric enzymes is assisted by factors that are not part of the mature enzyme but nevertheless essential in promoting its assembly into an active form. In humans, only 40% of the mutations of nuclear origin occur in structural subunits of Complex I and it is generally accepted that the other 60% of the patients is affected in factors that are recruited to assemble or regulate the complex.

In the recent years the use of model organisms has largely contributed to the enormous progress made in identifying factors involved in the assembly of respiratory complexes. Most of these studies have been carried out in the model organism *Saccharomyces cerevisiae*, which has a broad spectrum of genetic and molecular tools facilitating research (BARRIENTOS 2003). However, given that *S. cerevisiae* and its related species have lost the structural subunits during evolution, they are naturally depleted of Complex I (GRAY *et al.* 2001) and have no direct use in the study of Complex I assembly. Nevertheless, *S. cerevisiae* and other eukaryotes that do not contain a Complex I have been used in combination with other experimental approaches to reveal candidate Complex I assembly factors. An important advance in this respect has been recently published by the Mootha laboratory using substractive phylogenetic analyses together with mitochondrial proteomic data from Complex I bearing organisms (PAGLIARINI *et al.* 2008). Based on the outcome of the comparative strategy, the authors pulled out a number of candidate assembly factors of which one, C8orf38, was found to be mutated in a Complex I deficient patient. A main limitation of the subtractive phylogenetic approach is that the discovery power is restricted to assembly factors that are assumed to have been systematically lost from organisms lacking Complex I, hence excluding the possibility of finding conserved genes that have acquired a novel function in Complex I assembly. Therefore, there is still a need for a genetic approach that allows the discovery of novel loci controlling Complex I assembly on the basis of loss of function phenotype.

Several experimental systems have been used for the study of Complex I defects. Among them, the fungi *Neurospora crassa* (SCHULTE 2001; VIDEIRA and DUARTE 2002)

and *Yarrowia lipolytica* (KERSCHER *et al.* 2004), as well as *Caenorhabditis elegans* (GRAD and LEMIRE 2004), Chinese hamster cell lines, mice in the animal kingdom and *Arabidopsis thaliana*, *Nicotiana sylvestris* and *Zea mays* in plants (PINEAU *et al.* 2008) (MARIENFELD and NEWTON 1994; PLA *et al.* 1995). In *Yarrowia*, Complex I deficiency is lethal unless the Ndh2 alternative NADH dehydrogenase (ND) normally located at the IMS side of the mitochondrial inner membrane is ectopically expressed on the matrix side. In *Neurospora*, Complex I is only essential during the sexual growth phase (VIDEIRA and WERNER 1989). Although these systems have been used extensively to study the effects of specific mutations in Complex I function, they do not offer the advantage of an easy, inexpensive screening system for the isolation of Complex I mutants.

Chlamydomonas reinhardtii, a unicellular green alga, is a very promising experimental system to address the question of Complex I assembly (REMACLE *et al.* 2008). Often viewed as a "plant-like" organism because it was first successfully used in the study of photosynthesis, *Chlamydomonas* is in fact closer to mammalians by many aspects of its biology that are unrelated to photosynthesis (MERCHANT *et al.* 2007). It is an ideal organism to study mitochondrial biogenesis because respiratory mutants are viable if maintained in phototrophic (light) or mixotrophic (light + carbon source) conditions. This provides an obvious advantage to screen for Complex I mutants, as they show similar growth rates as those of the wildtype strains under mixotrophic conditions but reduced growth under heterotrophic conditions (dark+carbon source) (CARDOL *et al.* 2002; REMACLE *et al.* 2001a). In contrast, Complex III or Complex IV mutants display

arrested growth in the dark (**d**ar**k** dier or dk). The difference between a "slow" versus "arrested" growth is attributed to the fact that a Complex I mutant retains two respiratory complexes sites out of the three that still contribute to the formation of the proton electrochemical potential, and thus to ATP formation, whereas a *dk* mutant only keeps Complex I as proton pumping enzyme. Until now, several mutations in Complex I subunits encoded by the mitochondrial genome and one nuclear mutation (*amc2*, *assembly of mitochondrial complex I*) that has not been mapped to any locus have been described in *Chlamydomonas* (CARDOL *et al.* 2002; REMACLE *et al.* 2001a). Here, we followed a mutagenesis approach to search for additional *amc* mutants of nuclear origin. Six *amc* mutants defining five loci were isolated. The mutants are affected to different extents in Complex I activity and most of them resulted in the accumulation of subcomplexes, an indication that the assembly process of the membrane arm is compromised.

2.2. Results

2.2.1. Identification of complex I deficient (amc) mutants via insertional mutagenesis

Only one nuclear mutation resulting in a Complex I defect and obtained via chemical mutagenesis has been described in *Chlamydomonas* (CARDOL *et al.* 2002; REMACLE *et al.* 2001a). We have named this mutant *amc2*. To uncover additional *AMC* loci, we undertook an insertional mutagenesis and screened for nuclear mutations resulting in Complex I dysfunction. An insertional mutant library was generated by electroporation of an expression cassette conferring resistance to either of the protein synthesis inhibitors hygromycin B (*aphVII*) or paromomycin (*aphVIII*). The insertional mutagenesis approach has been extensively used in *Chlamydomonas* to produce cassette-tagged mutants (ADAM and LOPPES 1998; ERMILOVA *et al.* 2000; GALVAN *et al.* 2007; GUMPEL *et al.* 1995). To screen for mutants with defects in mitochondrial function, particularly in Complex I, the transformants were plated in replicas and maintained in the dark and in the light. Out of approximately 50,000 independent transformants, 22 showed either arrested (*dk*) or slow growth in the dark (*sid* for slow growth in the dark). Because our goal was to isolate Complex I mutants, we focused our attention on mutants displaying a *sid* phenotype as loss of Complex I function is known to result in such a phenotype in *Chlamydomonas* (REMACLE *et al.* 2008; REMACLE *et al.* 2001a). The growth phenotype of all *sid* mutants was confirmed (not shown and Figure 2.1, A). To determine if the observed phenotype was caused by a defect in Complex I activity, the rotenone-sensitive NADH dehydrogenase activity of partially purified membranes of the

22 *sid* candidates was evaluated (not shown and Figure 2.1, B). Complex I deficiency was verified for six *sid* mutants and we named them *amc1*, *amc3* through *amc7* (Figure 2.1, B). The other *sid* mutants were either not significantly or only marginally reduced in Complex I activity (p-value > 0.05) and were not further analyzed (not shown). All *amc* mutants showed a drastic decrease in Complex I activity. A milder reduction was observed in *amc3*, which still retained 40% of the level of Complex I activity.

We focused on the six isolated *amc* mutants in addition to *amc2* that was previously described (REMACLE *et al.* 2001a). In order to differentiate a defect in the ability to reduce quinone from a defect in the NADH: oxidase function of the complex, BN-PAGE followed by *in gel* NADH dehydrogenase activities were performed in all mutants (Figure 2.1, C). The typical purple bands observable at 950 kDa that correspond to the holoenzyme was absent in the partially purified membranes of *amc1*, *amc2*, *amc4*, *amc5*, *amc6* and *amc7*. In the case of *amc3*, a native complex of wildtype size was still detectable, although the staining was reduced. Note that wildtype Complex I is often resolved in more than one band of high molecular weight depending on solubilization conditions. These results were in agreement with those of the partially purified membranes. With the exception of *amc3* and *amc4*, all mutants accumulated a smaller band (approximately 700 kDa) that stained for NADH dehydrogenase activity in the BN-PAGE (not shown and Figure 2.1, C). We noted that the subcomplexes detected in *amc1* and *amc2* were labile based on the fact that they were not always detected in independent extractions (not shown). On the other hand, *amc5*, *amc6* and *amc7* always accumulated the subcomplexes and their abundance was fairly constant. It is worth mentioning that a

similar 700 kDa subcomplex is also detected in mitochondrial *nd4* or *nd5* mutants in *Chlamydomonas* (CARDOL *et al.* 2008). In *amc3*, a reduced amount of Complex I was systematically detected. We also noted that very small quantities of Complex I accumulated in *amc4* (Figure 2.2, C). Similarly to the subcomplexes detected in *amc1* and *amc2*, this accumulation appeared to be dependent upon extraction, an indication that Complex I is not stable in the presence of the *amc4* mutation.

To further evaluate the Complex I NADH oxidoreductase function in the mutants, total NADH: ferricyanide oxidoreductase activity was determined. Total NADH: ferricyanide oxidoreductase activity reflects the activity of Complex I but also of other cellular NADH dehydrogenases (QUILES *et al.* 1996). However, because most of the NADH: ferricyanide activity in *Chlamydomonas* is due to the NADH activity of the peripheral arm of Complex I, the level of this activity is reduced in Complex I mutants. A strong reduction was observed in all mutants except *amc3*, which showed a mild decrease (Figure 2.1, D). Overall, the levels of reduction correlated with the reduced *in gel* staining for NADH dehydrogenase activity (Figure 2.1, B) in the mutants accumulating a 700 kDa subcomplex with NADH dehydrogenase activity. All *amc* mutants show decreased whole cell respiration when compared to wild type (Table 2.1). In accord with the defect in Complex I activity, the respiration in the *amc* mutants was rotenone insensitive.

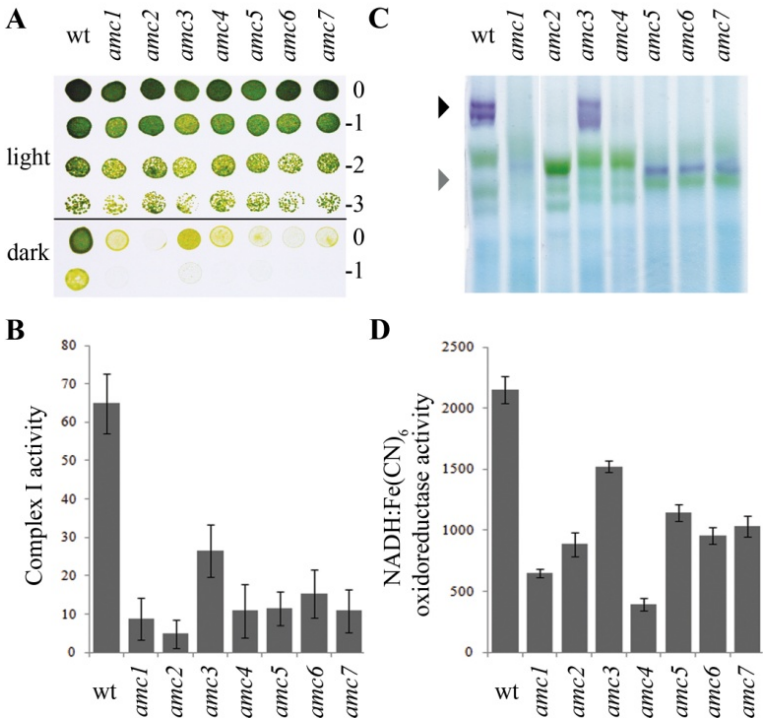

Figure 2.1. Six novel *sid* mutants display a defect in Complex I activity.

A. Ten-fold dilution series of *amc1* to *amc7* mutants and wild type (wt) cells were plated on acetate containing medium and incubated three days in the light and five days in the dark, respectively. **B.** Complex I-specific (rotenone-sensitive NADH: dehydrogenase) of the *amc* mutants are indicated as averages of ten independent measurements. Activities are expressed in nmol NADH reduced per minute per mg of protein. **C.** BN-PAGE and *in gel* NBT staining of the NADH dehydrogenase activity. Note that Complex I is often resolved in two or several bands of high molecular weight. The black and grey arrows indicate the position of mature Complex I and the700 kDa subcomplex, respectively. **D.** NADH: ferricyanide oxidoreductase activity. Activities are expressed in nmol K_3Fe reduced per minute per mg protein. The results represent the average of three independent determinations. B and D. Error bars indicate standard error (SE).

Strain	Respiration ($\mu mol\ O_2\ h^{-1}\ mg_{Chl}^{-1}$)	
	- rotenone	+ rotenone
wt	61.0 ± 2.0	42.0 ± 4.0
amc1	44.2 ± 3.2	39.8 ± 5.7
amc2	42.7 ± 0.8	41.0 ± 5.4
amc3	44.6 ± 5.0	40.1 ± 6.8
amc4	43.9 ± 5.3	43.7 ± 7.8
amc5	37.0 ± 4.2	33.4 ± 5.9
amc6	36.2 ± 4.6	34.4 ± 3.1

Table 2.1. Complex I-dependent oxygen consumption of mutants representing the six *amc* loci

Wildtype and mutant strains representing mutants of the six different *AMC* loci were grown mixotrophically (TAP+ arginine, light) Oxygen consumption was measured in the dark with or without the addition of 100 µM rotenone to specifically inhibit Complex I. Values represent the average of three independent measurements and ± indicates the standard error.

2.2.2. The amc mutants display complex I assembly defects

To verify that the 700 kDa bands showing NADH dehydrogenase activity observed in *amc1, 2, 5, 6* and *7* were *bona-fide* subcomplexes of Complex I, we carried out immunoblot analyses. Polyclonal antibodies directed against two subunits of the hydrophilic arm (49 kDa and 51 kDa) were used to analyze the steady-state level of subunits separated under native conditions. As expected for a *bona-fide* assembly intermediate of Complex I, the 700 kDa subcomplex was detected by the two Complex I-specific antibodies (Figure 2.2, A and B). In *amc1*, the 49 and 51 kDa are detected in the subcomplex but accumulate in lower amount than in the *amc5*, *amc6* and *amc7* mutants. In *amc2*, the subcomplex is not always detected with the anti-51 kDa antibody. This low

accumulation of 51 kDa correlates with the weak detection of *in gel* activity for the *amc1* and *amc2* mutant as the 51 kDa is the subunit required for NADH dehydrogenase activity (FECKE *et al.* 1994). Intermediate assembly subcomplexes of similar size were not observed in the wildtype or in the *amc3* and *amc4* mutants. Lower amount of Complex I was evidenced in *amc4* using the anti-49 kDa antibody in extractions where the weak NADH dehydrogenase activity was also detected by in gel staining (Figure 2.2, C).

Down-accumulation of structural subunits has been observed under Complex I deficiency (SAADA *et al.* 2009). We then decided to evaluate the steady-state levels of four Complex I subunits (49 kDa, 51 kDa, TYKY and NuoA9/39 kDa) in the *amc* mutants. TYKY is a subunit of the hydrophilic arm while NuoA9 is a subunit associated with module Iα, anchored to the membrane and including the hydrophilic arm of Complex I (LAZAROU *et al.* 2009). No significant variation of the steady-state level of the NuoA9 subunit was detected in any of the mutants. This suggests that this subunit is stable even when not incorportated in Complex I. In contrast, the accumulation of TYKY and 51 kDa was severely reduced in all mutants with the exception of *amc3* (Figure 2.2, D). Detection with the anti-49 kDa subunit revealed two species and peptide competition assays demonstrated that only the upper band is specific to the 49 kDa subunit (not shown). All mutants appear to be depleted for this subunit (Figure 2.2, D). Among all the mutants, *amc2* seems the most affected for the accumulation of 51 kDa, TYKY and the 49 kDa subunits. The lower abundance of TYKY, 49 kDa and 51 kDa in *amc3* appears to correlate with the reduced level of Complex I activity in this mutant.

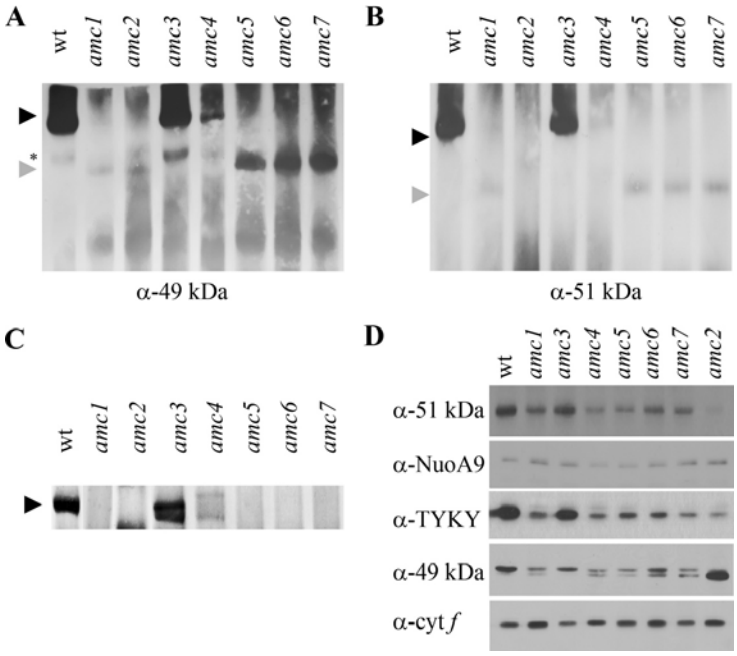

Figure 2.2. The *amc* mutants are deficient in Complex I assembly.

A and B. Immunoblot analysis of membrane fractions separated by BN-PAGE using anti-49 kDa (A) and anti-51 kDa (B) subunits. 150 µg protein of partially purified membranes were loaded per lane. The figures show the most representative blots of three independent experiments. The black and grey arrows indicate the position of mature Complex I and the 700 kDa subcomplex, respectively. The symbol (*) indicates the presence of a 49 kDa containing complex. Note that this complex is not always detected in independent extractions. **C.** BN-PAGE and in gel NBT staining of the NADH dehydrogenase activity. Only the top part of the gel is shown here to emphasize the Complex I in *amc4*. **D.** Membrane fractions were separated by SDS-PAGE and immunoblot analyses were performed using polyclonal antibodies against subunit specific peptides. The subunits are 51 kDa, NuoA9, TYKY and 49 kDa. 10 µg of total protein per lane were loaded. Antibody specificity was evaluated by peptide competition assays (not shown). Only the top band is specific for the 49 kDa subunit. An antibody against the chloroplastic protein cytochrome *f* was used as a loading control. The results are representative from at least three independent membrane extractions.

2.2.3. Impact of the amc mutations on respiratory complexes II, III and IV

To determine whether the observed phenotypes were specific to Complex I or had a broad impact on the respiratory chain in general, Complex II+III, Complex II, Complex III and Complex IV activities were measured. In a wild type strain, succinate: cytochrome *c* oxidoreductase activity (Complex II+III combined) is low for most of Complex III uses electrons derived from NADH oxidation at Complex I. All Complex I mutants showed increased levels of Complex II+III combined activity, an indication that they compensate for the defect in Complex I (Figure 2.3, A). Such a compensatory effect has already been observed in Complex I mutants of mitochondrial origin (CARDOL *et al.* 2002; REMACLE *et al.* 2001a). Individually, Complex II and Complex III were not significantly affected (Figure 2.3, B and C), suggesting a respiratory membrane rearrangement in order to enhance the electron flow entering through Complex II. On average, the augmented Complex II+III combined activity correlated with the level of reduction of Complex I in all mutants. All *amc* mutants but *amc3* displayed wildtype levels of complex IV activity (Figure 2.3, D). The *amc3* mutant exhibited 30-45 % of the wildtype Complex IV activity. However, through genetic analysis, we noted that the Complex IV defect unlike the Complex I phenotype was not inherited in the progeny (not shown). We concluded that all *amc* mutants resulted in isolated Complex I deficiency.

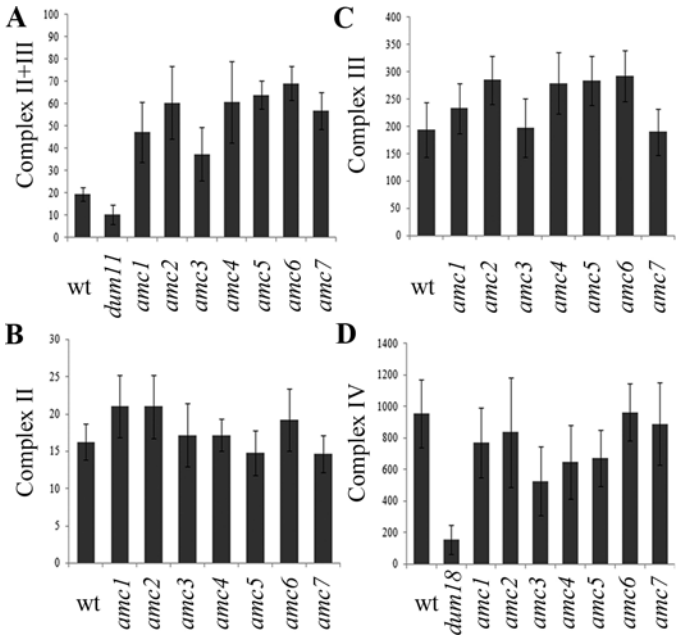

Figure 2.3. Effects of the *amc* mutations on other respiratory complexes.

A. Complexes II+III (succinate: cytochrome *c* oxidoreductase) combined activities of ten independent determinations. *dum11*, a Complex III mutant, was used as a control (DORTHU *et al.* 1992). **B.** Complex II (succinate: DCIP oxidoreductase) activity. Three independent determinations were averaged and activities expressed as nmol DCIP reduced per minute per mg of protein **C.** Complex III (DBH_2: cytochrome *c* oxidoreductase) activity. Activities were measured as nmol of cytochrome *c* reduced per minute per mg of protein. Averages from three independent measurements are shown. **D.** Complex IV (cytochrome *c* oxidase) activity. *dum18* is a complex IV mutant (REMACLE *et al.* 2001b). Average activities of ten independent determinations are expressed in nmol cytochrome *c* oxidized per min per mg protein. For A, B, C and D, error bars indicate S.E.

2.2.4. Genetic analyses reveal four AMC loci

Genetic analysis of the *amc* mutants was very difficult as most mutants showed defects in diploid/zygote formation, germination and/or spore survival.

To our knowledge, all reported mutations affecting Complex I are recessive and are loss of function mutations. In order to evaluate if the *amc* mutations were also recessive, we constructed heterozygous diploids by crossing each of the *amc* mutants with a wildtype strain of opposite mating type. All the diploids were verified for the presence of markers of both mating types by diagnostic PCR on colonies (not shown). In the heterozygote state, all *amc* mutants displayed wildtype or wildtype-like levels of Complex I activity (Figure 2.4, A). Statistical analyses showed that the lower activity observed in the *amc4/+* diploid was significantly different than that of the wildtype strain 137c (*p=0.002)*. However, as observed for the other diploids, both phenotypes, i.e. growth in the dark and Complex I assembly assessed via BN-PAGE were restored to wild type levels (not shown and Figure 2.4, B and C). Therefore, we concluded that all *amc* mutations were recessive. Progeny analyses based on the segregation of the *sid* phenotype showed that all the *amc* mutations are monogenic (not shown). In addition, the *amc1*, *amc3*, *amc4, amc6, amc7* mutations were not tagged with the antibiotic resistance cassette based on the fact that we recovered *sid* spores displaying sensitivity to the antibiotic (Table 2.2). It has already been reported that around 50% of the mutants isolated by insertional mutagenesis are not tagged with the resistance marker (DENT *et al.* 2005). For *amc5*, the antibiotic resistance (Pm^R) co-segregated with the *sid* phenotype

and we concluded that the affected locus was tagged with the insertional marker (χ^2= 51.06, n =1, p = 8.9 10^{-13}).

To establish if all *amc* mutants belonged to different complementation groups or defined alleles of the same complementation group, we performed a test of allelism. We aimed to obtain diploids between the seven *amc* mutants. Despite several attempts, we were unable to obtain diploids strains from *amc1xamc5* and *amc2x amc4* crosses. The other 19 diploid strains could be constructed and were further analyzed for Complex I function by BN-PAGE followed by *in gel* activity staining, NADH-ubiquinone activity and restoration of wildtype-like growth in the dark (Figure 2.5). Although activity levels did not always reach those of the wildtype strain, we observed restoration of a fully assembled Complex I in most diploids (Figure 2.5, A). This restoration correlated with the recovery of wildtype growth in the dark (Figure 2.5, B) and NADH dehydrogenase activity (not shown and Figure 2.5, C). Only two combinations of diploids (*amc5*x*amc7*) and (*amc1*x*amc7*) diploids showed a low level of Complex I activity (Figure 2.5, A).

The *amc5*/*amc7* diploid accumulated the same intermediate assembly subcomplex as each single mutant and displayed a *sid* phenotype (Figure 2.6, A), suggesting that *amc5* and *amc7* are allelic to each other. Alternatively, *amc5* and *amc7* could constitute a case of non-allelic non-complementation (reviewed in (HAWLEY and GILLILAND 2006). To distinguish between these two possibilities, we generated meiotic spores and analyzed them for their *sid* phenotype. All the progeny (100 meiotic products) from the *amc5* to *amc7* cross displayed a *sid* phenotype (Figure 2.6 B, left). Accordingly, the spores exhibiting a *sid* phenotype were also deficient in Complex I activity (Figure 2.6, B, right).

Strain	CI Activity	Fully assembled (950 kDa)	Subcomplex (700 kDa)	Cassette	Analysis	Progeny segregation	Monogenic	Allelism	Tagged
wt	100	++++	-						
amc1	12	-	+	iHyg	bulk	29 *sid*/42 WT	yes	no	no
amc2	4	-	+	none		(REMACLE *et al.* 2001a)	yes	no	no
amc3	41	+++	-	iHyg	bulk and tetrad	24 *sid*/36 WT	yes	no	no
amc4	14	+	-	iHyg	bulk	27 WT/32 *sid*	yes	no	no
amc5	14	-	++	iPm	bulk	51 *sid*/43 WT	yes	yes, *amc7*	yes
amc6	22	-	++	iPm	bulk	27 WT/23 *sid*	yes	no	no
amc7	14	-	++	iPm	bulk	45 *sid*/51 WT	yes	yes, *amc5*	no

Table 2.2. Phenotype and molecular genetics of *amc* mutants.

Complex I activity (CI) is indicated in % of wild type (100). ++++, ++, +,- indicate the relative levels of fully assembled complex I or 700 kDa subcomplexes.

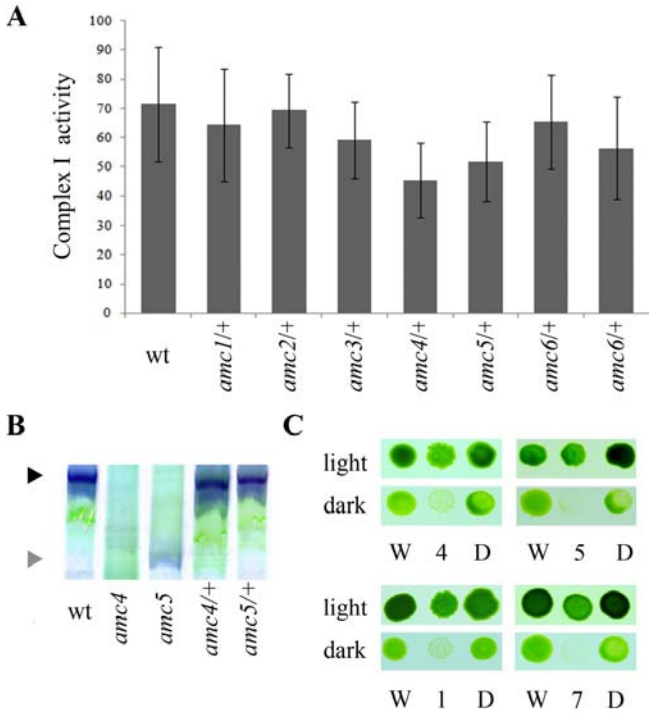

Figure 2.4. The *amc* mutations are recessive.

Heterozygous diploid strains (*amc*/+) were generated by crosses with the wildtype. **A.** Complex I (rotenone-sensitive) activities (nmol NADH oxidized per minute per mg protein). Columns represent the average of ten independent determinations, with S.E. as the error bars. **B.** BN-PAGE and *in gel* NBT staining of the NADH dehydrogenase activity shows restoration of assembly in the diploids strains. The black and grey arrows indicate the position of mature Complex I and the 700 kDa subcomplex, respectively. **C.** light/dark growth comparison of wildtype (W), *amc* mutants (cardinal) and the respective heterozygous diploids (D). Cells were plated on acetate containing medium and incubated three days in the light and five days in the dark, respectively. For B and C, only representative *amc*/+ diploids are shown. All diploids exhibit restoration of the growth in the dark and Complex I assembly phenotypes (not shown).

Thus, we concluded that *amc5* and *amc7* are alleles of the same locus. The *amc1/amc7* diploid displayed a low level of Complex I activity (Figure 2.5, A) but was restored for the growth in the dark (Figure 2.6, A) and Complex I assembly when assessed by BN-PAGE (not shown). We concluded that *amc1* and *amc7* define distinct loci.

Since we were not able to recover diploids from the *amc1xamc5* cross, we analyzed the few meiotic progeny obtained from these two mutant strains. All of the five *amc1xamc5* spores we were able to recover grew extremely slowly in the light and most of them died after a few rounds of replication. The two surviving spores were Complex I deficient (not shown). Hence, we were not able to determine allelism because of the insufficient number of spores. However, if *amc5* and *amc7* define a same locus and *amc1* and *amc7* are alleles of distinct loci, then *amc1* and *amc5* are non allelic. Similarly, because we were unable to generate *amc2xamc4* diploids, we analyzed the segregation of the meiotic spores originating from this cross. Several spores from the *amc2xamc4* progenies were recombinant and grew as wildtype in the dark (Figure 2.7, top). Wildtype levels of Complex I activity were also confirmed by enzymatic activity measurements (Figure 2.7, bottom). Therefore, we concluded that *amc2* and *amc4* belong to different complementation groups. In summary, all the seven *amc* mutants define six nuclear loci.

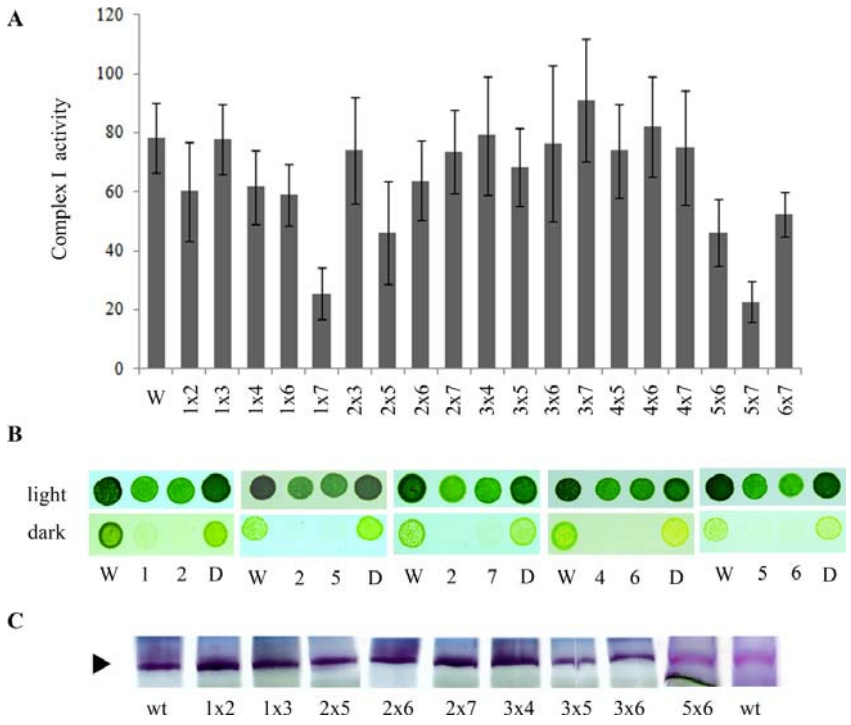

Figure 2.5. Diploid complementation analyses define alleles of *AMC* loci.

A. Complex I activity of the wildtype (wt) and the 19 diploids strains (*amc* x *amc*). For each strain, ten independent replicas were taken and the average is indicated. The error bars represent the standard error. **B.** light/dark growth comparison of wildtype (W), *amc* mutants (cardinal) and the respective heterozygous diploids (D). Cells were plated on acetate containing medium and incubated three days in the light and five days in the dark, respectively. **C.** BN-PAGE and *in gel* NBT staining of the NADH dehydrogenase activity shows restoration of assembly in the diploids strains. The black arrow indicates the position of mature Complex I. For B and C, only representative *amcxamc* diploids are shown. All diploids exhibiting restoration of the growth in the dark phenotype also showed restoration of Complex I assembly assessed by NBT staining (not shown).

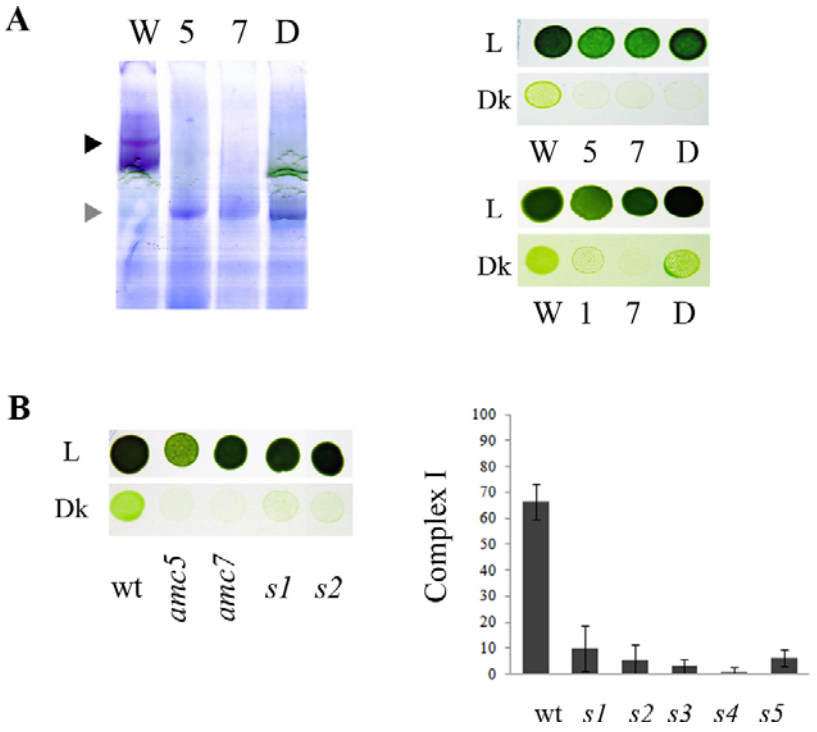

Figure 2.6. *amc5* and *amc7* define alleles of the same *AMC* locus.

A. *(left)* Detection of Complex I and the 700 kDa subcomplex via NADH dehydrogenase activity on membrane fractions separated by BN-PAGE. The black and grey arrows indicate the position of mature Complex I and the 700 kDa subcomplex, respectively**.** *(right)*: light (L)/dark (DK) growth comparison of wildtype (W), *amc1, amc5* and *amc7* mutants (cardinal) and the respective heterozygous diploids (D). Cells were plated on acetate containing medium and incubated three days in the light and five days in the dark, respectively. **B.** (*left*) Light (L) versus dark (DK) growth of wildtype (wt), *amc5*, *amc7* and two representative spores (*s1* and *s2*) from the *amc5xamc7* cross. (*right*). Complex I (rotenone-sensitive) activities (nmol NADH oxidized per minute per mg protein) of wildtype (wt) and representative spores (*s1* through *s5*) originating from the *amc5xamc7* cross. Columns represent the average of ten independent determinations, with S.E. as the error bars

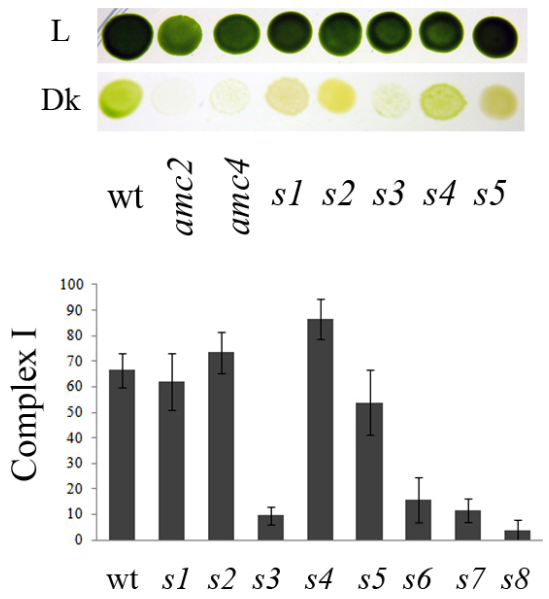

Figure 2.7. *amc2* and *amc4* define alleles of different AMC loci.

Top: Light (L) versus dark (DK) growth of wildtype (wt), *amc2*, *amc4* and several representative spores (*s1* through *s5*) from the *amc2xamc4* cross. *Bottom*: Complex I (rotenone-sensitive) activities (nmol NADH oxidized per minute per mg protein) of wildtype (wt) and representative spores (*s1* through *s8*) originating from the *amc2xamc4* cross. Columns represent the average of ten independent determinations, with S.E. as the error bars.

2.3. Discussion

The assembly of mitochondrial Complex I is an intricate process involving coordination of multiple factors to yield a holoenzyme with more than 40 subunits, one FMN molecule and 8 FeS clusters. Based on the generalized hypothesis that the assembly process is conserved overall among eukaryotes, we aimed to further dissect this process and pursued a forward genetics approach in the green alga *Chlamydomonas reinhardtii* to look for mutations (*amc*) resulting in loss of Complex I function. We took advantage of the fact that in this alga, mutations inactivating Complex I are not lethal and result in a slow growth in the dark phenotype which facilitates visual screening of mutant candidates (REMACLE *et al.* 2008). Out of approximately 50,000 mutants generated by insertional mutagenesis, we isolated six new Complex I deficient mutants, four of them resulting in the formation of intermediate assembly subcomplexes. Based on our genetic analyses, all *amc* mutations are recessive and fall into six complementation groups (Table 2.2). The finding that *amc5* and *amc7* are the only recovered allelic mutations indicates that our screen is not saturated and more *AMC* loci could be revealed through mutagenesis. Even though all *amc* mutations result in a defect in Complex I activity, they appear different when examined at the level of Complex I assembly (Table 2.2). While *amc1,2,5/7, 6* accumulated a Complex I assembly intermediate in the form of a subcomplex, *amc3* and *amc4* showed reduced level of a fully assembled complex and did not accumulate any subcomplexes. The five mutants displaying 700 kDa subcomplexes are presumably arrested in the late phases of the assembly process.

Preliminary data using an antibody against the 78 kDa subunit from *Neurospora crassa* had already suggested the presence of a 700 kDa subcomplex in *amc2* (P. Cardol and L. Boutaffala, unpublished data). Cardol *et al.* showed that the mitochondria encoded ND4 and ND5 subunits of the membrane arm are also required to proceed from the 700 kDa subcomplex towards the mature 950 kDa complex in *Chlamydomonas* (CARDOL *et al.* 2008). Solubilization analyses with increasing concentrations of dodecyl maltoside in that study suggested that the 700 kDa was loosely associated with the membrane in the *nd5* mutant (CARDOL *et al.* 2008).

Using BN-PAGE, we have explored the presence of different subunits using antibodies specific to the NADH dehydrogenase subunits (51 kDa and 49 kDa) to assess potential differences in the subcomplex composition. Our result suggest that in *amc1* and *amc2*, the 51 and 49 kDa subunits are probably weakly associated to the 700 kDa subcomplex. On the other hand, the subcomplex in the *amc5, amc6* and *amc7* mutants stably bound these two subunits. Interestingly, TYKY was always associated with the 700 kDa subcomplex in *amc1*, *amc2*, *amc5/7* and *amc6* (not shown). This result reinforces our view that 49 and 51 kDa are loosely bound to the subcomplex in *amc1* and *amc2*. Recently, important advances in modeling Complex I holoenzyme overall structure were achieved through a combination of crystallographic data from the soluble arm of *T. thermophilus* (SAZANOV and HINCHLIFFE 2006) and electron microscopy imaging in *Y. lypolitica* (CLASON *et al.* 2007; ZICKERMANN *et al.* 2003), *A. aeolicus* and *Bos taurus* (CLASON *et al.* 2009). The models derived from these structural informations place the 51 and 49 kDa on the same side of the peripheral arm with 49 kDa facing the membrane arm

and 51 kDa distal to it (see Figure 3 in (ZICKERMANN *et al.* 2009) or Figure 1.2). The instability of the 51 and 49 kDa subunits binding to the ~700 kDa intermediate in *amc1* and *amc2* but not in *amc5/7* and *amc6* suggests that the mutations produce a change in the local environments. Overall, the accumulation of the subcomplex indicates that *amc1, 2, 5/7* and *6* are disrupted for the assembly of the membrane arm of Complex I (Figure 2.8). The *amc3* and *amc4* mutants appear to accumulate lower amount of a wildtype Complex I and are probably not deficient for the assembly process per se but rather for the stability of the enzyme. This instability appears more pronounced in the *amc4* mutant than in presence of the *amc3* mutation.

The identity of the *AMC* gene products revealed through our mutant screen is unknown and can only be speculated upon at the present time. One possibility is that the *AMC* loci correspond to genes encoding *bona fide* subunits of the Complex. Indeed, mutations in the structural subunits of Complex I are expected to be recovered in our screen for mutants displaying a Complex I defect. Alternatively, *AMC* loci could encode Complex I assembly factors that do not remain in the mature Complex I but nevertheless are recruited for its maturation. Orthologs for well characterized assembly factors, NDUFAF3 (SAADA *et al.* 2009), CIA30 (DUNNING *et al.* 2007), C20orf7 (GERARDS *et al.* 2009; SUGIANA *et al.* 2008), Ind1 (BYCH *et al.* 2008; SHEFTEL *et al.* 2009) and candidate assembly factors (C2orf56, PhyH, C10orf65) (PAGLIARINI *et al.* 2008) are present in the predicted proteome of *Chlamydomonas*. In *Arabidopsis*, L-galactono-1,4-lactone dehydrogenase (GLDH), an enzyme involved in ascorbate biosynthesis has also

been identified as a Complex I assembly factor (PINEAU *et al.* 2008). This is a plant specific Complex I assembly factor that is also conserved in *Chlamydomonas*.

To our knowledge, this is the first report of a mutagenesis screen yielding mutants with isolated Complex I deficiency. The variety in assembly defects in the *amc* mutants suggests that the corresponding gene products (either structural subunits or assembly factors) act at different steps of the assembly process. This further stresses the value of *Chlamydomonas* as an experimental model to address the question of Complex I assembly. This question has now received considerable attention as most of Complex I-linked diseases in humans still have no molecular explanation (LAZAROU *et al.* 2009).

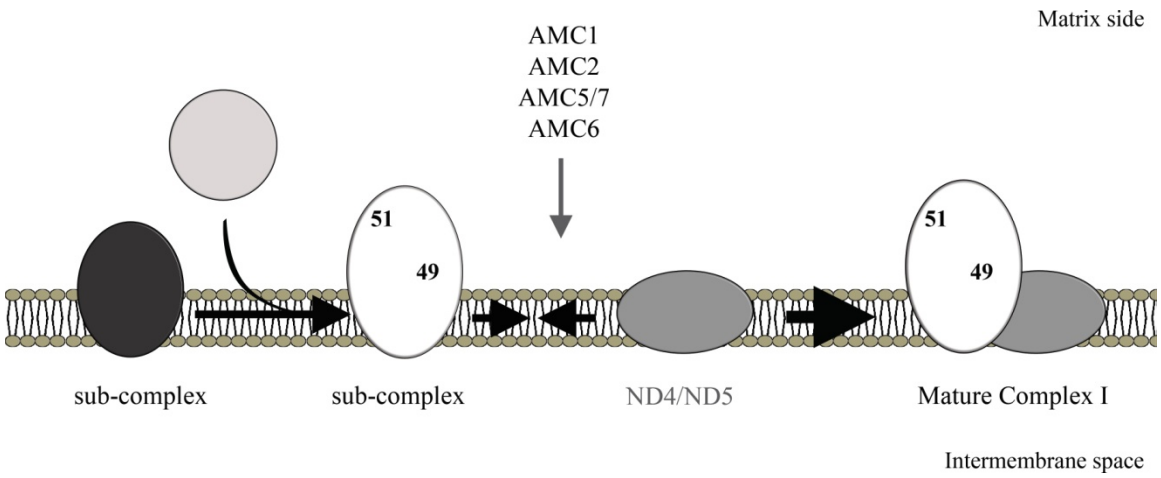

Figure 2.8. Schematic representation of the site of action of the AMC gene products during the assembly process.

The black oval and the grey circle symbolize assembly intermediates. The membrane and soluble arms of Complex I are represented by light and dark grey ovals, respectively. The 49-kDa subunit (49) is positioned relative to the membrane arm according to the model described in ref. (ZICKERMANN *et al.* 2003). The 51-kDa (51) subunits is positioned relative to the 49-kDa (49) subunits following the model structure from (SAZANOV and HINCHLIFFE 2006). AMC1, 2, 5/7 and 6 are probably involved in the assembly of the membrane arm or in connecting the membrane and soluble arms of Complex I.

2.4. Experimental procedures

2.4.1. Strains and culture conditions

Strains were grown at 22–25 °C in TAP or arginine supplemented TAP liquid or solid medium (HARRIS 1989) under continuous light (50 μmol/m^2/s) for *amc* and wild type strains as described in (HOWE *et al.* 1992). Wildtype strains 3A+ and 4C- (*arg7-8*) of opposite mating types were used for transformation (J. D. Rochaix, University of Geneva, Switzerland) and strains $137c^+$ and $137c^-$ were used for backcrosses. Strain *dn26* 169 (*mt-*) (REMACLE *et al.* 2001a) and a mt^+ derivative, renamed here as *amc2*, were used for crosses and as Complex I deficient controls.

2.4.2. Insertional mutagenesis and identification of the amc mutants

Autolysin-treated 3A+ (*mt^+ arg7-8*) or 4C- (*mt^- arg7-8*) cells were transformed by electroporation with 100 ng of either a hygromycin B (iHyg) or paromomycin (iPm) resistance cassette as described in (SHIMOGAWARA *et al.* 1998). Both cassettes were amplified by PCR from the pHyg3 (BERTHOLD *et al.* 2002) or pSL18 (POLLOCK *et al.* 2003) plasmids and carry *Chlamydomonas* endogenous promoters and terminators in addition to a *Chlamydomonas* intron. Oligonucleotides Aph7-F (TCGATA TCAAGCTTCTTTCTTGC) and Aph7-R (AAGCTTCCATGGGATGACG), specific for the beta-tubulin promoter and *RBCS2* terminator, were used for amplification of the 1743 bp iHyg cassette. The amplification of the iPm cassette was carried out with Aph8-F2 (TCAGGCAGACGGGCAGGTG) and Aph8-R (TCAGGCAGACGGGCAGG TG) to

produce a 1848 bp product which included part of the *RBSC2* promoter, *HSP70* promoter and the *RBSC2* terminator. Transformants were selected on solid TAP +arginine media containing 25 μg/ml of either hygromycin B or paromomycin in the light. After 7-10 day incubation under continuous light (50 μmol/m^2/s), primary transformants were transferred individually to 96 well plates and grown in selective liquid media. Individual colonies were replica plated on omnitrays containing solid TAP+arginine medium and incubated in the dark and in the light for seven additional days before scoring. Transformants showing slow growth in the dark, typically having very small colonies, were subcloned to single colony and retained for further analyses.

2.4.3. Molecular genetic analysis of the amc mutants

Gamete formation was induced by nitrogen deprivation as previously described (HARRIS 1989). In some cases, 50 mM dibutyryl-cAMP (Sigma) was added to stimulate cell-wall release and mating structure activation. To isolate vegetative diploids, the mating mixture was directly plated on selective media and incubated in the light. Individual colonies were subcloned and verified by diagnostic PCR for the presence of mating type specific genes (WERNER 1998).

2.4.4. Measurement of respiratory enzyme activities

Respiratory activities were measured as previously described (REMACLE *et al.* 2001a; REMACLE *et al.* 2004) using partially purified membranes extracted from two- to three-day old cultures. Specific activities were calculated using extinction coefficients $\varepsilon_{340\ nm}$ = 6.22 mM^{-1} cm^{-1} for Complex I, $\varepsilon_{550\ nm}$ = 19.6 mM^{-1} cm^{-1} for Complex II+III and

Complex IV, with or without complex-specific inhibitors, 15 μM rotenone, 7.5 μM myxothiazol and 1 mM KCN, respectively. NADH: ferricyanide oxidoreductase was measured as described in (CARDOL *et al.* 2002) and calculated using $\varepsilon_{420\ nm} = 1.05\ mM^{-1}\ cm^{-1}$. Complex II (succinate: DCIP oxidoreductase) activity was determined from partially purified membranes incubated with 20 mM sodium succinate, 10 mM MOPS-KOH, pH 7.4 for five minutes followed by addition of 74 μM 2,6 dichloroindophenol (DCIP). The reaction was inhibited with 8 mM malonate. Complex III (cytochrome *c*: DBH_2 oxidoreductase) was measured from partially purified membranes in 10 mM MOPS-KOH, pH 7.4, 0.2% Tween 20, 1 mM KCN, 0.7 mg horse heart cytochrome *c* (C2506, Sigma) with addition of 60 μM decylubiquinone (DBH_2). The reaction was inhibited with 7.5 μM myxothiazol. Activities were determined using extinction coefficients $\varepsilon_{600\ nm} = 21\ mM^{-1}\ cm^{-1}$ for Complex II and $\varepsilon_{550\ nm}$ of $19.6\ mM^{-1}\ cm^{-1}$ for Complex III, respectively.

2.4.5. Antibody production

Protein A purified polyclonal antibodies directed against Complex I subunit-specific peptides were custom synthesized in rabbits by GeneScript (Piscataway, NJ) using the following peptide antigens: Nuo7 (49-kDa), CGIDWDLRKTQPYDA; Nuo6 (51-kDa), SLEGKQGKPRLKPPC; Nuo8 (TYKY), YASDWENDPTFKRTC; NuoA9 (39 kDa), IRNDDDIKRAISRSC.

2.4.6. Protein extraction, SDS-PAGE and immunoblot analyses

Total protein was isolated from two-day old light-grown plates using the freeze/thaw method (HOWE and MERCHANT 1992) . SDS-PAGE was performed using standard protocols (SAMBROOK *et al.* 1989). To assess antibody specificity, protein extracts were competed with the peptides used to generate the polyclonal antibodies (HOWE and MERCHANT 1992). A polyclonal antibody directed against the plastid protein cytochrome *f* was used as a loading control.

*2.4.7. BN-PAGE and i*n *gel-activity*

Separation of Complexes and subcomplexes was done by BN-PAGE (SCHÄGGER and VON JAGOW 1991) using 3-12% gels. Partially purified membranes were obtained as described for Complex IV activity determination. Membranes were partially solubilized by adding 0.5 volumes of 750 mM aminocaproic acid, 0.5 mM EDTA, 50 mM BisTris and 1% w/v sodium n-dodecyl-β-D-malto*sid*e, pH 7.0 before adding 0.1 volume of loading buffer (750 mM aminocaproic acid, 5% Coomasie Blue R-250). For in gel NADH dehydrogenase activity, gels were incubated in 20 mM MOPS buffer, pH 8.0 containing 122 μM p-nitro blue tetrazolium chloride (NBT, Fisher Scientific) and 188 μM NADH (Amresco).

2.5. Supplementary infomation

This section contains additional preliminary information that complements but is not included in the body of the Chapter.

2.5.1. Nature of the 700 kDa subcomplex

The 700 kDa subcomplex that accumulates in several *amc* mutants is similar to the 700 kDa subcomplex previously observed in *Chlamydomonas* (CARDOL *et al.* 2008; CARDOL *et al.* 2006; CARDOL *et al.* 2002; REMACLE *et al.* 2006). Peptides corresponding to the 49, 51 kDa and TYKY subunits have been detected by mass spectrometry analysis of the 700 kDa subcomplex in the *nd5* mutant (CARDOL *et al.* 2008) (Figure 2.9), and by BN-PAGE/immunoblot in all the *amc* mutants. In contrast with *Chlamydomonas,* the 830 kDa subcomplex in humans, presumably equivalent to the 700 kDa subcomplex described here, does not appear to include the NDUFV1/51-kDa subunit, which is believed to be incorporated at a later step after attachment of the membrane arm (LAZAROU *et al.* 2007; VOGEL *et al.* 2007c). Mass spectrometry composition analysis of the 700 kDa subcomplex in the *nd5* mutant in *Chlamydomonas* (CARDOL *et al.* 2008) revealed that some the detected subunits were also present in a 650 kDa subcomplex found in muscle mitochondria from patients with Complex I deficiency (ANTONICKA *et al.* 2003): NuoA9 (39 kDa, NDUFA9), Nuo7 (49 kDa, NDUFS2), Nuo5 (24 kDa, NDUFV2), Nuo9 (30 kDa, NDUFS3), Nuo10 (PSST, NDUFS7), also suggesting that these two subcomplexes could be equivalent. Unfortunately, there is not enough information available on the composition of the 830 kDa and 650 kDa subcomplexes.

Interestingly, the 700 kDa subcomplex was detected in *amc1* and *amc2* mitochondrial preparations using an antibody against the the Nuo17 (ESSS) accessory subunit (not shown). In previous studies, this subunit was identified as part of subcomplex Iβ (CARROLL *et al.* 2003; HIRST *et al.* 2003) using detergent fractionation and so far has not been associated with subcomplex Iα, presumed to be represented by the 700 kDa subcomplex in *Chlamydomonas* (CARDOL *et al.* 2008). Although Nuo17 was not previously found in the 700 kDa subcomplex by mass spectrometry, other subunits that are believed to form part of the interface between subcomplexes Iα and Iβ were found. Consistent with the need for Nuo17 in the assembly of the 700 kDa subcomplex, an ESSS Chinese Hamster cell mutant line was completely depleted from NADH dehydrogenase activity (POTLURI *et al.* 2004). However, because the authors did not pursue immunoblot analyses on samples separated under native conditions, the presence of a subcomplex in the absence of the ESSS subunit cannot be ruled out. The carbonic anhydrase subunit (not shown) was also detected in the mature complex and in the 700-kDa subcomplex of *amc1, 2, 5/7* and *6*, in agreement with its finding in the 700 kDa subcomplex in the *nd5* mutant (CARDOL *et al.* 2008).

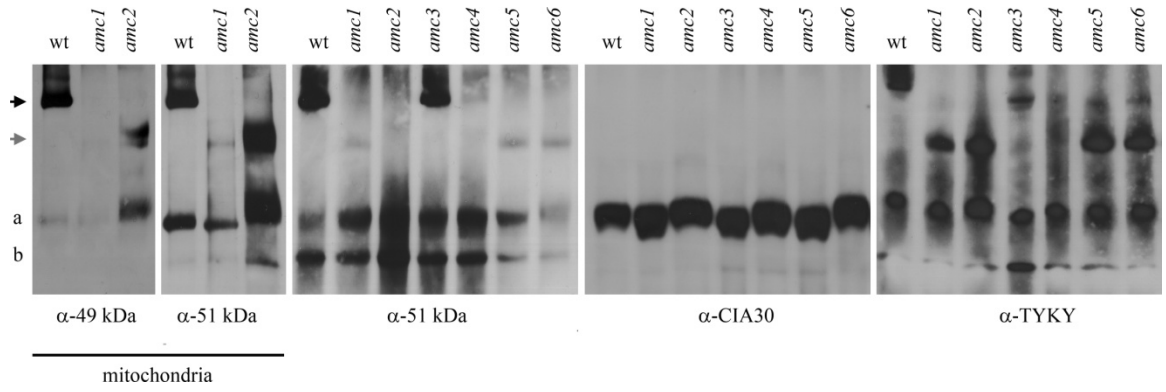

Figure 2.9. Additional subcomplexes are apparently detected in wildtype and mutant strains.

2.5.2. Additional subcomplexes are detected with the 49-kDa, 51-kDa subunit and CIA30 antibodies

In addition to the 700 kDa subcomplex observed in *amc1*, *amc2*, *amc5/7* and *amc6*, two other bands of lower molecular weight were detected with TYKY, 51 and 49-kDa subunit antibodies in the membrane extracts of the wildtype and all mutant strains (Figure 2.9, bands *a*, *b*). The bands are likely to be subcomplexes containing Complex I subunits, as they were also found in mitochondrial extracts. A band of size similar to band *a* was also detected in membrane extracts using an antibody against the CIA30 assembly factor. This antibody was generated using a *Chlamydomonas* CIA30 synthetic peptide (GeneScript, Piscataway, NJ) and was shown to be specific by competition assay (data not shown). It also recognizes a purified recombinant form of CIA30. Because the antibody against CIA30 also detected non specific bands in immunoblots against

membrane proteins separated under denaturing conditions it was not clear if the bands shown here correspond to Complex I-related subcomplexes. CIA30 was associated with 440-500 kDa and 600-800 kDa subcomplexes in fibroblast-derived mitochondria but not with the 950 kDa mature Complex I (DUNNING *et al.* 2007). On the other hand, association of NDUFAF1 (CIA30) with high molecular weight subcomplexes was still observed in fibroblasts from patients with mutations in Complex I subunits and in the mitochondrial translation Elongation Factor G1 (EFG-1), both resulting in almost complete absence of Complex I, although with less intensity (VOGEL *et al.* 2007d). Based on this lack of correlation, the authors suggested that these two subcomplexes may be unrelated to Complex I and represent other associations of CIA30. However, the study did not use any antibody equivalent to the ones used in the BN-PAGE immunoblots shown here. Association of CIA30 with Complex I subunits has been clearly demonstrated (DUNNING *et al.* 2007) by coimmunoprecipitation. Pulse-chase labeling of mitochondria encoded subunits followed by incubation in Sepharose columns coupled to CIA30 antibody resulted in the enrichment of membrane-associated subunits ND1, ND2 and ND3 at early chase times. ND1 was also identified by coimmunoprecipitation analyses with CIA30, as well as some nuclear encoded subunits -NuoA9 (NDUFA9), Nuo9 (NDUFS3), Nuo10 (NDUFS7)- (DUNNING *et al.* 2007). Based on the relative abundance of the 830 and 460 kDa bands, these associations most likely represent the 460 kDa subcomplex, which would preced the assembly of the 830 kDa subcomplex (LAZAROU *et al.* 2007). ND6 subunit was also found in the 440 and 830 kDa subcomplexes in another study (LAZAROU *et al.* 2007). Therefore, based on its similar

composition to the 460 kDa subcomplex, it is likely that *Chlamydomonas* subcomplex *a* detected with the 51 kDa, 49 kDa, CIA30 and TYKY antibodies is a *bona fide* subcomplex of Complex I, possibly also corresponding to the 460 kDa subcomplex observed in association with CIA30 (DUNNING *et al.* 2007). Even though in *Chlamydomonas* immunoblots CIA30 was not found associated with the 700 kDa subcomplex (Figure 2.9), in the paper by Dunning *et al.* the intensity of the CIA30 band associated with the 830 kDa subcomplex was significantly low compared to the intensity of the 460 kDa band, suggesting that most of CIA30 is not associated with the 830 kDa band. A minor band (*b*) of around 400 kDa was detected in both mitochondria and partially purified membranes with the 51 kDa subunit and TYKY (only analyzed in partially purified membranes) antibodies, but not with the 49-kDa antibody, which could correspond to the 480 kDa band observed in a patient with a mutation in NDUSF4 (18 kDa) (LAZAROU *et al.* 2007). Although the bands observed here accumulated as subcomplexes that seem to be related to Complex I assembly, the results presented here are only preliminary, and further analyses have to be pursued. Composition analyses combining two-dimensional electrophoresis and mass spectrometry in addition to genetic studies will be crucial to characterize these subcomplexes and their role in Complex I assembly. The detection of non-specific bands highlights the need to obtain a CIA30 mutant to further verify the specificity of this antibody in *Chlamydomonas* extracts, and to determine if the detected subcomplex is indeed related to CIA30.

2.5.3. Amc3 progeny displays different levels of Complex I activity

Visual scoring of *amc3x*wt progeny based on the *sid* phenotype showed a large degree of variation that was separated in three classes: class I, corresponding to wildtype-like spores; class II, corresponding to spores with *sid* phenotype similar to that of the original *amc3* mutant; and class III, spores that had a more pronounced slow growth in the dark phenotype. Together, classes II and III constituted 50% of the progeny. The combined bulk and tetrad segregation values for this cross are indicated in Table 2.2. To further elucidate if this variation was caused by a second-site mutation, we focused in the ten complete tetrads obtained from this cross. Each tetrad contained either a class II and a class III spore, two class II spores or two class III spores; the other two progeny were wildtype (class I). Complex I and IV activities were measured for the progeny of two tetrads containing a class II and a class III spore (Figure 2.10, top). Complex I activity correlated with the degree of *sid* phenotype. That is, class II spores had intermediate levels of Complex I activity while class III spores were totally depleted of Complex I activity. Because a mild effect in Complex IV was observed in the *amc3* parental strain (Figure 2.3), we wondered if the partial effect in Complex I activity (classII) was cosegregating with Complex IV deficiency and if we would be able to observe a more severe Complex IV defect in the class III spores. Complex I and Complex IV activity levels were not associated to each other and it is apparent that Complex IV deficiency segregates independently of Complex I. However, a more thorough analysis, including a

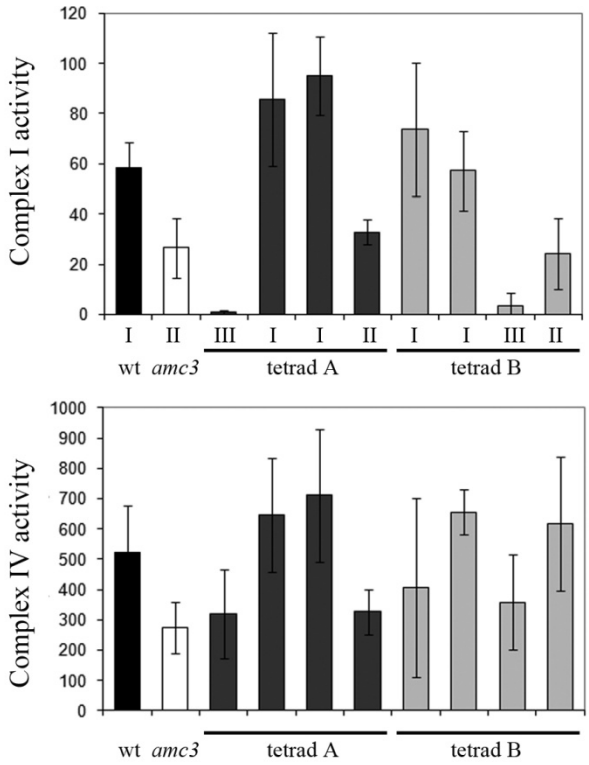

Figure 2.10. Progeny segregation of *amc3* unmasks two different levels of Complex I deficiency.

Complex I and IV activities were measured from partially purified membranes of wt, *amc3* and the eight spores originated from two tetrads (A and B). I, II and III indicate the classes defined on the basis of dark growth phenotype. Class I corresponds to wildtype, Class II indicates a *sid* phenotype similar to the parental *amc3* and Class III indicates a strong *sid* phenotype. The bars indicate the average of three independent determinations with S.E. indicated by the error bars. Activity units are indicated in nmol substrate oxidized per minute per mg of protein, NADH for Complex I and cytochrome *c* for Complex IV.

larger number of spores should follow to determine if Complex IV partial defect constitutes a second site mutation.

What causes the atypical *amc3* Complex I segregation pattern? It is likely that the original *amc3* is a monogenic mutation, based on the 2:2 segregation values. However, a polymorphism present in the wildtype strain 137c^{-} (different from the mutant background strain 3A+) could result in the enhancement of the *amc3* phenotype when present in the same strain as seen in Figure 2.10. However, this polymorphism alone would not have an effect *per se.* Analysis of the progeny of both Class II and Class III spores would help understand the nature of this segregation pattern. First, the progeny of one of the class II spore in a cross with 137c strain should produce a similar pattern as before with spores segregating 2:1:1 for Class I: Class II: Class III. Second, the progeny of a class II spore with 3A+ should segregate 2:2 for Class I: Class II. Third, progeny of a class III spore with 137c should segregate 2:2 Class I: Class III. Finally, progeny of a class III spore crossed with 3A+ should segregate 2:1:1 for class I: class II: class III. Ultimately, identification of the *AMC3* locus will provide clues to understand this complex segregation pattern.

CHAPTER 3

MOLECULAR IDENTIFICATION OF *AMC2* AND *AMC5*

3.1. Introduction

The initial studies in the assembly of Complex I in *Chlamydomonas reinhardtii* were directed towards the generation of mutants in structural subunits encoded by the mitochondrial genome. Such mutagenesis experiments have been carried out using the chemical mutagens acriflavine or ethidium bromide (REMACLE *et al.* 2001b), which produce small insertions or deletions and substitutions. Most of the respiratory mutants generated by those studies displayed mitochondrial inheritance (*dum, dark uniparental transmission by the minus parent*). One of them showed slow growth in the dark associated with Complex I deficiency and nuclear inheritance; hence, its name *dn26* (*dark +/- phenotype, nuclear inheritance*). In Chapter 2, this mutant was renamed *amc2* to agree with the nomenclature followed by the newly found insertional mutants. *amc2* accumulates an unstable 700 kDa subcomplex which does not proceed to a mature form of Complex I. A similar subcomplex was found in for the *amc1*, *amc5/7* and *amc6* mutations. In Chapter 2 we concluded that *amc2* was distinct from *amc1* and *amc5* based

on diploid complementation analyses. We found that *amc1xamc7* diploid was able to restore the assembly of a mature complex and growth in the dark, but failed to restore wildtype levels of activity. Based on the growth and assembly complementation, we concluded that *amc1* and *amc7* constituted mutations of different genes. We also showed that *amc5* and *amc7* were allelic to each other, based on the absence of recombination between the two mutations.

Because the inability to form a fully assembled Complex I can result either from mutations in structural subunits or *yet-to-be-identified* assembly factors, we decided to determine the molecular identity of this mutant. Accumulation of the 700 kDa subcomplex is diagnostic of an impairment in the assembly of the membrane arm (CARDOL *et al.* 2008; REMACLE *et al.* 2006), so mutations in subunits previously found or predicted to be in the region connecting the 700 kDa subcomplex and the membrane arm are also likely to disrupt the assembly of the membrane arm and display a subcomplex accumulation. Some preliminary sequencing evidence indicated that most of the subunits predicted to be in the periphery of the membrane in the subcomplex Iα were unaffected in the *amc2* mutant (Layla Boutaffala, unpublished data). Therefore, a derived hypothesis is that *amc2* constituted a mutation in a gene encoding a novel **A**SSEMBLY OF **M**ITOCHONDRIAL **C**OMPLEX I (AMC2) factor. On the same basis, *amc1* and *amc5/7* could carry mutations in structural subunits. Therefore, we pursued different strategies to understand the molecular identity of these mutations.

3.2. Results

3.2.1. Mapping of amc2 mutation to chromosome 10: AMC2, a new assembly factor?

The most direct approach for complementing the *amc2* mutation was to transform an arginine auxotroph mutant strain with the indexed *Chlamydomonas* cosmid genomic library generated by Dr. Jean David Rochaix's laboratory (U. of Geneva, Switzerland). Unfortunately, the *amc2* mutant had extremely low transformation efficiency so that this approach was not viable, even after optimizing the transformation conditions. In general all *amc* mutations showed very low or even null transformation efficiency, regardless of the transformation method employed (electroporation, glass beads, biolistics). A cell wall deficient background was tried for *amc1* and *amc2*, also unsuccesfuly. We do not know to this point what could be the cause of the lack of transformability.

Therefore, we decided to pursue a second strategy, molecular mapping starting with the PCR mapping kit available from the *Chlamydomonas* Stock Center (RYMARQUIS *et al.* 2005). For this, *amc2* was crossed to the highly polymorphic strain S1-D2 and 54 independent *amc2* spores were manually dissected from 54 tetrads. The *amc2* spores were selected on the basis of their *sid* phenotype (Figure 3.1).

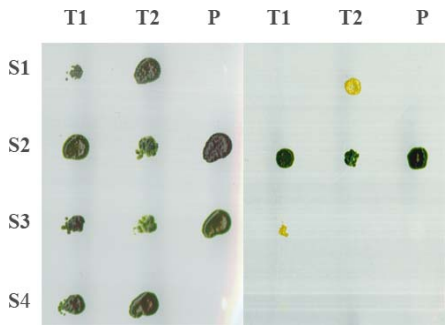

Figure 3.1. Tetrad segregation for *AMC2* mapping.

Individual colonies derived from the four spores (S1-S4) of two independent tetrads (T1-T2) are shown. The strains were grown during seven days under light, mixotrophic (*left panel*) or dark, heterotrophic (*right panel*) conditions. The column labeled P indicates the two parental strains: wt: S1-D2 on top, and the *amc2* mutant on the bottom.

Linkage analyses were done with Mapmaker 3.0 (see Experimental Procedures for more details). Markers *KAT1* and *CNA83* in chromosome 10 (LGX) had the highest LOD scores (3.31 and 2.95, respectively) among the group of markers studied, followed by *PF25* (LGX, LOD score = 1.71) and *MBB1* (LGIX, LOD score = 1.71). Neither *PPX1* nor *PSBO*, the two other markers from LGIX, had a LOD score above 0.50. Based on these preliminary mapping it is very likely that *AMC2* is located in LGX. This chromosome contains three genes encoding for Complex I subunits: *NUO6*, *NUOA9* and *NDUFA1*. Based on the recombination values, *AMC2* lies 26.2 and 27.5 cM apart from *KAT1* and *CNA83* markers, enclosing only *NUOA9* locus. The low LOD score value observed for *PF25* marker can be explained by the fact that it is located on the other side

of the centromeric region, in a distal position. Because *NDUFA1* is proximal to *PF25*, it is highly unlikely to cause the *amc2* phenotype. To refine the position of *AMC2* within LGX and to determine whether *NUOA9* and *amc2* mapped to the same locus, additional markers: *PF6* (AAK38270.1; sequence tagged site, STS), *GP441* (e_gwW.8.206.1, single nucleotide polymorphism, SNP), and *c226* and *c225* (STS), *c1982* (dCAP), were used. Primers *c226, c225* and *c1982* were designed in Dr. D. Stern's laboratory (Boyce Thomsom Institute for Plant Research, Ithaca, NY) but not tested so far. Marker *PF6* lies within the *NUOA9* coding region, so, lack of recombination between the *AMC2* and *PF6* would be suggestive that *amc2* is a mutation of *NUOA9*. In the final map, *AMC2* was located in a narrowed region of around 315 kb, 5.9 cM apart from marker *c225* and 16.6 cM from marker *c1982*, distant from *PF6/NUOA9*. Therefore, *AMC2* and *NUOA9* comprise different loci. Because no other subunits are present in the region framed by markers *c225* and *c1982*, *AMC2* has to be a non-structural factor involved in assembly. Based on the results from Chapter 2, this factor should be needed to proceed from the 700-kDa subcomplex to a mature Complex I by attachment of subunits in subcomplex Iβ.

In the last assembly of *Chlamydomonas* genome the 350 kb region contains 43 predicted genes. Six of them, predicted to be mitochondrial proteins (au5.g284_t1, au.g296t_1, au.g300t_1, au.g307t_1, au.g317t_1 and au.g321t_1) but only two of them with high probability –au.g296t_1 and au.g321t_1. Two other genes are predicted cyclin-dependent kinases (CDKs, au.g291t_1, au.g293t_1). CDKs have been long proposed to be important for Complex I function. For instance, although it is not the only way to regulate its function, human Cdk2 can activate Sp1 zinc-finger transcription factor

(BANCHIO *et al.* 2004), which in turn binds to the *NDUFV1* (51-kDa subunit) and *NDUFV2* (49-kDa subunit) promoters to activate their expression (BEN-SHACHAR and KARRY 2007). Also, because targeting to more than one organelle can occur, some genes encoding proteins with predicted plastid localization were sequenced. In addition to these, sequencing of the coding regions of some other genes mapping close to marker *GP441* was pursued.

	KAT	***c226***	***c225***	***gp441***	***AMC2***	***c1982***	***PF6***	***CNA83***
c226	30.1							
	2.50							
c225	36.9	7.9						
	1.57	*9.26*						
gp441	26.3	9.7	5.9					
	3.31	*8.51*	*10.40*					
AMC2	**26.3**	**9.7**	**5.9**	**0.0**				
	3.31	***8.51***	***10.40***	***16.26***				
c1982	49.8	10.1	14.4	16.6	**16.6**			
	0.63	*7.99*	*6.26*	*5.50*	***5.50***			
PF6	51.0	12.2	16.9	18.0	**18.0**	6.3		
	0.61	*7.08*	*5.28*	*5.25*	***5.25***	*9.58*		
CNA83	42.6	26.1	32.5	27.5	**27.5**	19.8	14.4	
	1.09	*3.09*	*2.02*	*2.95*	***2.95***	*4.39*	*6.26*	
PF25	39.1	33.7	41.5	35.9	**35.9**	32.5	21.2	26.1
	1.38	*1.94*	*1.13*	*1.71*	***1.71***	*2.02*	*4.18*	*3.09*

Table 3.1. Final genetic distances and LOD score table of markers in Chromosome 10. The double entry table indicates the genetic distances (in cM, top values) for each pair of markers. LOD-score values (bottom) are indicated in italics. Genetic distances and values for *AMC2* locus are indicated in bold.

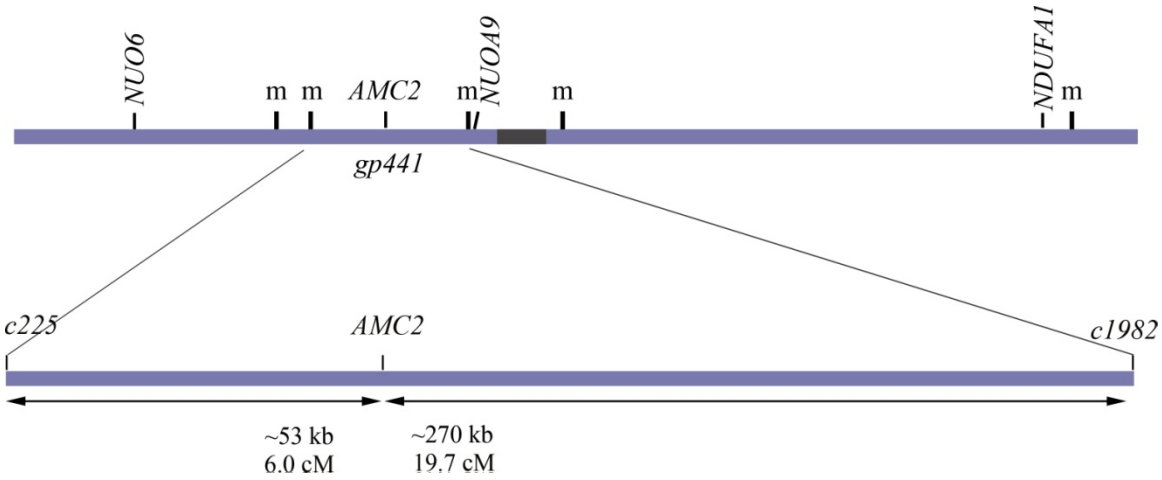

Figure 3.2. PCR-based mapping of the *AMC2* locus

Crude mapping was done using a defined set of PCR markers (m) available at the Chlamydomonas Resource Center. Additional available marker sequences were tested for the amplification of polymorphic bands. S indicates the location of known Complex I subunits in Chromosome 10. The grey band shows the position of the centromere. Markers *c225, gp441* and *c1982* are the closest to the *AMC2* locus based on the data.

Gene ID	genomic (bp)	TargetP	Description	Sequencing		Sequencing results
				bp from ATG	bp from STOP	
au5.g284	3844	M (0.555)	Sulphatase Alkaline-phosphatase-like, core domain	-505	+ 984	wt
au5.g290	2044	C (0.785)	similar to putative drought-induced protein in *Oryza sativa* (*japonica* cultivar-group); Fb25 of *Gossypium barbadense* - DnaJ-class molecular chaperone with C-terminal Zn finger domain	-270	+ 530	wt
au5.g291	8978		Serine/threonine protein kinase-related	-99	+ 1471	wt
au5.g292	1638	C (0.556)	COG0539, RpsA, Ribosomal protein S1	-431	+ 714	wt
au5.g293	8498		Serine/threonine protein kinase-related	-362	+ 815	wt
au5.g294	13144		hypothetical protein	-1568	+254	95% complete
au5.g295	7768		hypothetical protein	-200	+ 573	wt
au5.g296	4354	M (0.936)		-174	+ 72	wt
au5.g297	9238		hypothetical protein ankyrin domain	-880	-1151	wt
au5.g299	5924		Voltage-dependent potassium channel	-59	+ 886	wt
au5.g300	12678	M (0.519)	Alkaline-phosphatase-like, core domain Sulphatase	-365	-5965	50 % complete
au5.g307	3244	M (0.664)	hypothetical protein ankyrin domain	-219	+ 429	wt
au5.g317	5804	M (0.576)	WD40-repeat	-110	+685	wt
au5.g321	3734	M (0.902)	Putative RNA methylase, Bacterial Fmu (Sun)/eukaryotic nucleolar NOL1/Nop2p, conserved site	-1866	+440	wt

Table 3.2. Sequenced genes in the *AMC2* locus region

None of the genes sequenced to this point contains mutations in the coding regions (Table 3.2). At this point, sequences for two of the tested genes are incomplete: au5.g294 and au5.g300. No specific sequence could be obtained from the missing regions. Indeed, the whole region has an extremely high GC content, thus rendering difficult the PCR amplification attempts. au5.g300 contained numerous $(CA)_n$ and $(GT)_n$ repeats and palindromic sequences. au5.g294 also contained numerous repeats, typically $(GCC)_4$ as well as palindromic sequences. In several cases, we were able to recover long sequences beyond the predicted ATG and stop codons. In *Chlamydomonas*, promoter regions tend to be short, usually regulatory elements are within the first hundred base pairs. (Dr. Sabeeha Merchant, personal communication). However, so far there has not been a systematic characterization of promoter regions in this organism.

Several Complex I assembly factors have been predicted based on substractive phylogenetic analyses of mitochondrial proteins (PAGLIARINI *et al.* 2008), see Table 1.2. Also, other genes involved in Complex I assembly have been experimentally identified in plants, fungi and humans (see section 1.2.2.3). *In silico* analyses of the predicted genes in the 350 kb region did not identify any of them as homolog or functionally related to the currently proposed assembly factors. Because the *amc2* mutation lies somewhere within this region, we can conclude that the *AMC2* gene is a novel factor involved in Complex I assembly. Alternatively, *amc2* (as well as other *amc* loci for this matter) could also be mutants in genes controlling the expression of mitochondrial ND subunits, for instance translational activators. The identification of the *AMC2* gene is crucial to further unveil

its function in the context of Complex I assembly and its degree of conservation in eukaryotes.

3.2.2. Sequencing of subunits in the amc1 mutant

As previously mentioned, the molecular identity of the *amc* mutants is currently unknown. Attempts to transform *amc1* and other *amc* mutants yielded an extremely low number of transformants thus, preventing the use of a *Chlamydomonas* indexed cosmid genomic library to complement the mutations. Additional efforts to cross *amc1* with a polymorphic strain failed to produce sufficient amount of progeny to make molecular mapping feasible. We reasoned that the *amc1* subcomplex accumulation could be caused by a mutation in one of the subunits that are incorporated at the later steps of assembly. Mutations in the mitochondrially encoded ND4 and ND5 subunits, which are subunits of module Iβ incorporated in the last assembly step, result in the accumulation of the 700 kDa subcomplex (CARDOL *et al.* 2008; REMACLE *et al.* 2006). Because *amc1* is a mutant of nuclear origin, we decided to sequence nuclear-encoded subunit genes that are predicted to form part of the interface between subcomplexes Iα and Iβ and whose mutation could result in the formation of a 700 kDa assembly intermediate which is unable to bind ND4 and ND5 (Table 3.3). To the extent of our results, none of these subunits carries a mutation in the *amc1* mutant. Therefore, it is likely that the *AMC1* locus encodes an assembly factor. However, mutations in the promoter region cannot be discarded, as we did not extend far upstream of the translation start codon. At this point, characterization of *Chlamydomonas* promoter regions has not been pursued thoroughsly,

with only a few described promoters (e.g. (BAURAIN *et al.* 2003; DENG and ERIKSSON 2007; GOLDSCHMIDT-CLERMONT 1986).

3.2.3. AMC5/7 locus corresponds to the gene encoding Complex I subunit NUOB10

Several methods are available for gene identification of *Chlamydomonas* insertional mutants. The most common methods, TAIL-PCR (LIU *et al.* 1995) and inverse PCR (CHEN *et al.* 1996) initially yielded unsuccessful results in recovering sequence flanking the *AMC5* locus. Therefore, Ligation Mediated Suppression PCR (LMS-PCR) was used as an alternative approach (STRAUSS *et al.* 2001) to walk the genome outside the iPm cassette in the *AMC5* locus. A PvuII genomic library was ligated to the LMS adaptor and PCR was carried out using primers specific to the cassette. Sequencing of a 800 bp band showed that the inserted fragment extended beyond the length of the iPm cassette and contained part of the pSL18 vector backbone that was used to generate the iPm cassette, suggesting that the mutant had been transformed with a piece of contaminating vector. In addition the sequencing results revealed that the insertion of the plasmid fragment had been rearranged. In the obtained sequence (light blue in Figure 3.3) the plasmid backbone contiguous to the iPm cassette was immediately followed by a part of the PsaD terminator that is located after the *bla* selective marker. The PsaD terminator fragment was inverted with respect of the original orientation and the *bla* gene was deleted.

Chlamydomonas subunit	*Accession number*	sub-complex	*H.sapiens*	*B.taurus*	Sequence obtained		Sequencing result
					bp from ATG	bp from STOP	
ACP1	AAQ73138	α, βS	NDUFAB1	SDAP	-57	+32	wt
NDUFA11	AAS58499	α, λ	NDUFA11	B14.7	-99	+372	wt
NUO17	AAS48192	β	NDUFB11	ESSS	-109	+130	wt
NUOA8	AAQ55460	α, λ	NDUFA8	PGIV	-8	+43	wt
NUOB10	AAQ55459	βL, βS	NDUFB10	PDSW	-57	+130	wt
NUOB12	AAS48194	β	NDUFB3	B12	-140	+338	wt
NUOB18	AAQ73135	βS	NDUFB7	B18	-13	0	wt
NUOB22	AAQ73134	βS	NDUFB9	B22	-3	+20	wt
NUOP2	AAS48193	α, βS	NDUFB4	B15	-182	+69	wt
NUOP1	AAS58501	α, λ, βS	n.i.	n.i.	-133	+570	wt
NUOP4	AAS58498	α, λ, βS	n.i.	n.i.	-18	+215	wt
NUOA1	AAS48198	α	NDUFA1	MWFE	-63	+488	wt
NUOA9	AAQ55458	α	NDUFA9	39	-233	+177	wt
NUOB16	AAQ64637	α, λ	NDUFA13	B16.6	-151	+656	wt
NUOB8	AAQ63699	α, λ	NDUFA2	B8	-75	+527	wt
assembly factor							
NUOAF1	ACN88152		NDUFAF1	CIA30	-13	+288	wt

Table 3.3. Sequencing results for Complex I subunits whose mutation could result in the formation of a 700 kDa subcomplex in the *amc1* mutant.

Subcomplex assignment subcomplex is based on the predicted organization shown in (LAZAROU *et al.* 2009). n.i.: not identified. The location of NUOP1 and NUOP4, only identified in *Chlamydomonas* has not yet been determined experimentally.

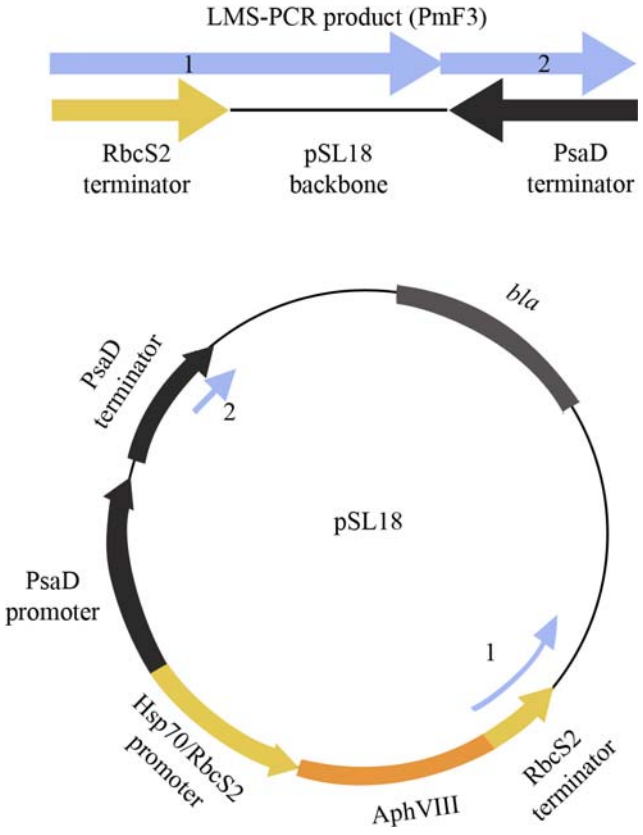

Figure 3.3. LMS-PCR reveals a genomic rearrangement with the insertion in the *amc5* mutant.

Nested primers PmF1, PmF2 in the AphVIII ORF, and PmF3 in the RbcS2 backbone were used in combination with AP1-lms and AP2-lms primers to generate a 800 bp PCR product associated with the Pm resistance. The resulting sequence (blue) spans the RbcS2 terminator and plasmid backbone (1) and continues in the PsaD terminator region (2). Note that the PsaD terminator region in the insertion is inverted with respect to its original orientation in the plasmid by comparing the blue arrows (continuous from 1 to 2) on the top panel and in the plasmid.

In the light of these results, we wondered if the original TAIL-PCR results, in which bands of small sizes incompatible with the presence of an intact cassette, were obtained, could be caused by a partial deletion of the RbcS promoter. Four different degenerate primers available in the literature -AD1 and AD2, (LIU *et al.* 1995)- and RM227 and RMD228 (DENT *et al.* 2005)- were used in combination with primers PmR1, PmR2 and PmR3, for primary, secondary and tertiary reactions, respectively. PmR1 was designed to hybridize within the coding region of *AphVIII* while PmR2 and PmR3 were specific for the promoter region. None of the primers had significant homologies with *Chlamydomonas* genomic regions. No band amplification was observed in the wildtype strain (not shown). Degenerate primers AD2 and RMD227 amplified two bands of around 600 and 400 bp in the *amc5* mutant primary reaction. In the secondary reaction, only a 300 bp band was observed. The distance between primers PmR1 and PmR2 is predicted to be around 100 bp, so it was likely that the 400 bp and 300 bp products were specific for the insertion. The PmR3 primer (72 bp downstream of PmR2) failed to yield a product in combination with any of the primers, suggesting that the promoter region had been removed during the insertion process. Sequence analysis of the 400 bp band amplified with PmR1 as the specific primer and AD1 and RMD227 as the degenerate primers yielded similar products that contained 50 bp from the RbcS2 sequence and continued in the third intron of *NUOB10*, in reverse orientation (see Figure 3.4). The mutation was verified by amplification of the genomic region spanning the insertion using primers PSDW-7F and PSDW-6R. A band of the expected size (641 bp) was amplified in the wildtype strain but not in *amc5*, confirming that the gene encoding the

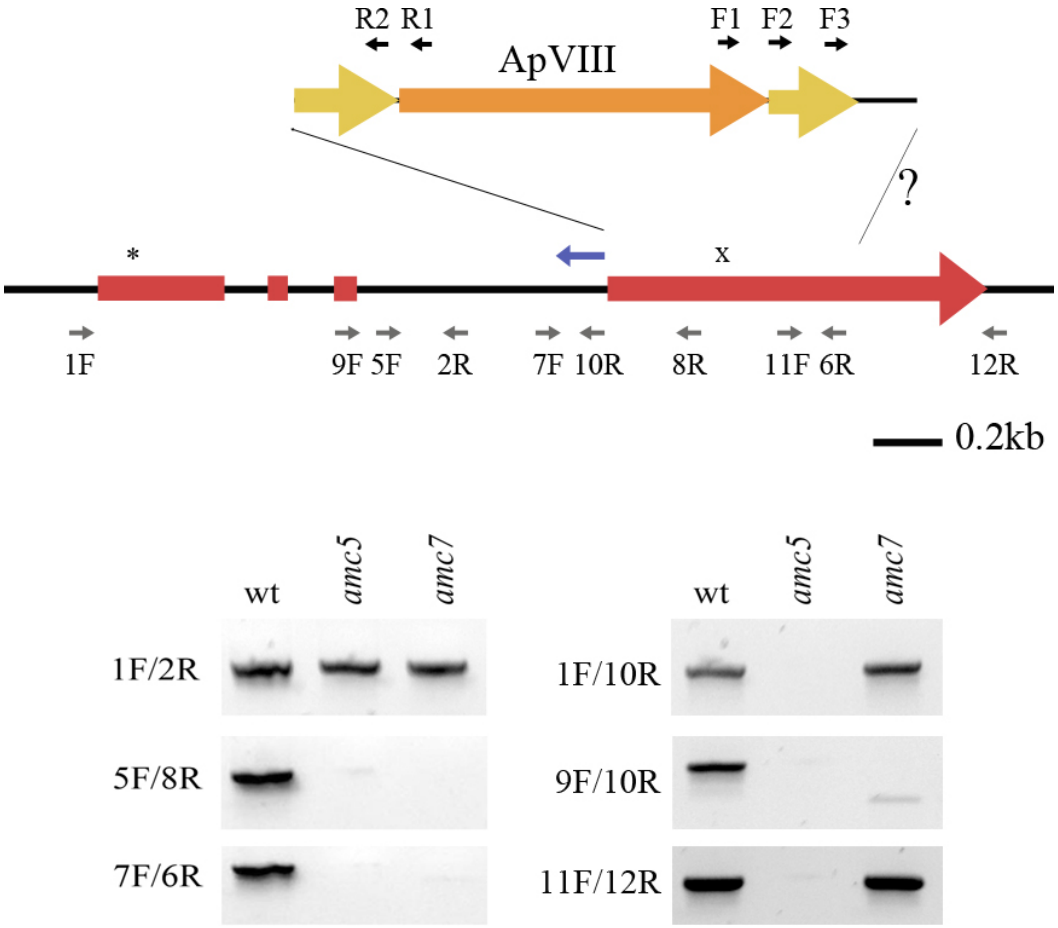

Figure 3.4. Cloning of *AMC5* reveals its identity as *NUOB10*, encoding the 17.8 kDa Complex I subunit

The approximate position of the insertion is indicated. The red segments indicate NUOB10 exon regions; the asterisk indicates the position of the ATG codon and x indicates the position of the stop codon. The blue arrow represents the sequence obtained from TAIL-PCR. Orientation of the AphVIII insert is based on the continuity between the RbcS2 promoter and the region represented by the blue arrow. Black arrows indicate primers specific for the insertion (PmF1, PmF2, PmF3, PmR1, PmR2) while gray arrows represent NUOB10 primers (PSDW1F/2R, 5F/ 8R, 7F/6R, 9F/10R, 11F/12R).

NUOB10 subunit is interrupted causing a truncated transcript lacking the last exon. Also, as no product was detected with primers PSDW-5F and 8R (Figure 3.4) or using primers PSDW-7F in combination with PmR1 or PSDW8 in combination with PmF1 (not shown), it is likely that a more complex rearrangement, possibly an inversion/deletion, had occured. New primers are being tested to evaluate this possibility.

In Chapter 2, we showed by genetic analyses that *amc5* and *amc7* were alleles of the same gene. Therefore, *amc7* should carry a mutation in the *NUOB10* gene. PCR amplification of *amc7* using *NUOB10* specific primers failed to amplify a fragment including part of the third intron and part of the fourth exon (Figure 3.4). This allowed us to conclude that *amc7* and *amc5* carry molecular lesions in *NUOB10*.

Although the diploid *amc1xamc7* was described in Chapter 2 as "complementing for assembly" but did not restore wildtype Complex I activity levels, identification of *amc5/7* was essential to definitely discard the possibility that *amc1* constituted a third allele of the same gene. In section 3.2.2 we described the sequencing of genes encoding several Complex I subunits that could affect the transition from the 700 kDa subcomplex in *amc1* to the fully assembled 950 kDa Complex I (Table 3.3, and 1.1). *NUOB10* sequence in the *amc1* background did not reveal any mutation in the coding region.

Alignment of members of the NUOB10/PSDW/NDUFB10 family (Figure 3.5) reveals the presence of a $C(X)_{11}C$ motif involving the two absolutely conserved cysteines Cys79 and Cys91 (following *Chlamydomonas* numbering). Cys79 and 91 belong to two adjacent predicted alpha helical regions. The helixes are separated by only two residues, Gly84 (conserved) and Thr85 (not conserved). The two helices are not predicted to form

a coiled-coil domain. However, it is possible that an otherwise unstable structure is stabilized by the formation of a disulfide bond between these two cysteines.

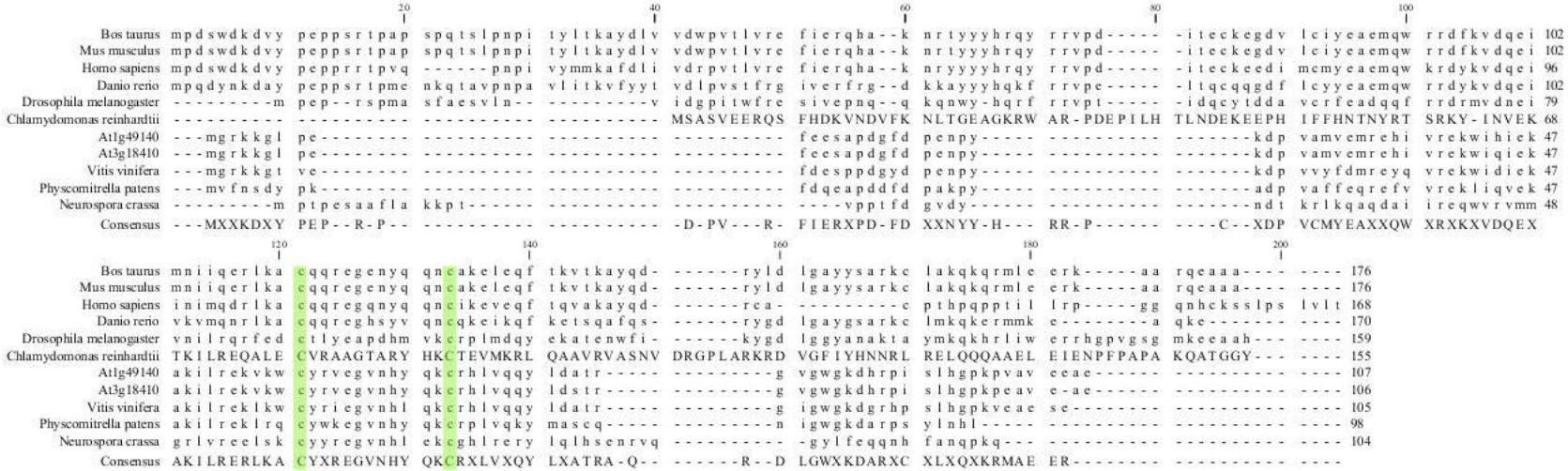

Figure 3.5. Alignment of NUOB10/PSDW proteins

PSDW/NUOB10 proteins were aligned using ClustalW and CLC Sequence Viewer. The two absolutely conserved cysteines in the $C(X)_{11}C$ motif are highlighted in green. Accession numbers: (*B.taurus*), NP080960 (*M.musculus*), AAH07509 (*H.sapiens*), Q6PC16 (*D.rerio*), Q9VQR2 (*D.melanogaster*), XP_001694041 (*C.reinhardtii*), NP_566608 (*Arabidopsis thaliana-2*), NP56540 (*Arabidopsis thaliana-1*), XP_001770976 (*V.vinifera*), XP_001770976 (*P.patens*), CAA48768 (*N.crassa*).

3.3. Discussion

Here we described different approaches to identify mutations affecting the assembly of Complex I and resulting in the formation of a 700 kDa subcomplex. In the case of *amc2* and *amc1* no molecular tag was linked to the mutation and therefore, in the case of *amc2* a molecular mapping approach was pursued. Based on the mapping results, we were able to narrow down the the mutation to a 350 kb region in chromosome 10 of *Chlamydomonas*. The region contains an average GC content of 62%, making sequencing of subunits extremely difficult. In addition, a very high frequency of repeats was present all through the 350 kb. Based on the mapping results we were able to determine that none of the known subunits of Complex I, particularly those found in subcomplex Iβ (HIRST *et al.* 2003), were encoded in this region. Moreover, none of the known assembly factors described so far (see section 1.2.2.3) is also present in this region. Although we could not definitely identify the *amc2* mutation and its associated gene, *AMC2*, we can conclude that *amc2* mutation affects a novel locus that has a role in Complex I assembly.

The forward genetics approach that we used in Chapter 2 resulted in the isolation of Complex I deficient mutations. Several mutations in Complex I structural subunits are known to have an effect in the assembly of the Complex (see sections 1.2.2.1 and 1.2.2.2). Thus, finding of mutations in nuclear encoded subunits would provide proof of concept for our screening and analyses. Here we identified *amc5* and *amc7* mutations as alleles of the *NUOB10* locus, encoding the homolog to the PSDW subunit in *Bos taurus* (CARDOL *et al.* 2004; HIRST *et al.* 2003). This subunit has been identified in purified

Complex I from *Chlamydomonas* (CARDOL *et al.* 2004). A subcomplex accumulation has been already reported in the *nuo12.3* mutant, the homolog in *Neurospora crassa* (DUARTE *et al.* 1995). The assembly of the peripheral and membrane domains are somewhat different in *Neurospora*, in the sense that the membrane arm is assembled before the attachment of the module containing soluble subunits (see (VOGEL *et al.* 2007c) for a review). In that respect *Chlamydomonas* is closer to humans as far as the assembly process is concerned, given that the peripheral subunits dock on a preassembled membrane module before the final incorporation of the extended membrane arm.

NUOB10 family (pFAM 10249) is a poorly characterized protein family with members sharing little conservation. NUOB10 proteins are between 100 and 180 aminoacids in length and are characterized by a $C(X)_{11}C$ motif (Figure 3.5). The proteins are predicted to be hydrophilic are the secondary structure is postulated to be composed mainly of helices. Despite their hydrophilic nature, characterized by the presence of several charged aminoacids, the bovine homolog has been found in the membrane arm (subcomplex Iβ) by chromatographic fractionation (HIRST *et al.* 2003) and as an integral membrane protein in *Neurospora crassa* based on its lack of extractability in alkali treated samples (VIDEIRA *et al.* 1993).The authors also reported that the *Neurospora* PSDW subunit migrated according to its size after solubilization of mitochondrial membranes with SDS under reducing or oxidative conditions. So it was concluded that no covalent associations with other proteins were present and that the subunit was protected by other subunits in the membrane environment (VIDEIRA *et al.* 1993). No additional data have been reported so far about the role of NUOB10/PSDW in assembly of Complex I

and no reports of patients with defects in the human homolog *NDUFB10* have been documented to our knowledge. Other Complex I subunits, such as PGIV, also contain conserved cysteine pair motifs where the cysteines are separated by long stretches of low conserved aminoacids and it was proposed that alternative to disulfide bond formation, the cysteines could be involved in the assembly of Fe-S clusters (CARDOL *et al.* 2004). However, all the detected Fe-S clusters in Complex I are coordinated by *core* subunits (see Chapter 1), making this alternative unlikely. An important question arising here is on the role of NUOB10/PSDW in the assembly of the membrane arm given its hydrophilic nature. One possible explanation could be that the incorporation of NUOB10 and possibly other accessory proteins in the interphase between subcomplex Iα and Iβ provides support for an otherwise labile structure. In this context, mutation of NUOB10 would result in the formation of a very transient 950 kDa complex that rapidly reverts to its 700 kDa precursor. Alternatively, addition of NUOB10 could be a necessary step offering a recognizable surface by chaperones with a role in the incorporation of the membrane arm. This step could be redox dependent, involving the $C(X)_{11}C$ motif. The two cysteines could form disulfide bonds with each other to stabilize an unstable antiparallel helix-folding. Complex III subunit 8 (also known as the hinge protein and Qcr6 in yeast) is stabilized by the formation of disulfide bonds (reviewed in (KOEHLER and TIENSON 2009). The formation of this disulfide bond could be associated to the assembly into Complex I, and possibly requires the function of additional chaperones. The topology of these cysteines is currently unknown. Depending on its orientation the disulfide bond formation could be catalyzed by a system such as the Erv1-Mia40 relay,

which drives a redox-regulated import of proteins harboring $C(X)_nC$ motifs into the intermembrane space (HELL 2007). None of the NUOB10/PSDW/NDUFB10 protein sequences analyzed contained mitochondrial targeting sequences, suggesting that they may not be imported to the matrix and could indeed be targets of the Erv1-Mia40 relay system and small Tim chaperone proteins that reside in the intermembrane space (KOEHLER and TIENSON 2009). A partial reduction in Complex I activity was observed in a patient with a R194H substitution in GFER, the human homolog of Erv1 (DI FONZO *et al.* 2009) but not further analyses have been done to link Erv1 requirements in Complex I function. Any hypotheses described here will remain speculative until a detailed functional characterization of NUOB10 is undertaken.

3.4. Experimental procedures

3.4.1. DNA analyses

DNA was extracted in proteinase K buffer (10 mM Tris-HCl, pH 8.0, 10 mM EDTA, 10 mM NaCl, 15 % glycerol, 0.5% SDS, 10 µg/ml proteinase K, Invitrogen) at 55^{o}C for 1 hour, followed by phenol: chloroform purification and ethanol precipitation. For sequencing analyses, PCR products were gel-purified using the NucleoSpin Gel-Extraction Kit (Clontech) following the manufacturer's instructions. GoTaq Polymerase (Promega) with addition of 2.5% DMSO was used for standard reactions. For difficult PCR amplifications, KlenTaq DV Ready Mix (Sigma) was used.

3.4.2. PCR-based mapping

Crosses between *amc2* (*arg7-8 mt+*) and S1-D2 (CC-2290) (*ARG7-8 mt-*) were performed as in section 2.4.3 and tetrads were manually dissected. Spores were confirmed by evaluation of the independent segregation of the *arg7-8* marker.

One *amc2* progeny (based on *sid* phenotype) was selected from each tetrad for mapping. The PCR mapping kit (RYMARQUIS *et al.* 2005) was obtained from the *Chlamydomonas* Center. All primer pairs were tested against the parental strains to confirm the expected size differences between the strains and PCR conditions. GoTaq DNA polymerase (Promega) was used for all PCR reactions and supplemented with 2.5% DMSO. For linkage analyses, the F2 backcross formatting option in Mapmaker 3.0 was used. Each spore was considered heterozygous (H) for a given marker if the size of the

PCR amplicon equaled the size of that amplicon in the *amc2* parent. Otherwise, it was considered homozygous (A).

3.4.3. Molecular identification of AMC5: TAIL-PCR and LMS- PCR

LMS-PCR was essentially performed as previously described (STRAUSS *et al.* 2001). An adapter was constructed by annealing of Adapter-a LMS (5'-CTAATACGA CTCACTATAGGGCTCGAGCGGCCGCCCGGGCAGGT-3') and Adapter-b LMS (3'-H_2N- CCCGTCCA-P-5') in equimolar amounts. Ten micrograms of purified DNA were digested with 60 units of PvuII overnight and purified by phenol: chloroform extraction and ethanol precipitation. Five micrograms of purified DNA were ligated to 5 µM adapters with 10 units of T4 DNA ligase (Invitrogen) overnight to generate an adapter-*amc5* library. The library was amplified using insert specific primers PmF1 (5'-GTG GGATGGGGCGGTATCGGAG-3'), PmF2 (5'-GGCTGTTGGACGAGTTCTTCTGAG G-3') and PmF3 (5'-GTGTTGGTGGCTGGGTAGGGTTGCG-3') for the primary, secondary and tertiary reactions, respectively, in combination with adaptor specific primers AP1-lms (5'-GGATCCCTAATACGACTCACTATAGGG-3') for the primary reaction and AP2-lms (5'-AATAGGGCTCGAGCGGC-3') for the secondary and terciary reactions. The primary PCR amplification was done using 0.05 units/µl of Pfu Turbo Polymerase (Stratagene), 2.5% DMSO, 0.4 µM AP1-lms primer, 1 µM PmF1 primer, 1 µl adapter-*amc5* library DNA, 0.8 mM dNTP mix, 1x Pfu buffer. PCR cycles were run according to the manufacturer's conditions with annealing temperature at 58°C, and 4 minutes extension at 72°C. One microliter of a 1:50 dilution of the PCR product was used

for the secondary and tertiary reactions using AP2-lms primer and the insert specific primers.

Amplification of insertion-linked by TAIL-PCR products followed the same cycling conditions as described in (DENT *et al.* 2005) with 1.25 units/µl GoTaq DNA Polymerase, 1x Green Buffer GoTaq Reaction Buffer, 2.5% DMSO, 1.55 µM specific primers (PmR1, PmR2 or PmR3 for primary, secondary and tertiary reactions, respectively) and 0.4 µM of degenerate primers (AD1, AD2, RMD227 or RMD228) were used. Oligonucleotides AD1 (5'-NTCGA(G/C)T(A/T)T(G/C)G(A/T)GTT-3') and AD2 (5'-NGTCGA(G/C)(A/T)GANA(A/T)GAA-3') were described in (LIU *et al.* 1995). Olignucleotides RMD227 (5'-NTCGWGWTSCNAGC-3') and RMD228 (5'-WGNT CWGNCANGCG-3') were described in (DENT *et al.* 2005). Primers specific for NUOB10 are listed in Table 3.4.

Primer	Sequence (5'→3')
PSDW-1F	CACCTGGTGCACATTGCTGTA
PSDW-2R	TTCATGCTTGCCCGAGAAG
PSDW-5F	GACCAAGGGCTTTCTGACTG
PSDW-7F	AGCCTCAGGCATATTGCGC
PSDW-6R	ATCGCACATGACGGCAG
PSDW-8R	GTAGATGAAGCCCACGTCG
PSDW-9F	GTCATGAAGCGCCTGCAGG
PSDW-10R	GGAACTGGGTAAGGTTCTAAGC
PSDW-11F	CACTGCCTGAAAGCCTGCC
PSDW-12R	GAGGAGAGCAGTGGCATCGTG

Table 3.4 NUOB10 Primers used in this work.

CHAPTER 4

CONSERVATION OF THE ROLE OF CIA30 AND OXA1 ASSEMBLY FACTORS IN *CHLAMYDOMONAS REINHARDTII*

4.1. Introduction

Several Complex I assembly factors have been already identified by subtractive genomics (PAGLIARINI *et al.* 2008) and proteomics in humans and other systems (BYCH *et al.* 2008; KUFFNER *et al.* 1998; OGILVIE *et al.* 2005; VAHSEN *et al.* 2004; VOGEL *et al.* 2005) (Table 1.2); and at least 50 % find a orthologous gene in *Chlamydomonas*. This chapter focuses on the function of two proteins that have been associated with Complex I activity and assembly in other eukaryotes: Oxa1 (BONNEFOY *et al.* 1994a; SELLEM *et al.* 2005; STIBUREK *et al.* 2007) and CIA30 (KUFFNER *et al.* 1998; VOGEL *et al.* 2005). In view of this conservation, the following hypothesis is proposed:

Complex I assembly is conserved for Chlamydomonas and Chlamydomonas orthologs of known assembly factors in other eukaryotes also have a role in the assembly of the complex, supporting the idea that similar factors are recruited in all Complex I-containing organisms to produce a mature and functional Complex I.

To test whether *Chlamydomonas* Oxa1 is involved in the assembly of respiratory complexes, I followed a heterologous complementation approach using a deletion mutant of yeast Oxa1 as the recipient strain.

4.1.1. Oxa1 as an assembly factor for multiple respiratory complexes

Oxa1 is a polytopic inner membrane protein originally discovered in a *Saccharomyces cerevisiae* genetic screen as a cytochrome oxidase (Complex IV) assembly factor (BONNEFOY *et al.* 1994a). This protein belongs to the Alb3/Oxa1/YidC family of membrane protein chaperones carrying a five-transmembrane domain signature (Figure 4.1) with a chaperone role in facilitating insertion of proteins into the membrane (reviewed in (KUHN *et al.* 2003) and (BONNEFOY *et al.* 2009)). Alb3 is involved in the insertion of light-harvesting complexes and photosystems into the thylakoid membranes (BELLAFIORE *et al.* 2002; GOHRE *et al.* 2006; OSSENBUHL *et al.* 2004; SPENCE *et al.* 2004; SUNDBERG *et al.* 1997; WOOLHEAD *et al.* 2001). YidC members of the family are involved in the insertion of subunits of several energy transducing complexes into the periplasmic membrane, including subunits a and c of F_1F_0 ATPase (VAN DER LAAN *et al.* 2003; YI *et al.* 2003), cytochrome *o* oxidase- the bacterial counterpart to Complex IV (VAN DER LAAN *et al.* 2003; YI *et al.* 2003), NuoK subunit of NADH dehydrogenase (PRICE and DRIESSEN 2008), and also nitrate and fumarate reductases (PRICE and DRIESSEN 2008). Two subfamilies of Oxa1 proteins are only found in mitochondria: Oxa1 and Cox18 (BONNEFOY *et al.* 2009).

Complex IV assembly requires the insertion of the mitochondrially encoded subunits (Cox1, Cox2, Cox3) into the mitochondrial inner membrane. The role of Oxa1

both as a cotranslational chaperone for translocation of proteins across the inner membrane was suggested from crosslinking evidence that Oxa1 interacts with nascent polypeptides of Cox2 and Cox3 (HELL *et al.* 1998), cofractionation and *in vitro* binding of ribosomes with the mitochondrial facing C-terminus of Oxa1 (JIA *et al.* 2003; SZYRACH *et al.* 2003), and interactions of Oxa1 with the mitochondrial ribosomal subunits Mrp20 and MrpL40 (JIA *et al.* 2003; JIA *et al.* 2009). Moreover, Oxa1 is required to export the N-terminus of Cox2 to the intermembrane space (HE and FOX 1997). A role of Oxa1 in posttranslational export to the intermembrane space was also suggested, base on the fact that the C-terminal domain of Cox2 also requires the presence of Oxa1, independently of its N-terminal part (HE and FOX 1997). In addition to Oxa1, Mss2 and Cox18 are also required to export the C-terminal domain of Cox2, supporting the posttranslational role of Oxa1 in Cox2 export (FIUMERA *et al.* 2007; SARACCO and FOX 2002). In contrast with Oxa1, whose mutation results in deficiency in the assembly of several respiratory complexes (see below), Cox18 deficiency results in isolated deficiency of Complex IV (HIKKEL *et al.* 1997; SACCONI *et al.* 2009; SOUZA *et al.* 2000).

Oxa1 has been reported to have effects in the assembly of other respiratory complexes other than Complex IV. It has been reported that Oxa1 deficiency has deleterious effects in the assembly of yeast Complex V (ALTAMURA *et al.* 1996). *Podospora anserina* Oxa1 is able to complement respiratory growth in a yeast *oxa1* null mutant and an *oxa1* thermosensitive mutant (*oxa1*^{ts}) shows a strong reduction in Complex I, IV and V activities as measured by *in gel* staining (SELLEM *et al.* 2005). Similarly, Oxa1 is essential for viability in *N. crassa* and Oxa1-depleted mitochondria have a strong

reduction in the amounts of the 29.9 and 24 kDa Complex I and Cox2 and Cox3 Complex IV subunits (NARGANG *et al.* 2002). A role of Oxa1 in Complex V assembly has been shown by RNA interference knockdown of human HEK293 cell lines in humans (STIBUREK *et al.* 2007). However, although the authors report an effect in Complex I accumulation, the magnitude of this effect is not evident. Nevertheless, accumulation of the NDUFA9 and NDUFB6 subunits is slightly decreased in the knockdown lines. Recently, a decrease in accumulation of NuoK, the homolog of ND4L subunit in *E. coli*, was shown in the absence of YidC (PRICE and DRIESSEN 2008). NuoK is a small subunit with three transmembrane domains (KAO *et al.* 2005). Using proteinase K-treated inner membrane vesicles, it was shown that NuoK insertion into the membrane is affected by deficiency of YidC in *E. coli* and NuoK co-purified with YidC (PRICE and DRIESSEN 2010). The *Arabidopsis* version of Oxa1 is also able to restore respiratory growth in yeast *oxa1* mutants (HAMEL *et al.* 1997). Nonetheless, the conservation level of the Oxa1 proteins is very low, sharing only about 20-30 % identity with the founding member of the family (HAMEL *et al.* 1997; NARGANG *et al.* 2002; SELLEM *et al.* 2005; STIBUREK *et al.* 2007). Despite this low level of sequence conservation, Oxa1 seems to have a general role in facilitating the biogenesis of respiratory complexes and its function is conserved in eukaryotes. The current model is that Oxa1 acts as an insertase/translocase for membrane subunits that are synthesized in the mitochondrial matrix.

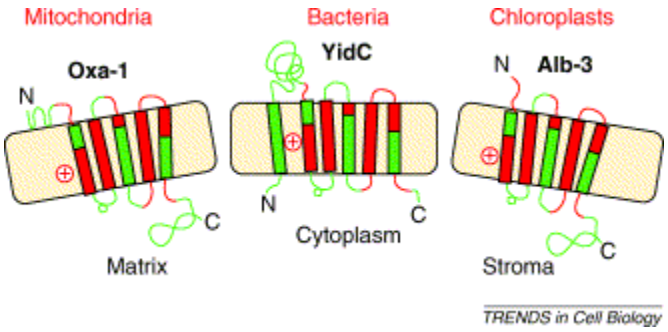

Figure 4.1. Topology of the Alb3/Oxa1/YidC family.

All members have at least five transmembrane domains and a conserved arginine (+) in the membrane. Except for YidC that has an extra transmembrane domain, all members have an N-out C-in topological organization. Conserved regions are coloured in red. Source: (KUHN *et al.* 2003).

Differently from other eukaryotes, *Chlamydomonas* COX2 and COX3 are nucleus encoded (PEREZ-MARTINEZ *et al.* 2001; PEREZ-MARTINEZ *et al.* 2000). Similarly, NAD4L Complex I core subunit, whose bacterial counterpart –NuoK- requires YidC for membrane insertion (PRICE and DRIESSEN 2010), is nucleus encoded in *Chlamydomonas* (CARDOL *et al.* 2006). Therefore, these subunits have to be imported into the mitochondrial matrix prior to their insertion in the mitochondrial inner membrane, which is necessarily posttranslational. Alternatively they could be inserted in the membrane from the intermembrane space side. *Chlamydomonas* COX2 is atypical as it forms a heterodimer of two polypeptides COX2A and COX2B, encoded by two different genes (PEREZ-MARTINEZ *et al.* 2001). COX2A is equivalent to the N-terminal part yeast Cox2

while COX2B is equivalent to the C-terminus. The long mitochondrial targeting sequence of COX2A has been proposed to function also during assembly. COX2B lacks the targeting sequence and its N-sequence is highly charged. Therefore it was suggested that COX2A would be imported into the mitochondrial inner membrane while COX2B would be directly imported to the intermembrane space. In the previous paragraphs yeast Oxa1 and Cox18 function in the insertion of proteins synthesized in the mitochondrial matrix was discussed. Particularly, since Cox18 is involved in the insertion of Cox2 C-terminal domain, its function would not be longer required in *Chlamydomonas* (COX2B does not seem to be imported into the matrix). On the other hand OXA1 could still sustain a role for insertion of COX2A and NAD4L, both carrying long N-terminal mitochondrial targeting sequences that were proposed to facilitate mitochondrial import and inner membrane insertion (FIGUEROA-MARTINEZ *et al.* 2008). Consistently, only one member of the Oxa1/Cox18 subfamily is found in *Chlamydomonas* genome, but its role on the assembly of respiratory complexes has not been studied so far.

4.1.2. Evidence for CIA30 in Complex I assembly

CIA30 was first isolated by gel filtration chromatography from a purified large membrane-associated subcomplex that accumulated in the *Neurospora crassa nuo21* mutant, depleted from the 21.3 kDa Complex I subunit (KUFFNER *et al.* 1998). Disruption of CIA30 in *Neurospora* and mitochondrial membrane solubilization with Triton X-100 results in the accumulation of two subcomplexes recovered in different fractions after sucrose gradient centrifugation: a 200 kDa membrane arm, containing the hydrophobic

subunits ND2 and ND5, and a 400 kDa soluble matrix arm containing the 49-kDa subunit.

The involvement of the human homolog of CIA30 (NDUFAF1) was originally observed using a small interference RNA (siRNA) knockdown approach in HeLa cells (VOGEL *et al.* 2005), which resulted in compromised Complex I activity and a shift in the subcomplex migration profile, increasing the accumulation subcomplexes of intermediate sizes. Similarly to *Neurospora*, NDUFAF1 was found in association with two membrane subcomplexes of 600 and 700 kDa when using n-dodecyl β-D-maltoside to solubilize the membranes (VOGEL *et al.* 2005). Co-immunoprecipitation analyses showed that CIA30 associates with subunits ND1 (mitochondrial), NDUFA9, NDUFS3, NDUFS7, NDUFB6, NDUFS5 and NDUFA6 (DUNNING *et al.* 2007). However, solubilization of mitochondria with Triton X-100 after *in vitro* labeling of newly synthesized proteins, showed CIA30 in association to an abundant 460 kDa complex and a less abundant 830 kDa complex but not with the mature Complex I (DUNNING *et al.* 2007). Two missense mutations in the third exon of *NDUFAF1* were identified after observing depletion of CIA30 in the patient's fibroblast cells (DUNNING *et al.* 2007). The two mutations produced changes in two aminoacids conserved in mammals (T207P and K253R). However, these aminoacids are not conserved in *Neurospora*, the only other organism in which CIA30 function was experimentally explored.

Complex I assembly Tandem Affinity Purification of mitochondrial lysates (VOGEL *et al.* 2007b) identified Ecsit as a partner for CIA30 in human mitochondria. Ecsit (evolutionary conserved signaling intermediate in Toll pathways) was initially

identified as a cytoplasmic protein with roles in pathways regulating innate immunity and embryonic development in *Drosophila* and humans (reviewed in (MOUSTAKAS and HELDIN 2003). Ecsit's involvement in human Complex I assembly was evidenced by knockdown analyses which resulted in a severe assembly reduction (VOGEL *et al.* 2007b). In humans, CIA30 is believed to accompany the assembly intermediates of Complex I until the latest stages of assembly (LAZAROU *et al.* 2009), and therefore, it is reasonable to picture direct interactions of CIA30 with at least some Complex I subunits and/or with other factors which in turn associate with structural subunits. To our surprise, no further interaction studies for CIA30 have been reported in the past years. To increase our understanding of CIA30 role in Complex I assembly, we performed yeast-two hybrid analyses and looked for direct interaction partners.

4.2. Results

4.2.1. The predicted topology of Chlamydomonas Oxa1 is similar to Oxa1 proteins in other organisms

Oxa1 is a ubiquitous protein with chaperone activity in the assembly of respiratory complexes present in the eukaryotic mitochondrial inner membrane (BONNEFOY *et al.* 2009). We reasoned that if our hypothesis of assembly conservation was correct, we would be able to find a homolog of yeast Oxa1 in *Chlamydomonas.* We used *Saccharomyces* Oxa1 to perform a BLAST search against the *Chlamydomonas* genome. The highest score hit (26% I, e-value $1e^{-08}$) matched a protein annotated as "Cox18, cytochrome oxidase assembly factor" (Accession number XM_001699133). The next hit corresponded to *Chlamydomonas* ALB3, a gene of the same family that is involved in assembly of chloroplast membrane proteins (BELLAFIORE *et al.* 2002; GOHRE *et al.* 2006; OSSENBUHL *et al.* 2004) and therefore, it was unlikely to be involved in mitochondrial function. The annotation for the cytochrome oxidase assembly factor (fgenesh1_est.C_scaffold_45000014) indicated a protein much shorter (OXA1S, 237 residues) than the fungal, mammalian and *Arabidopsis* versions which are around 400 aminoacids long (BONNEFOY *et al.* 1994a; BONNEFOY *et al.* 1994b; HAMEL *et al.* 1997). Importantly, prediction analysis of the topology of this protein only revealed three transmembrane domains, in contrast with the five transmembrane domains that constitute the signature of the Oxa1 family. We decided to analyze the *OXA1* genomic region using GreenGenie2, a gene prediction algorithm that was trained with *Chlamydomonas*

sequences (KWAN *et al.* 2009). The gene structure resulting from this analysis contained a coding sequence similar in length and topological organization to the known Oxa1. We named it OXAlL (for OXA1 long, Figure 4.2). Indeed, a transmembrane domain prediction by hydropathy analyses revealed five transmembrane domains and this prediction placed the N-terminus on the outside (intermembrane) space and the C-terminus on the inside (matricial) space, consistent with the the general organization of Oxa1 in other organisms (HERRMANN *et al.* 1997; SATO and MIHARA 2009). Bases 12 to 534 from OXA1S overlapped completely with bases 648 to 1170 in the OXA1L model, and the reading frame was also conserved. A change in the four aminoacids at the beginning of the protein was observed for OXA1S compared to the adjacent aminoacids in OXA1L.

To confirm the gene structure prediction, we used *OXA1L* sequence in a search for available ESTs at the *Chlamydomonas* EST index (Kazusa DNA Research Institute, http://est.kazusa.or.jp/en/plant/chlamy/EST/blast.html). We found two available EST sequences with GenBank accessions AV626960 (483 bp), at the 5' end of *OXA1L* mRNA, and BI529086 (429 bp), spanning bases 648 to 1057 (one to 421 of *OXA1S*). Full sequencing of the inserts showed that the ESTs represented two different cDNAs, one corresponding to *OXA1S* (1165 bp, accession number FJ589129) and the other carrying the long version of OXA1 (1928 bp, accession number FJ577501) (Figure 4.2). Because both libraries were grown under different conditions we performed RT-PCR analyses to evaluate if there were variations in transcripts by growing *Chlamydomonas* wildtype strains under heterotrophic (dark + acetate) or mixotrophic (light +acetate) conditions.

Transcripts exclusive for OXA1L were detected under both conditions (not shown). The short and long cDNAs were identical for most of the sequence, starting at position 20 from the short cDNA. The first 19 bases of this cDNA, however, differed from the long form and included a short sequence from an adjacent intron, providing an alternative translation start codon, suggesting that two transcripts coexist with different transcription start sites. Alternatively, transcription could start from a similar start site and the short transcript could reflect an alternative splicing site, or a partially spliced site including the immediately upstream intron. For example, three splicing forms exist for *Chlamydomonas* immunophilin FKB16-2, defining three different final localizations: thylakoid lumen, chloroplast stroma, and mitochondrion (VALLON 2005). Also, the possibility that the short transcript is an artifact produced by a partially spliced full-length transcript that was truncated cannot be disregarded. Examples of introns that are processed slowly and give the idea of two coexisting alternative splice forms have already been documented *Chlamydomonas* (HILL *et al.* 1991; KROPAT *et al.* 2005).

4.2.2. Chlamydomonas Oxa1 restores respiratory growth of a yeast Δoxa1 mutant

Alignment of yeast Oxa1 and *Chlamydomonas* OXA1L proteins showed a very low level of conservation (20% identity) similar to what had been reported to other Oxa1 proteins. These other proteins are still capable of functionally complement *oxa1* deficiency in yeast (BONNEFOY *et al.* 1994b; HAMEL *et al.* 1997). Therefore, we decided to pursue a heterologous complementation approach by transforming in the Δ*oxa1* NBT1 mutant strain with plasmids expressing the long (pYES-Oxa1L) and short (pYES-Oxa1S)

versions of *Chlamydomonas* OXA1. Strains transformed with OXA1S or the empty vector failed to grow in the respiratory media. Similarly, the Oxa1-related proteins ALB3.1 and ALB3.2, involved in the assembly of light-harvesting complexes and photosystems in the chloroplast (BELLAFIORE *et al.* 2002; GOHRE *et al.* 2006; OSSENBUHL *et al.* 2004), were unable to complement the yeast mutation. On the other hand, only OXA1L was able to sustain growth in ethanol plates (respiratory), although this growth was slow compared with the positive control, transformed with a wildtype copy of yeast Oxa1 (Figure 4.3).

To further confirm that the restoration of respiratory growth was due to the functional complementation by OXA1L of the assembly of respiratory complexes, we compared the whole cell absorbtion spectra of another yeast *oxa1* mutant strain (CNB1: *oxa1-79,* intron-less background (BONNEFOY *et al.* 1994a) carrying either the endogenous Oxa1 or CrOXA1L. The respiratory defect of *oxa1* mutants is associated with its inability to properly assembly the cytochrome oxidase cytochromes *a*+*a3* and cytochrome *b* from Complex III (BONNEFOY *et al.* 1994a) and Figure 3.4. This deficiency is evidenced by the absence of a 602 nm peak, characteristic of cytochromes *a*+*a3* from the cytochrome oxidase complex. As previously reported, the endogenous copy of Oxa1 was able to restore assembly of cytochromes *a*+*a3*. Expression of CrOXA1L also restored the assembly of both cytochromes, although to a lesser extent and in agreement with the partial restoration of respiratory growth. Therefore, it was concluded that only the long form of Oxa1, OXA1L, is the *Chlamydomonas* functional homolog of yeast Oxa1.

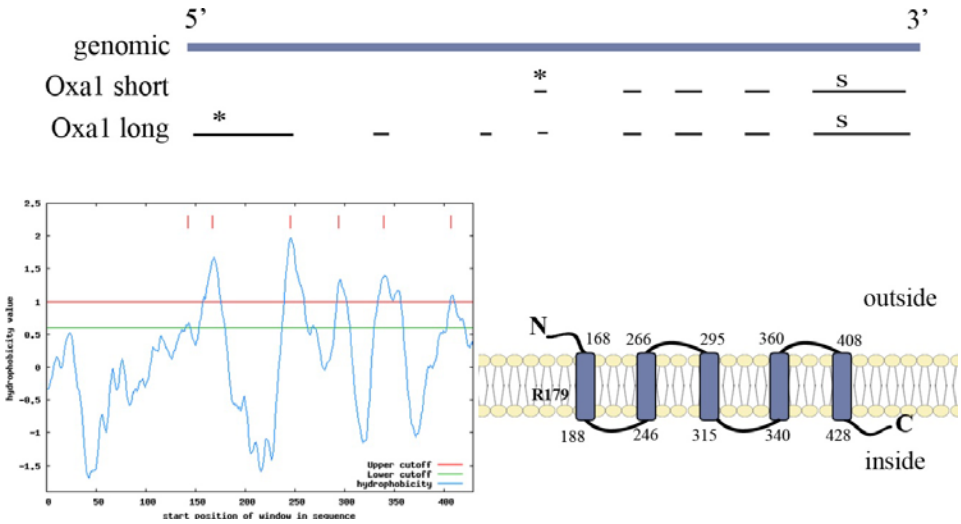

Figure 4.2. Genomic structure and topological prediction of *Chlamydomonas* OXA1 proteins reveal a similar organization as its homologs in other systems.

Top: Schematic alingment of the two cDNAs with different length and different start codons (*) with the genomic sequence of *OXA1*. "s" indicates the position of the stop codon. *Bottom:* hydropathy plot of translated *OXA1L* cDNA (left) and its predicted membrane topology (right). The organization is similar to other Oxa1 proteins with a role in mitochondrial respiratory complexes assembly.

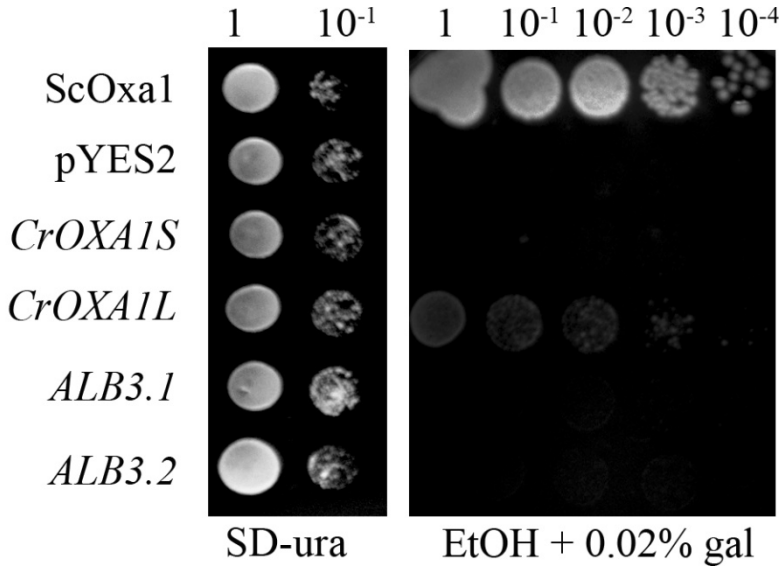

Figure 4.3. *Chlamydomonas OXA1L* cDNA complements the respiratory growth of the respiratory deficient Δ*oxa1* mutant in yeast

The yeast Δ*oxa1* NBT1 strain (BONNEFOY *et al.* 1994a), unable to growth in respiratory media was transformed with the galactose inducible expression vector pYES2 carrying the either the yeast Oxa1 ORF (ScOxa1), *CrOXA1L* cDNA, *CrOXA1S* cDNA or cDNAs for *Chlamydomonas* ALB3.1 and ALB3.2. Dilution drops of freshly grown liquid cultures were incubated for three days in uracil drop-out minimal media (SD-ura) and ethanol, 0.02% galactose at 28°C.

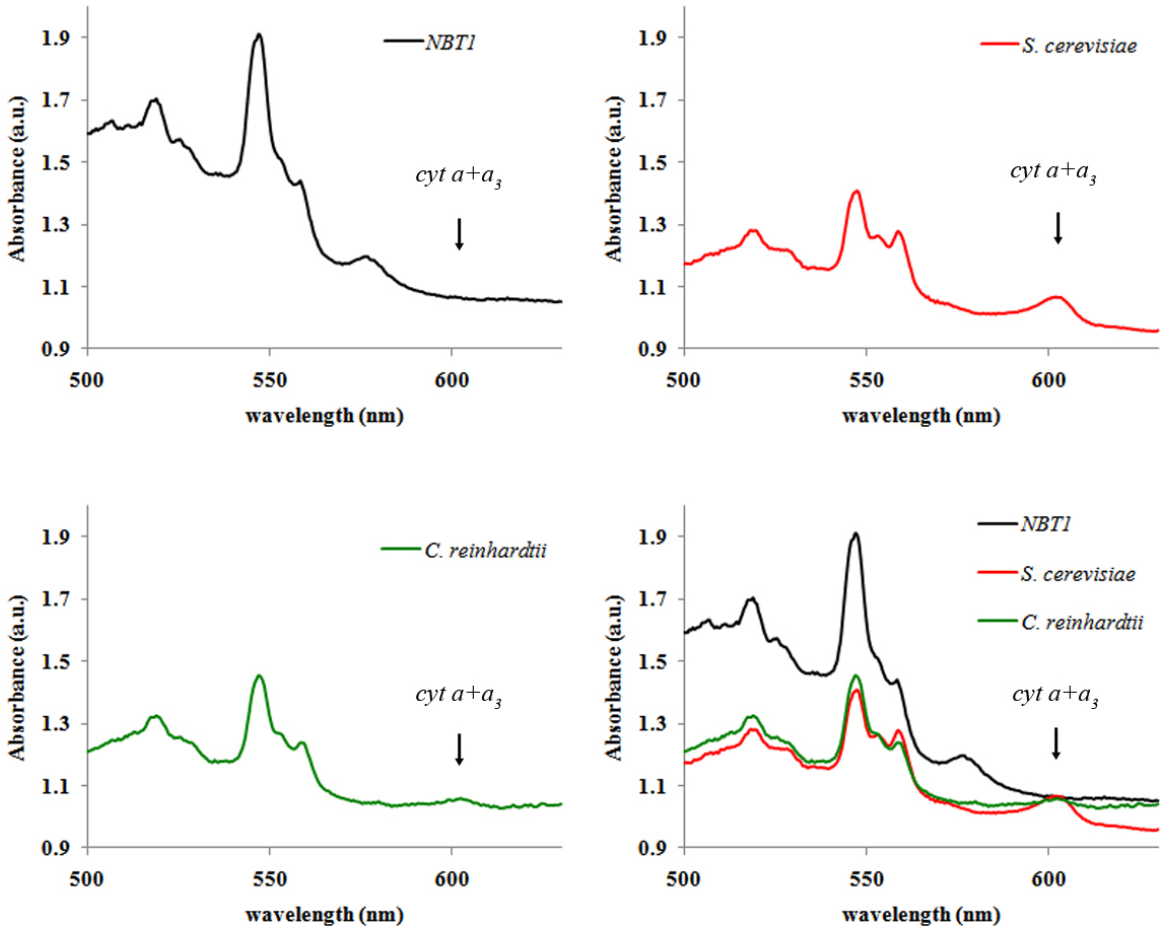

Figure 4.4. Whole cell absorbtion spectra confirms CrOXA1L functional complementation of cytochrome assembly

4.2.3. CIA30 conservation in the green lineage

CIA30 superfamily (pfam 08547) can be subclassified in 13 different subfamilies, based on the presence of other protein domains in addition to the CIA30 motif. The members of this family are loosely related and present in many organisms, some of which are devoided of Complex I. In humans and *Neurospora crassa*, CIA30 protein is localized in the mitochondria (KUFFNER *et al.* 1998; VOGEL *et al.* 2005). *Arabidopsis* contains two copies of CIA30, At1g17350 (AtCIA30a) and At1g72240 (AtCIA30b), with 227 and 228 aminoacids, respectively. *Chlamydomonas* contains a single copy encoding a 277 aa protein, CrCIA30. CrCIA30 is only 28% identical to the human version (e-value 9^{-16}). Likewise, identity levels in *Arabidopsis* are 26% for At1g17350 (e-value 3^{-10}) and 24% for At1g17240 (e-value 5^{-10}). A similar low level of conservation was also found in *Neurospora* (27% I, e-value 3^{-09}). ClustalW alignment of several CIA30 sequences from diverse organisms shows that the region between residues 200 and 240 (with human sequence as a reference) has the highest similarity among all sequences (Figure 4.5).

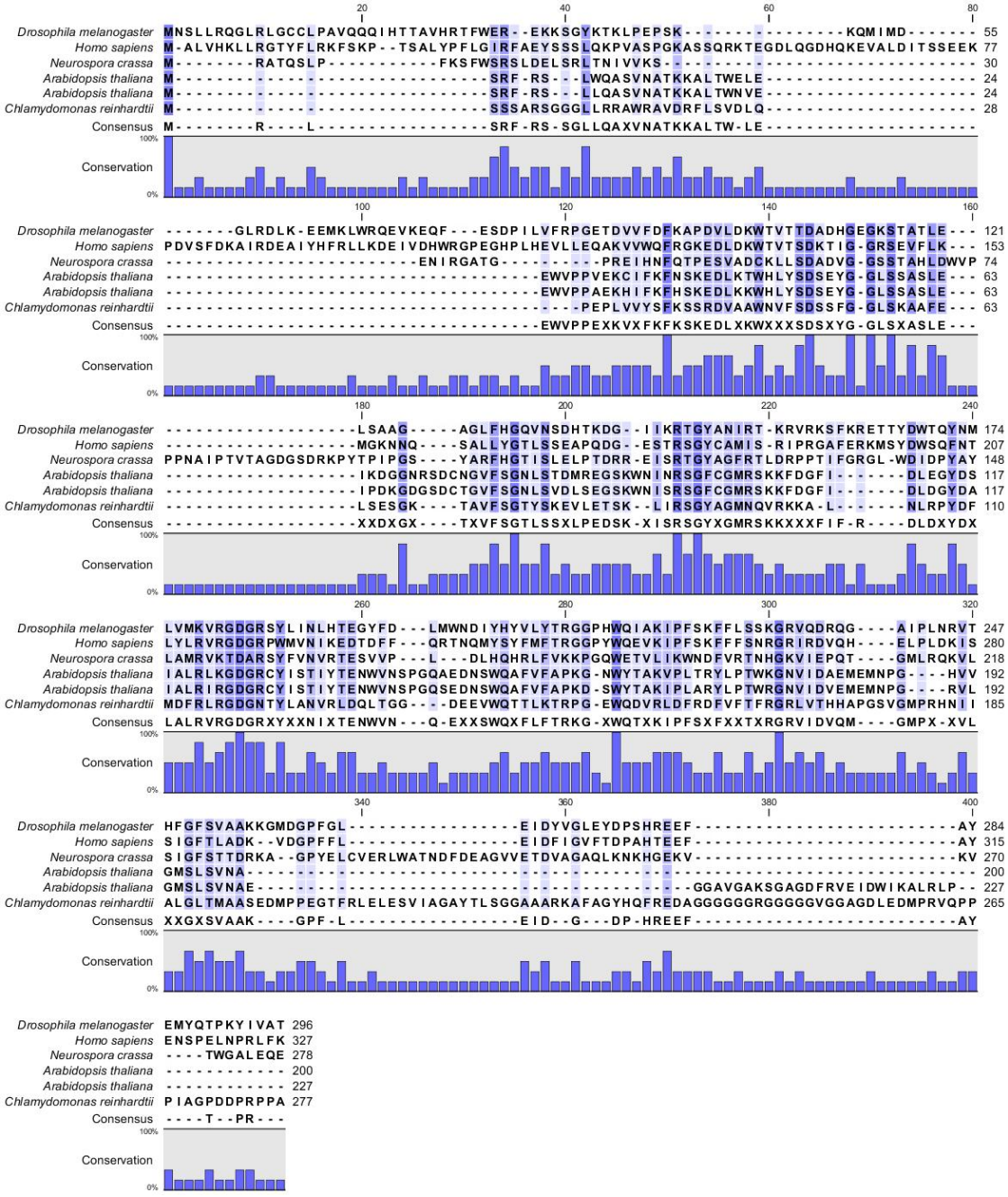

Figure 4.5. Alignment of CIA30 proteins of animals, fungi and plants.

The alignment was generated using ClustalW within the CLS Sequence Viewer Package (CLC bio, Cambridge MA). The blue coloring indicates the degree of conservation (darker being more conserved)

4.2.4. Silencing of Chlamydomonas reinhardtii OXA1and CIA30 using an artificial microRNAi strategy leads to the finding of new respiratory mutants

We aimed to characterize the respiratory function of *Chlamydomonas* OXA1 and CIA30 proteins. Because there is no stable mutant collection in *Chlamydomonas*, we generated artificial microRNAi OXA1 and CIA30 constructs (amiOXA1 and amiCIA30) and transformed them into a *Chlamydomonas* wildtype strain to generate Oxa1 knockdowns according to a recently developed strategy (MOLNAR *et al.* 2009). For Oxa1 we targeted the 5'-region of the gene with constructs amiOXA1L1 and amiOXA1L2, and the coding region with constructs amiOXA1S1 and ami1OXA1S2. For CIA30, we used constructs amiCIA30.2 (5'-region) and amiCIA30.1 (3'-UTR). After transformation and selection in the appropriate conditions, transformants were analyzed for the presence of either *sid* or dark dier phenotypes, characteristic of respiratory mutants in *Chlamydomonas* (REMACLE *et al.* 2008). A total of 2,000 transformants were analyzed for each construct and none of them displayed a respiratory phenotype. Therefore, a double transformation approach, with distinct or identical miRNA constructs, was used and an additional 3,000 transformants were obtained. Using this strategy, four transformants showing a *sid* phenotype were isolated: two for OXA1 (Oxa #6 and Oxa-F8) and two for CIA30 (CIA30#1 and CIA30#3) (Figure 4.6). Mutant F8 also displayed a very slow growth under mixotrophic conditions, evidenced by small colony size.

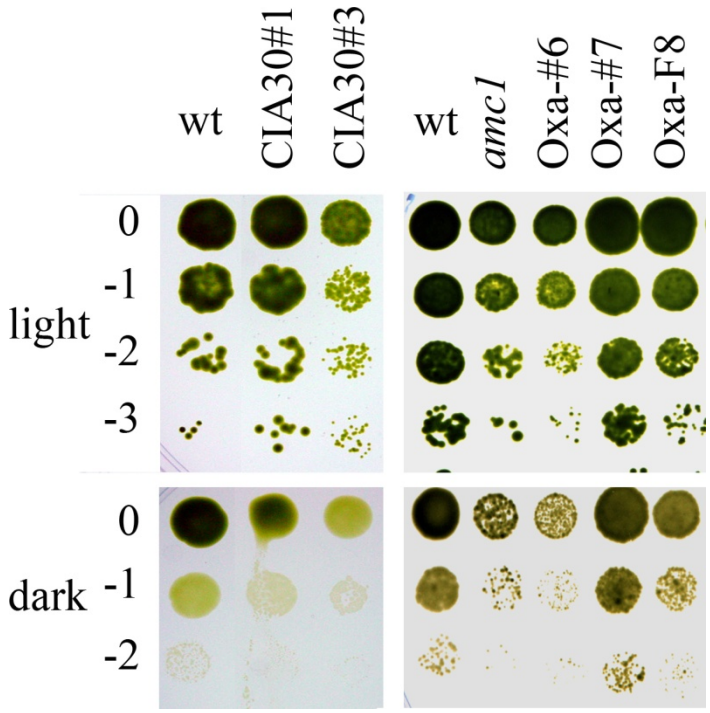

Figure 4.6. The putative transformants by microRNAi-directed knockdown of *Chlamydomonas reinhardtii CIA30* and *OXA1* show a *sid* phenotype.

The numbers on the left indicate serial one-tenth dilutions. *amc1* mutant was used as a control for the *sid* phenotype and Oxa-#7 transformant as a control for a transformant with wildtype growth in the dark. Plates were grown for three days under mixotrophic conditions (light + acetate) or for five days under heterotrophic conditions (dark + acetate).

Strains Oxa-#6 and Oxa-F8 accumulated reduced amounts of Complex I (Figure 4.7 , C) and CIA30#3 displayed no Complex I at all in BN-PAGE followed by *in gel* activity staining (Figure 4.8, A). On the contrary, the empty vector transformants and CIA30#1 showed wildtype levels of Complex I accumulation. The growth rate of CIA30#3 mutant was also reduced under mixotrophic conditions in liquid cultures (Figure 4.8, C), but the mutant was able to reach wildtype cell numbers over time, indicated that the rate of cell division was reduced. All of the mutants were evaluated for Complex I-specific NADH oxidation. Strains Oxa-#6 and CIA30#3 showed a strong depletion of Complex I activity while Oxa-F8 was only partially reduced (Figure 4.7, A and Figure 4.8, B). CIA30-1 Complex I activity was similar to that of the wildtype. It is interesting to notice that despite the strong reduction in Complex I activity, strains #6 and F8 still accumulated a reduced amount of Complex I, capable of NADH oxidation as observed in the *in gel* activity staining. This is contrasting with CIA30-3, which does not display a mature complex at all.

Oxa1 has a role in Complex IV assembly in yeast and other systems. Also, in the previous section, a conserved role for the Oxa1 function was suggested based on the ability of *Chlamydomonas* Oxa1 to complement the *Δoxa1* mutation in the NBT1 yeast strain. Because an effect in most organisms studied so far Oxa1 mutation results in a Complex IV deficient phenotype (see (BONNEFOY *et al.* 2009), we expected to see a defect in Complex IV activity in the Oxa1 microRNAi lines. Only strain #6 showed a depletion of Complex IV activity (Figure 4.7, B) and this strain produced a very weak activity stain on BN-PAGE (Figure 4.7, D).

Phenotypically, both CIA30#3 and Oxa-#6 had behaviors consistent with a knockdown of the respective genes. To verify that these phenotypes were caused by a reduced expression of the *CIA30* and *OXA1* genes in the transformed strains, transcript accumulation was evaluated using semiquantitative RT-PCR. Neither *OXA1* (Figure 4.9) nor *CIA30* (Figure 4.10) transcripts were reduced compared to the wildtype strain, indicating that these two strains, although showing respiratory phenotypes consistent with the reported functions for the function of these proteins, were caused by independent mutations, possibly by insertion of the construct in a locus controlling respiration.

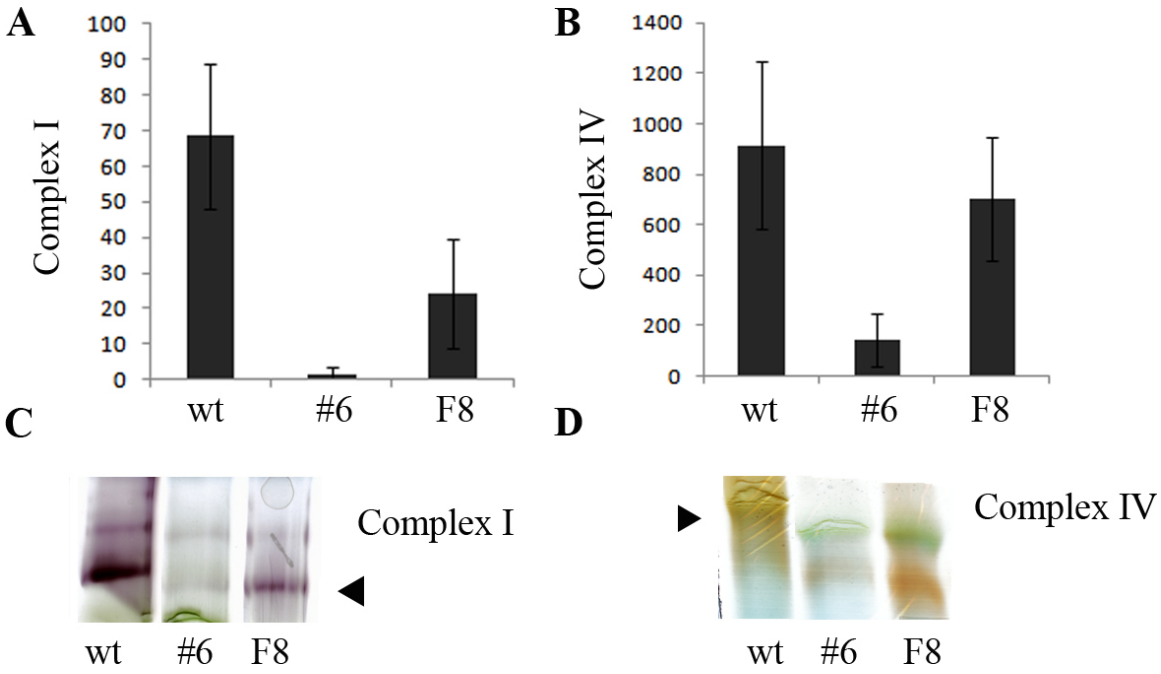

Figure 4.7. Oxa1 putative knockouts are affected in the assembly of respiratory complexes.

Partially purified membranes were extracted from three-day old cultures. **A**. Complex I activity (rotenone-sensitive) using NADH and duroquinone as substrates. Activity expressed in nmol NADH oxidized per minute per mg protein. **B**. Complex IV activity. Activity is expressed in nmol cytochrome *c* oxidized per minute per mg protein. **C and D**. BN-PAGE and Complex I (C) and Complex IV (D) *in gel* activity from partially purified membranes. Notice that Complex IV runs sometimes as a poorly defined smear. The brown band in case of F8 is more accurate to compare the reduction of Complex IV levels in strain Oxa-#6.

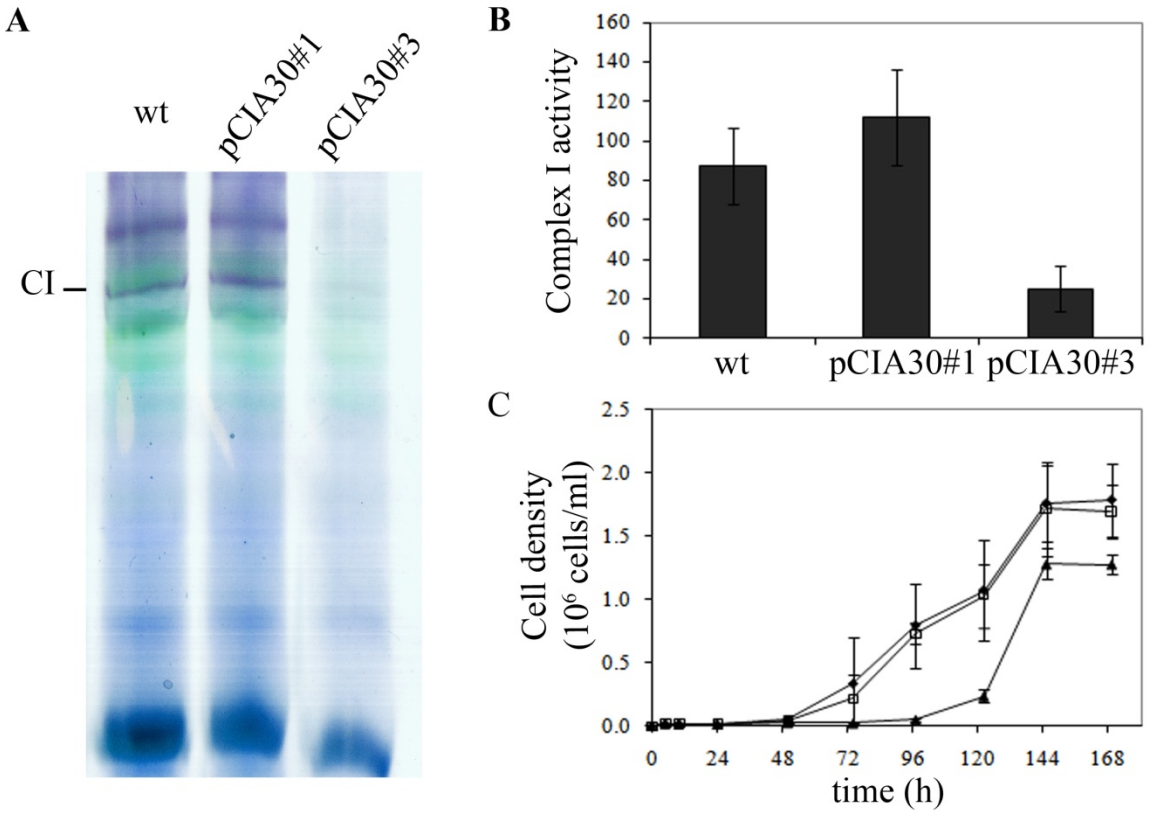

Figure 4.8. Complex I mutant phenotype in one of the transformants with amiCIA30-1.

A. BN-PAGE and *in gel* staining of Complex I. **B**. Complex I-specific activity (rotenone-sensitive) of partially purified membranes. **C.** Growth curve of transformants with *sid* phenotype. ◆, wildtype; ○, transformant CIA30#1; ▲, transformant CIA30#3.

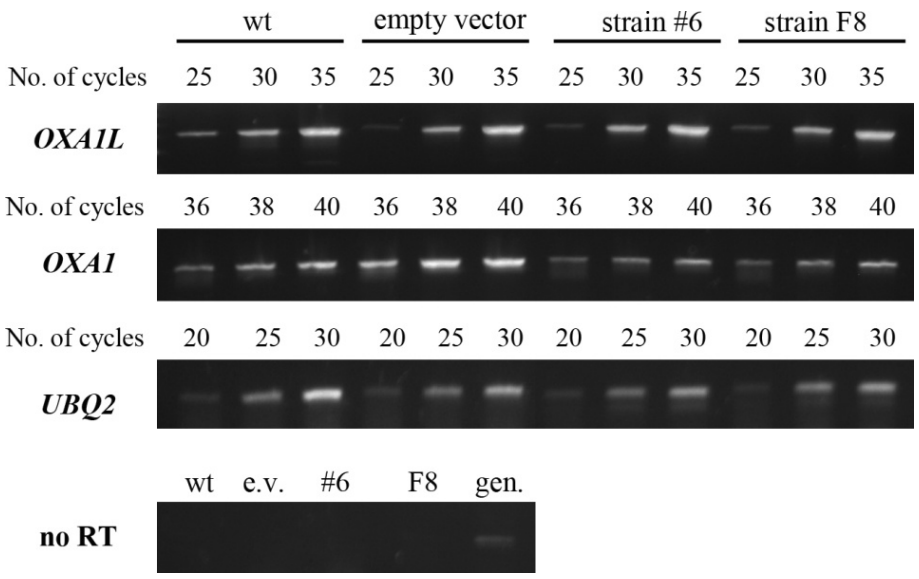

Figure 4.9. Semiquantitative RT-PCR expression analysis of the *OXA1* microRNAi transformants shows similar expression levels as the unstranformed controls

Oxa1L mRNA (*Oxa1L*) was specifically detected with Oxa1-EST1F and Oxa1-3R. Primers Oxa1F and Oxa2R were used to detect both forms of Oxa1 mRNA, generically *OXA1*. *UBQ2* mRNA was used as a loading control.

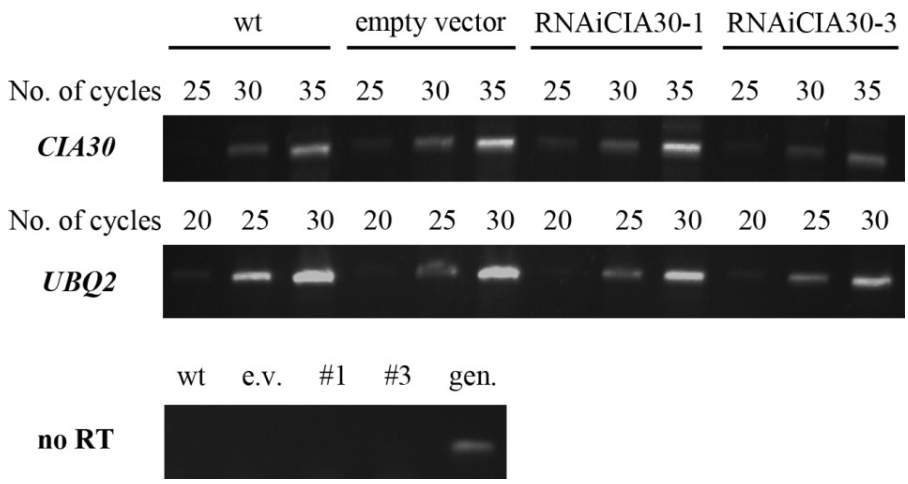

Figure 4.10. Semiquantitative RT-PCR of the CIA30 microRNAi transformants reveals that none of the to transformants with *sid* phenotype is depleted of *CIA30* mRNA.

CIA30 mRNA was specifically amplified with P9CIA30 and P10CIA30 primers. *UBQ2* mRNA was used as a loading control.

4.2.5. Interaction partners of CIA30

Because the deficiency of CIA30 produces a Complex I phenotype in most organisms studied, we aimed to identify possible interaction partners that could be involved in the Complex's assembly process. For this, we developed a yeast two-hybrid screening analysis using AtCIA30a cDNA as a bait in the pAS1 vector (DURFEE *et al.* 1993). A leaf and root *Arabidopsis* cDNA library available from the *Arabidopsis* Biological Resource Center (ABRC, The Ohio State University) was used as a prey and co-transformed into pJ69.4a strain (JAMES *et al.* 1996). The use of *Arabidopsis* instead of *Chlamydomonas* was aimed to avoid expression problems in yeast caused by the high GC

content of *Chlamydomonas* cDNAs. Co-transformants were selected for their growth in SD minus leucine (-L) and tryptophan (-W) plates. Positive interactions were selected in plates lacking leucine, tryptophan, histidine and adenine (-LWHA). Out of 120,000 transformants, 43 were confirmed positives based on the stringent selection on SD – LWHA, and SD-A (Figure 4.11). Prey plasmids were rescued from the positive interacting strains, retransformed in *E.coli* and sequenced.Table 4.1. Genomic annotation of confirmed interactions with pAS1-AtCIA30. Table 4.1 summarizes the identities of the interaction partners.

To our surprise, none of the positive interaction partners corresponded to Complex I subunits or proteins targeted to the mitochondria, the bulk of the identified interacting proteins being targeted to the chloroplast. The actual localization has been confirmed by mass spectrometry in several of these proteins as well as their role in chloroplast metabolism. It is therefore possible that AtCIA30a in *Arabidopsis* is targeted to the chloroplast instead of the mitochondria. This possibility originally ruled out based on the availability of mass spectrometry analyses of mitochondrial proteins in *Arabidopsis*, which positively showed the presence of AtCIA30a in this organelle (HEAZLEWOOD *et al.* 2004; KRUFT *et al.* 2001). The mitochondrial fractions in these two studies were 90 and 98.5 % pure, respectively. So far only a mitochondrial localization has been documented for AtCIA30. No data for chloroplast or secretory pathway localization (including proteomic and GFP data) for either isoform of AtCIA30 have been reported. Therefore, it is likely that the positive interactions that were found in this screening are not meaningful.

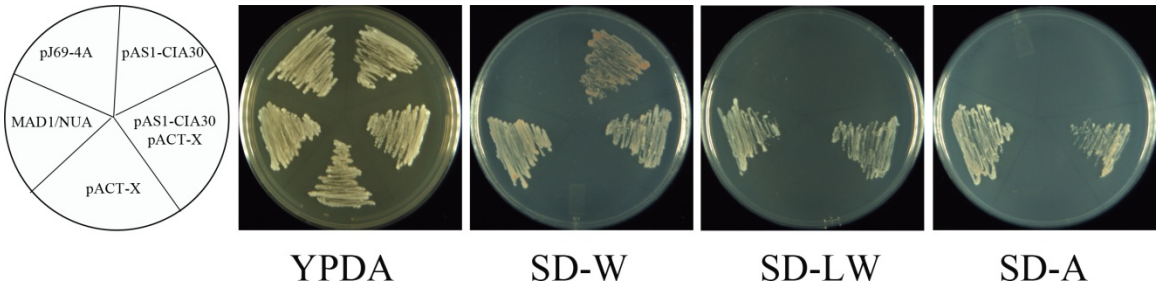

Figure 4.11. Example of the selection of a positive interacting strain X.

Strains were plated on YPDA, glucose dropout plates (SD) without tryptophan (-W) for selection of the bait vector, leucine and tryptophan (-LW) for selection of the bait and the prey, or adenine (-A) to test for interaction independently in the absence of vector selection. None of the preys in the positive interactions grew on SD-L or SD-A (not shown). MAD1/NUA was a kind gift of Siva Muttuswamy (PCMB, The Ohio State University) and was used as a positive control.

Accession	*n*	Description	TAIR Location	TargetP	Subcellular localization evidence
At1g29920	1	CAB2 (Chlorophyll a/b-binding protein 2); chlorophyll binding	thylakoid-integral	Chloroplast	chloroplast (FRISO *et al.* 2004)
At1g49380	1	cytochrome c biogenesis protein family	n.d.	Chloroplast	n.d.
At1g49720	1	ABF1 (Abscicic acid response binding factor 1); DNA binding / transcription activator/ transcription factor	n.d.	_	n.d.
At1g67090	3	RBCS1A; ribulose-bisphosphate carboxylase	plastid stroma	Chloroplast	chloroplast stroma (PELTIER *et al.* 2006)
At1g70760	2	subunit of the chloroplast NAD(P)H dehydrogenase complex, involved in PSI cyclic electron transport. Located on the thylakoid membrane. Mutant has impaired NAD(P)H dehydrogenase activity.	thylakoid-integral	Chloroplast	chloroplasts (SHIMIZU *et al.* 2008)
At1g78760	1	F-box family protein	nucleus	_	n.d.
At1g78830	1	curculin-like (mannose-binding) lectin family protein	apoplast	Secreted	cell wall proteome (IRSHAD *et al.* 2008)

Continued

Table 4.1. Genomic annotation of confirmed interactions with pAS1-AtCIA30.

n indicates the number of times a given accession was identified in the screen.

Table 4.1 continued

Accession	*n*	Description	TAIR Location	TargetP	Subcellular localization evidence
At2g30860	1	ATGSTF9 (Arabidopsis thaliana Glutathione S-transferase (class phi) 9); glutathione transferase	not plastid	_	plasma membrane (MARMAGNE *et al.* 2007), vacuole (CARTER *et al.* 2004), plastid (FRISO *et al.* 2004)
At2g45300	1	3-phosphoshikimate 1-carboxyvinyltransferase / 5-enolpyruvylshikimate-3-phosphate / EPSP synthase	chloroplast	Chloroplast	chloroplast (ZYBAILOV *et al.* 2008)
At3g12120	2	FAD2 (Fatty Acid Desaturase 2); delta12-fatty acid dehydrogenase	endoplasmic reticulum	_	n.d.
At3g14420	1	(S)-2-hydroxy-acid oxidase, peroxisomal, putative / glycolate oxidase, putative / short chain alpha-hydroxy acid oxidase, putative	peroxisome	_	nucleus (BAE *et al.* 2003), peroxisome (REUMANN *et al.* 2009), chloroplast (KLEFFMANN *et al.* 2004)
At3g20080	1	CYP705A15 (cytochrome P450, family 705, subfamily A, polypeptide 15); oxygen binding	endomembrane protein	Secreted	n.d.
At4g19420	1	pectinacetylesterase family protein	endomembrane system	Secreted	n.d.

Continued

Table 4.1 continued

Accession	*n*	Description	Location	TargetP	Subcellular localization evidence
At4g21860	1	MSRB2 (Methionine sulfoxide reductase B 2); peptide-methionine-(S)-S-oxide reductase	plastid stroma	Chloroplast	chloroplast (ZYBAILOV *et al.* 2008)
At4g29810	1	ATMKK2 (MAP KINASE KINASE 2); MAP kinase kinase/ kinase	plasma membrane	_	plasma membrane (BENSCHOP *et al.* 2007)
At5g02160	1	unknown protein	thylakoid membrane	Chloroplast	Thylakoid-stripped (PELTIER *et al.* 2004)
At5g04590	1	SIR (sulfite reductase); sulfite reductase (ferredoxin)	plastid stroma	Chloroplast	chloroplast (ZYBAILOV *et al.* 2008)
At5g11170	1	DEAD/DEAH box helicase, putative (RH15)	nucleolus	_	nucleolus (PENDLE *et al.* 2005)
At5g14260	2	SET domain-containing protein	plastid	Chloroplast	chloroplast (ZYBAILOV *et al.* 2008)
At5g23240	1	DNAJ heat shock N-terminal domain-containing protein	chloroplast	Chloroplast	n.d.
At5g42790	1	PAF1 (proteasome alpha subunit F1); peptidase	plasma membrane	_	plasma membrane (BENSCHOP *et al.* 2007)
At5g54770	1	THI1 (thiazole requiring)	mitochondria; plastid stroma	Chloroplast	chloroplast (ZYBAILOV *et al.* 2008), mitocondria (CHABREGAS *et al.* 2003)

Continued

Table 4.1 continued

Accession	*n*	Description	Location	TargetP	Subcellular localization evidence
At5g54810	1	TSB1 (Tryptophane synthase Beta-subunit)	plastid	Chloroplast	chloroplast (ZYBAILOV *et al.* 2008)
At5g66570	1	OE33/OEE1/OEE33/PSBO-1/PSBO1 (Oxygen-evolving enhancer 33); oxygen evolving/ poly(U) binding	thylakoid-peripheral-lumenal-side	Chloroplast	thylakoid (FRISO *et al.* 2004)
AtCG00140	1	ATPase III subunit	thylakoid-integral	Secreted	thylakoid (FRISO *et al.* 2004)
AtCg00950	6	Ribosomal RNA 23S	chloroplast encoded		

4.3. Discussion

The main objective of this chapter was to test the hypothesis that the assembly process of Complex I in *Chlamydomonas* is similar to other organisms in terms of functional conservation of its assembly factors. Validating this hypothesis is central to establishing *Chlamydomonas* as a model system to study Complex I defects associated to human disease. Because the Oxa1 function in assembly of Complex IV can be directly evaluated in yeast, a heterologous complementation approach was followed. In the case of *Chlamydomonas OXA1*, the annotated sequence was shorter than all functional *Oxa1* genes described so far. Based on the fact that the original gene prediction software for *Chlamydomonas* genome had been trained using other organisms we reasoned that probably the annotated sequence was erroneous and that the actual *OXA1* gene in *Chlamydomonas* was indeed similar to the other *Oxa1* sequences. The hypothesis was confirmed by functional complementation analyses which showed that only the ORF predicted using a program trained in *Chlamydomonas*, *OXA1L*, was able to restore respiratory growth and cytochrome assembly in yeast. Therefore, it is possible to conclude that *Chlamydomonas* OXA1 function is conserved and important for the assembly of respiratory complexes.

A second aim of this project was to test the function of assembly factors in their own genomic context. For that I used a microRNAi approach to test two of these factors, OXA1 and CIA30, for their role in Complex I assembly. Although I was able to isolate transformants displaying Complex I and Complex I and IV deficiency, the phenotypes

were independent of the knockdown strategy. One possible caveat of the screening methodology is that performing a phenotypic screening does not look directly for RNA knockdown but rather gives a strong selection for a desired phenotype. Thus, real knockdowns not displaying a phenotype were not selected. This approach however, was followed because of the simplicity of the visual screening. A second strategy to produce OXA1 and CIA30 mRNAi knockdown mutants is currently under test. This strategy makes use of an antisense construct nested inside an antisense construct for the *MAA7* gene, which encodes the tryptophane synthase β-subunit (ROHR *et al.* 2004). The system allows the direct selection of transformants expressing the antisense construct based on the resistance to the tryptophane analog 5-fluoroindole. Succeding in this strategy is particularly important to have a direct evaluation of gene function, especially for factors that are exclusively associated with Complex I and therefore cannot be tested in yeast.

The 40 clones retrieved from the two-hybrid screenen represented 25 *Arabidopsis* proteins plus one ribosomal RNA. Of them, only At5g54770 encoding a thiamine biosynthesis gene, has been reported to encode a protein localized to mitochondria (CHABREGAS *et al.* 2003). The study reports the presence of an alternative translation initiation codon that results in targeting of the protein either to chloroplasts or mitochondria. Most of the proteins had been previously identified in other subcellular compartment by mass spectrometry, particularly in the chloroplast (14 nuclear encoded plus two chloroplast encoded). Two other plastid proteins were found in additional compartments, including peroxisome, nucleus and vacuole. Other proteins have a predicted or demonstrated localization in the secretory system, including the apoplast.

Also, the size of this screening (10^5 transformants) was unsufficient to saturate all possible interaction pairs. Therefore, it is likely that proteins that have a low representation in the cDNA library have been missed. The physiological relevance of these interactions should be analyzed in the context of AtCIA30 localization. Because CIA30 is a low structured chaperone it is possible that the specificity of its interactions requires physical compartimentalization inside the mitochondria. The yeast two-hybrid approach followed here could have allowed for direct interactions between two proteins that are normally located in different organelles. If this is the case, co-immunoprecipitation using purified mitochondria would be a more optimal strategy. The assembly factor Ecsit was already found using this approach (VOGEL *et al.* 2007b). Alternatively, some of these proteins could be present within the mitochondria and not have been detected in past proteomic efforts (HEAZLEWOOD *et al.* 2004; KRUFT *et al.* 2001) because of their low abundance. This possibility seems unlikely for proteins belonging to the photosynthetic chain and these could have been detected because of their high representation in the cDNA library. Although AtCIA30 has only been identified in mitochondria, it is also possible that its localization be not exclusive to this organelle and that CIA30, as other mitochondrial proteins such as the Complex I subunit NDUFA13 (GRIM-19) and Ecsit (REEVES *et al.* 2007; VOGEL *et al.* 2007b) localize to other compartments under certain conditions.

4.4. Experimental procedures

4.4.1. Chlamydomonas strains and growth conditions.

For all experiments the 3A+ (*arg7*, 137c background) strain was grown under mixotrophic conditions in TAP media supplemented with 40 mg/l arginine at 25^{o}C.

4.4.2. Functional complementation of the yeast Δoxa1 mutant

The NBT1 *Δoxa1* mutant strain (BONNEFOY *et al.* 1994a) was used as the recipient strain. Diploid complementation of the *rho*^{0} JM6 strain was used to verify that the stored NBT1 strain retained the mitochondrial genome. The full-length cDNA for *OXA1* (*OXA1L*), the truncated version of *OXA1* cDNA (*OXA1S*), *ALB3.1* and *ALB3.2* cDNA were cloned into the yeast expression vector pYES2 (*URA3*) using traditional cloning techniques and transformed into the NBT1 strain. Plasmids were maintained in minimum medium dropout for uracile (SD-ura) and replicated on respiratory media: ethanol-glycerol and ethanol-glycerol, 0.02% galactose.

Whole cell spectra were recorded by Dr. Cristina Pannozzo at the Centre de Génétique Moléculaire du C.N.R.S., France. The pYES2 plasmids containing the *OXA1* constructs were transformed into strain NBT1/252 and grown in CSM plates without uracil and with addition of 2% galactose, 0.1% glucose, and supplemented with adenine. The spectra recorded at low temperature as described in (CLAISSE *et al.* 1970).

4.4.3. microRNAi plasmid construction

The target sequences for amiOxa1 and amiCIA30 construction were chosen from a selection generated using the WMD microRNAi Designer tool (http://wmd2.weigelworld.org) (SCHWAB *et al.* 2006). The precursor sequences and the derived amiRNAi primer sequences are shown in Table 4.2 and Table 4.3. The amiRNAi primers were annealed and cloned into the SpeI site of pChlamiRNA1 and pChlamyRNA2 vectors to generate pChlamyCIA30.1 and pChlamyCIA30.2 plasmids and into pChlamyRNA3 and pHyg3 for *OXA1* using traditional molecular biology techniques.

4.4.4. Chlamydomonas transformation and knockdown screening.

Exponentially grown cells were transformed with 5 μg of plasmid by electroporation as previously described (SHIMOGAWARA *et al.* 1998) with minor modifications. Individual transformants were selected in TAP, 25 μg/ml paromomycin under light conditions were replica-plated in the dark to isolate slow growth in the dark (*sid*) mutants.

4.4.5. BN-PAGE and in-gel activity staining of respiratory Complexes.

BN-PAGE and Complex I activity staining were performed as described in section 2.4.7. For Complex IV *in gel* activity the gel was incubated in staining buffer IV: 0.05 mg/ml 3,3'-Diaminobenzidine (Rockland Immunochemicals), 1 mg/ml cytochrome *c* (horse heart, Sigma), 0.2 μg/ml catalase (Sigma), 75 mg/ml sucrose, 10 mM MOPS-KOH, pH 7.4).

4.4.6. RNA analyses.

Logaritmically-grown liquid mixotrophic cultures were used for total RNA isolation using a protocol modified from (SOMANCHI and MORONEY 1999). Precipitated cultures were lysed for in freshly prepared lysis buffer (10 mM Tris-HCl pH7.5, 30 mM NaCl, 30 mM EDTA, 4% SDS, 0.08 mg/ml proteinase K (Invitrogen) for 20 minutes at room temperature with gentle agitation. The lysate was extracted twice with phenol: chloroform: isoamyl alcohol (25:24:1), twice with chloroform: isoamyl alcohol, and precipitated with 6 M LiCl (4^{o}C) overnight. The pellet was resuspended in water and treated with DNAseI (Invitrogen), followed by a second phenol extraction and ethanol wash. For semiquantitative RT-PCR ImPromII reverse transcriptase (Promega Corp.) was used following the manufacturer's instructions with specific primers for the controls and tested genes were used. GoTaq Polymerase (Promega) was used as directed by the manufacturer with the addition of 2.5% DMSO. Primers are listed on Table 4.4.

4.4.7. Yeast-two hybrid analyses.

Bait plasmid construction. To generate the bait vectors, pAS1 (DURFEE *et al.* 1993) containing the GAL4 binding domain was used. To generate pAS-AtCIA30, AtCIA30 ORF was amplified by PCR from the vector U86534 containing AtCIA30 cDNA ORF was amplified with Pfu Turbo (Stratagene) and primers U86534-NdeF and U86534-NcoR. Annealing was performed at 55^{o}C. Primers are listed in Table 4.4. The PCR products and pAS1 were digested with NdeI and NcoI and ligated overnight with T4 DNA ligase (Invitrogen). The purified plasmid was sequenced and transformed into the reporter yeast strain Y190 (*MATa gal4 gal80 his3 trp-901 ade2-101 ura3-52 leu2-3,-112*

+URA3::GAL→lacZ, LYS2::GAL(UAS)→HIS3 cyh^{r}) (DURFEE *et al.* 1993) and selected on SD–W plates.

cDNA library preparation. To look for direct interaction partners of AtCIA30 the *Arabidopsis* Walker two-hybrid cDNA library (*Arabidopsis* Biological Resource Center and NSF/DOE/USDA Collaborative Research in Plant Biology Program, Research Collaboration Group in Plant Protein Phosphorylation -USDA*92-37105-7675*). 1.5 x 10^9 p.f.u were converted into plasmid in *E.coli* BNN132 with 30 % efficiency and purified using the PC2000 Mega Plasmid purification kit (Clontech) using the low-copy number plasmid protocol as directed by the manufacturer.

Library screening. Two micrograms of library plasmid were transformed into the recipient yeast strain carrying pAS-AtCIA30 and plated directly into SD media without tryptophane and leucine (SD-WL) for bait and prey selection, respectively, and grown for 4 days at 28^{o}C. Transformation efficiency was approximately 10^5 c.f.u./μg_{DNA}. Replicas were plated in SD-WL and drop out for histidine (-H) and adenine (-A) to select for positive interactions. To eliminate possible false positives, all interaction candidates were plated again on SD-A. Plasmids from positive clones were rescued in *E.coli* EC8 strain (*leu*$^{-}$ *trp*$^{-}$ *his*$^{-}$) and retransformed into Y190 alone or together with pAS-AtCIA30. Plasmids that restored the adenine prototrophy only when co-transformed with the bait plasmid were sequenced.

Precursor	Position	Primer name	amiRNAi primer sequence (5'→3')
amiCrCIA30-1	3'-UTR	amiForCIA30-1	ctagtGACGCGTTTACTTCGTCAATAtctcgctgatcggcaccatggg ggtggtggtgatcagcgctaTATTCACGAAGTAAACGCGTCg
		amiRevCIA30-1	ctagcGACGCGTTTACTTCGTGAATAtagcgctgatcaccaccaccc ccatggtgccgatcagcgagaTATTGACGAAGTAAACGCGTCa
amiCrCIA30-2	5'-UTR	amiForCIA30-2	ctagtCCGCACTTACATACAGACTTAtctcgctgatcggcaccatggg ggtggtggtgatcagcgctaTAAGACTGTATGTAAGTGCGGg
		amiRevCIA30-2	ctagcCCGCACTTACATACAGTCTTAtagcgctgatcaccaccaccc ccatggtgccgatcagcgagaTAAGTCTGTATGTAAGTGCGGa

Table 4.2. microRNAi constructs to target CIA30

Target gene	Precursor	Position	Primer name	amiRNAi primer sequence (5'→3')
OXA1S	amiCrOxaS1	exon 1	amiFor_CrOxaS1	ctagtAACCCCAATGTTCCCGTAGAAtctcgctgatcggcaccatg ggggtggtggtgatcagcgctaTTCTGTGGGAACATTGGGGTTg
			amiRev_CrOxaS1	ctagcAACCCCAATGTTCCCACAGAAtagcgctgatcaccaccac ccccatggtgccgatcagcgagaTTCTACGGGAACATTGGGGTTa
	amiCrOxaS2	3'-UTR	amiFor_CrOxaS2	ctagtCGCCCTTCCACTTTGTATGAAtctcgctgatcggcaccatgg gggtggtggtgatcagcgctaTTCAAACAAAGTGGAAGGGCGg
			amiRev_CrOxaS2	ctagcCGCCCTTCCACTTTGTTTGAAtagcgctgatcaccaccacc cccatggtgccgatcagcgagaTTCATACAAAGTGGAAGGGCGa
OXA1L	amiCrOxaL1	5'-UTR	amiFor_CrOxaL1	ctagtCGTCACAAAGTTATAAATGAAtctcgctgatcggcaccatg ggggtggtggtgatcagcgctaTTCAATTATAACTTTGTGACGg
			amiRev_CrOxaL1	ctagcCGTCACAAAGTTATAATTGAAtagcgctgatcaccaccac ccccatggtgccgatcagcgagaTTCATTTATAACTTTGTGACGa
	amiCrOxaL2	exon 1	amiFor_CrOxaL2	ctagtGCACGCGTTCTTTTCCCCATAtctcgctgatcggcaccatgg gggtggtggtgatcagcgctaTATGCGGAAAAGAACGCGTGCg
			amiRev_CrOxaL2	ctagcGCACGCGTTCTTTTCCGCATAtagcgctgatcaccaccacc cccatggtgccgatcagcgagaTATGGGGAAAAGAACGCGTGCa

Table 4.3. Constructs used for the microRNAi knockdown of *CIA30* and *OXA1*

Target gene	Primer name	Primer sequence (5'→ 3')	Annealing (°C)	Reference
CIA30	U86534-NdeF	CTTGGGTGGTCATATGTCAAGG TTTCGATCG	55	this work
	U86534-NcoR	ATCCGTAGCCATGGCTTACGGC AATCTCAAGG	55	this work
	P9CIA30	GAACCAAGTGCGCAAGA	60	this work
	P10CIA30	GCCTTGTCTTGAGTGTGGTC	60	this work
OXA1	Oxa1F	GCGCCATCTTCTTGTCCATC	55	this work
	Oxa2R	TCGTTGCGCAGTGTGAGGC	55	this work
	Oxa1-EST-1F	CAGTCCAGTGCAATCAGTTCC	55	this work
	Oxa13R	GATGGCGATGGACAAGAACC	55	this work
UBQ2	UBQ2-F	GCGATTTCTCGTTGGGCAGT	57	(ALLEN *et al.* 2008)
	UBQ2-R	TGGCCCATCCACTTGTCCTT	57	

Table 4.4. Primers used in Chapter 3.

CHAPTER 5

CONCLUSIONS AND PERSPECTIVES

In this work, we developed the green alga *Chlamydomonas reinhardtii* as a model system to study Complex I assembly. Although several other systems have been used so far, the discovery of novel assembly factors that could explain Complex I associated mitochondrial disease has been prevented by the lack of a straightforward screening approaches. In contrast to other organisms, we proposed that *Chlamydomonas* provides a main advantage to develop forward screening strategies in relation to mitochondrial deficiency by offering a visual phenotype that facilitates the isolation of a mutant population consisting of respiratory mutants. Currently, *Chlamydomonas reinhardtii* is the only available system where Complex I mutants can be screened using a forward genetics approach. The finding of five new *amc* loci in Chapter 2 (in addition to three additional mutants in Chapter 4) highlights the potential of this organism as a model system to study Complex I but also mutations in other complexes. Indeed, one of the mutants found in Chapter 4 (strain #6) is also affected in Complex IV activity.

Here we report the first molecular identification of a Complex I mutant of nuclear origin in *Chlamydomonas*. The mutation in *amc5* and *amc7* was identified as the *NUOB10* gene, encoding for the ortholog of the bovine PSDW subunit. This subunit has been poorly characterized in other systems and no information is available on its biochemical function, particularly on its role in assembly of the membrane arm. Particularly, the question of how NUOB10 interacts with other Complex I subunits to determine the assembly of a functional Complex I should be addressed. The lack of mitochondrial targeting sequence and the presence of a $C(X)_{11}C$ motif suggest that possibly NUOB10 is imported to the intermembrane space and uses a system similar to Erv1-Mia40 for its folding and insertion into Complex I. Because no experimental data on the localization of PSDW with respect to the mitochondrial inner membrane are available, this hypothesis has to be further evaluated.

The discovery potential of *Chlamydomonas* in relation to the finding of new factors involved in Complex I assembly is highlighted in *amc2* (Chapter 3), which was mapped to a region of chromosome 10 that does not encode subunits of the Complex I or known or proposed assembly factors. It was concluded that the recessive *amc2* mutation (see section 2.2.4) is affecting a locus involved in Complex I assembly. Sequencing results of several parts of the genomic region failed to identify this mutation so far. The sequencing effort will be continued, in an attempt to identify the new factor encoded by *AMC2*.

As a proof of concept for respiratory complex assembly conservation, a heterologous complementation approach was used. We were able to proove that the

Chlamydomonas ortholog of human and yeast Oxa1, a protein involved in the insertion of membrane subunits of several respiratory complexes, is able to restore respiratory growth in a yeast *oxa1* deletion mutant by restoring assembly of the cytochrome oxidase complex (Complex IV). *Chlamydomonas* OXA1 role conservation in the assembly of Complex IV was not evident since the most characterized substrate of Oxa1p in yeast, Cox2, is split in two genes *Chlamydomonas* and encoded by the nuclear genome. Particularly, the ability of *Chlamydomonas* OXA1 to assemble of the C-terminal part of Cox2 could have been lost, since COX2B in *Chlamydomonas* seems to be imported directly to the intermembrane space. The ability of *Chlamydomonas* OXA1 to act upon Cox2 when expressed in yeast does not imply that Cox2 is necessarily a substrate of OXA1 in *Chlamydomonas* mitochondria. One possibility is that OXA1 in *Chlamydomonas* is only required to insert mitochondrial ND subunits and hence is restricted to the assembly of Complex I. To explore this hypothesis, a microRNAi knockdown strategy was attempted using Oxa1 and CIA30 as targets, but yielded unsuccessful results. An alternative procedure for microRNAi knockdown is currently undergoing. In this new experimental approach to RNAi (ROHR *et al.* 2004), a direct selection of transformants expressing the RNAi is used. This approach is also being tested for the knock-down of CIA30.

Future projects will focus on the identification and characterization of the *amc* mutations at the molecular level and analyzing their role in the context of human disease.

Bibliography

ABDRAKHMANOVA, A., V. ZICKERMANN, M. BOSTINA, M. RADERMACHER, H. SCHAGGER *et al.*, 2004 Subunit composition of mitochondrial complex I from the yeast *Yarrowia lipolytica*. Biochim Biophys Acta **1658:** 148-156.

ABDRAKHMANOVA, A., K. ZWICKER, S. KERSCHER, V. ZICKERMANN and U. BRANDT, 2006 Tight binding of NADPH to the 39-kDa subunit of complex I is not required for catalytic activity but stabilizes the multiprotein complex. Biochim Biophys Acta **1757:** 1676-1682.

ADAM, M., and R. LOPPES, 1998 Use of the ARG7 gene as an insertional mutagen to clone PHON24, a gene required for derepressible neutral phosphatase activity in Chlamydomonas reinhardtii. Mol Gen Genet **258:** 123-132.

AGGELER, R., and R. A. CAPALDI, 1990 Yeast cytochrome c oxidase subunit VII is essential for assembly of an active enzyme. Cloning, sequencing, and characterization of the nuclear-encoded gene. J Biol Chem **265:** 16389-16393.

ALBER, B. E., and J. G. FERRY, 1994 A carbonic anhydrase from the archaeon Methanosarcina thermophila. Proc Natl Acad Sci U S A **91:** 6909-6913.

ALLEN, M. D., J. KROPAT and S. S. MERCHANT, 2008 Regulation and localization of isoforms of the aerobic oxidative cyclase in Chlamydomonas reinhardtii. Photochem Photobiol **84:** 1336-1342.

ALTAMURA, N., N. CAPITANIO, N. BONNEFOY, S. PAPA and G. DUJARDIN, 1996 The *Saccharomyces cerevisiae OXA1* gene is required for the correct assembly of cytochrome *c* oxidase and oligomycin-sensitive ATP synthase. FEBS Lett. **382:** 111-115.

ALVES, P. C., and A. VIDEIRA, 1998 The membrane domain of complex I is not assembled in the stopper mutant E35 of Neurospora. Biochem Cell Biol **76:** 139-143.

ANTONICKA, H., I. OGILVIE, T. TAIVASSALO, R. P. ANITORI, R. G. HALLER *et al.*, 2003 Identification and characterization of a common set of complex I assembly intermediates in mitochondria from patients with complex I deficiency. J. Biol. Chem. **278:** 43081-43088.

BAE, M. S., E. J. CHO, E. Y. CHOI and O. K. PARK, 2003 Analysis of the Arabidopsis nuclear proteome and its response to cold stress. Plant J **36:** 652-663.

BANCHIO, C., L. M. SCHANG and D. E. VANCE, 2004 Phosphorylation of Sp1 by cyclin-dependent kinase 2 modulates the role of Sp1 in CTP:phosphocholine cytidylyltransferase alpha regulation during the S phase of the cell cycle. J Biol Chem **279:** 40220-40226.

BARRIENTOS, A., 2003 Yeast models of human mitochondrial diseases. IUBMB Life **55:** 83-95.

BAURAIN, D., M. DINANT, N. COOSEMANS and R. F. MATAGNE, 2003 Regulation of the alternative oxidase Aox1 gene in Chlamydomonas reinhardtii. Role of the nitrogen source on the expression of a reporter gene under the control of the Aox1 promoter. Plant Physiol **131:** 1418-1430.

BELLAFIORE, S., P. FERRIS, H. NAVER, V. GOHRE and J. D. ROCHAIX, 2002 Loss of Albino3 leads to the specific depletion of the light-harvesting system. Plant Cell **14:** 2303-2314.

BEN-SHACHAR, D., and R. KARRY, 2007 Sp1 expression is disrupted in schizophrenia; a possible mechanism for the abnormal expression of mitochondrial complex I genes, NDUFV1 and NDUFV2. PLoS One **2:** e817.

BENSCHOP, J. J., S. MOHAMMED, M. O'FLAHERTY, A. J. HECK, M. SLIJPER *et al.*, 2007 Quantitative phosphoproteomics of early elicitor signaling in Arabidopsis. Mol Cell Proteomics **6:** 1198-1214.

BERRISFORD, J. M., and L. A. SAZANOV, 2009 Structural basis for the mechanism of respiratory complex I. J Biol Chem **284:** 29773-29783.

BERTHOLD, P., R. SCHMITT and W. MAGES, 2002 An engineered Streptomyces hygroscopicus aph 7" gene mediates dominant resistance against hygromycin B in Chlamydomonas reinhardtii. Protist **153:** 401-412.

BONHOMME, S., F. BUDAR, D. LANCELIN, I. SMALL, M. C. DEFRANCE *et al.*, 1992 Sequence and transcript analysis of the Nco2.5 Ogura-specific fragment correlated with cytoplasmic male sterility in Brassica cybrids. Mol Gen Genet **235:** 340-348.

BONNEFOY, N., F. CHALVET, P. HAMEL, P. P. SLONIMSKI and G. DUJARDIN, 1994a OXA1, a Saccharomyces cerevisiae nuclear gene whose sequence is conserved from prokaryotes to eukaryotes controls cytochrome oxidase biogenesis. J Mol Biol **239:** 201-212.

BONNEFOY, N., H. L. FIUMERA, G. DUJARDIN and T. D. FOX, 2009 Roles of Oxa1-related inner-membrane translocases in assembly of respiratory chain complexes. Biochim Biophys Acta **1793:** 60-70.

BONNEFOY, N., M. KERMORGANT, O. GROUDINSKY, M. MINET, P. P. SLONIMSKI *et al.*, 1994b Cloning of a human gene involved in cytochrome oxidase assembly by functional complementation of an oxa1- mutation in Saccharomyces cerevisiae. Proc Natl Acad Sci U S A **91:** 11978-11982.

BRADLEY, J. L., J. C. BLAKE, S. CHAMBERLAIN, P. K. THOMAS, J. M. COOPER *et al.*, 2000 Clinical, biochemical and molecular genetic correlations in Friedreich's ataxia. Hum Mol Genet **9:** 275-282.

BRANDT, U., 2006 Energy converting NADH:quinone oxidoreductase (complex I). Annu Rev Biochem **75:** 69-92.

BRANGEON, J., M. SABAR, S. GUTIERRES, B. COMBETTES, J. BOVE *et al.*, 2000 Defective splicing of the first nad4 intron is associated with lack of several complex I subunits in the Nicotiana sylvestris NMS1 nuclear mutant. Plant J **21:** 269-280.

BUDAR, F., P. TOUZET and R. DE PAEPE, 2003 The nucleo-mitochondrial conflict in cytoplasmic male sterilities revisited. Genetica **117:** 3-16.

BULTÉ, L., P. GANS, F. REBÉILLÉ and F.-A. WOLLMAN, 1990 ATP control on state transitions in vivo in Chlamydomonas reinhardtii. Biochimica et Biophysica Acta (BBA) - Bioenergetics **1020:** 72-80.

BUSI, M. V., M. V. MALIANDI, H. VALDEZ, M. CLEMENTE, E. J. ZABALETA *et al.*, 2006 Deficiency of Arabidopsis thaliana frataxin alters activity of mitochondrial Fe-S proteins and induces oxidative stress. Plant J **48:** 873-882.

BYCH, K., S. KERSCHER, D. J. NETZ, A. J. PIERIK, K. ZWICKER *et al.*, 2008 The iron-sulphur protein Ind1 is required for effective complex I assembly. Embo J **27:** 1736-1746.

CARDOL, P., J. ALRIC, J. GIRARD-BASCOU, F. FRANCK, F. A. WOLLMAN *et al.*, 2009 Impaired respiration discloses the physiological significance of state transitions in Chlamydomonas. Proc Natl Acad Sci U S A **106:** 15979-15984.

CARDOL, P., L. BOUTAFFALA, S. MEMMI, B. DEVREESE, R. F. MATAGNE *et al.*, 2008 In Chlamydomonas, the loss of ND5 subunit prevents the assembly of whole mitochondrial complex I and leads to the formation of a low abundant 700 kDa subcomplex. Biochim Biophys Acta **1777:** 388-396.

CARDOL, P., R. DE PAEPE, F. FRANCK, G. FORTI and G. FINAZZI, 2010 The onset of NPQ and Deltamu(H)+ upon illumination of tobacco plants studied through the influence of mitochondrial electron transport. Biochim Biophys Acta **1797:** 177-188.

CARDOL, P., G. GLOIRE, M. HAVAUX, C. REMACLE, R. MATAGNE *et al.*, 2003 Photosynthesis and state transitions in mitochondrial mutants of Chlamydomonas reinhardtii affected in respiration. Plant Physiol **133:** 2010-2020.

CARDOL, P., D. GONZALEZ-HALPHEN, A. REYES-PRIETO, D. BAURAIN, R. F. MATAGNE *et al.*, 2005 The mitochondrial oxidative phosphorylation proteome of Chlamydomonas reinhardtii deduced from the Genome Sequencing Project. Plant Physiol **137:** 447-459.

CARDOL, P., M. LAPAILLE, P. MINET, F. FRANCK, R. F. MATAGNE *et al.*, 2006 ND3 and ND4L subunits of mitochondrial complex I, both nucleus encoded in Chlamydomonas reinhardtii, are required for activity and assembly of the enzyme. Eukaryot Cell **5:** 1460-1467.

CARDOL, P., R. F. MATAGNE and C. REMACLE, 2002 Impact of mutations affecting ND mitochondria-encoded subunits on the activity and assembly of complex I in Chlamydomonas. Implication for the structural organization of the enzyme. J Mol Biol **319:** 1211-1221.

CARDOL, P., F. VANROBAEYS, B. DEVREESE, J. VAN BEEUMEN, R. F. MATAGNE *et al.*, 2004 Higher plant-like subunit composition of mitochondrial complex I from Chlamydomonas reinhardtii: 31 conserved components among eukaryotes. Biochim Biophys Acta **1658:** 212-224.

CARROLL, J., I. M. FEARNLEY, R. J. SHANNON, J. HIRST and J. E. WALKER, 2003 Analysis of the subunit composition of complex I from bovine heart mitochondria. Mol Cell Proteomics **2:** 117-126.

CARTER, C., S. PAN, J. ZOUHAR, E. L. AVILA, T. GIRKE *et al.*, 2004 The vegetative vacuole proteome of Arabidopsis thaliana reveals predicted and unexpected proteins. Plant Cell **16:** 3285-3303.

CHABREGAS, S. M., D. D. LUCHE, M. A. VAN SLUYS, C. F. MENCK and M. C. SILVA-FILHO, 2003 Differential usage of two in-frame translational start codons regulates subcellular localization of Arabidopsis thaliana THI1. J Cell Sci **116:** 285-291.

CHEN, H., P. A. ROMO-LEROUX and M. L. SALIN, 1996 The iron-containing superoxide dismutase-encoding gene from *Chlamydomonas reinhardtii* obtained by direct and inverse PCR. Gene **168:** 113-116.

CLAISSE, M. L., G. A. PERE-AUBERT, L. P. CLAVILIER and P. P. SLONIMSKI, 1970 [Method for the determination of cytochrome concentrations in whole yeast cells]. Eur. J .Biochem. **16:** 430-438.

CLASON, T., T. RUIZ, H. SCHAGGER, G. PENG, V. ZICKERMANN *et al.*, 2009 The structure of eukaryotic and prokaryotic complex I. J Struct Biol.

CLASON, T., V. ZICKERMANN, T. RUIZ, U. BRANDT and M. RADERMACHER, 2007 Direct localization of the 51 and 24 kDa subunits of mitochondrial complex I by three-dimensional difference imaging. J Struct Biol **159:** 433-442.

DAY, D. A., 1985 Interactions between the Glycine Decarboxylase, the Tricarbocylic Acid Cylce and the Respiratory Chain in Pea Leaf Mitochondria. Australian Journal of Plant Physiology **12:** 119-130.

DE PAEPE, R., P. CHETRIT, V. VITART, F. AMBARD-BRETTEVILLE, D. PRAT *et al.*, 1990 Several nuclear genes control both male sterility and mitochondrial protein synthesis in Nicotiana sylvestris protoclones. Mol Gen Genet **222:** 206-210.

DENG, X., and M. ERIKSSON, 2007 Two iron-responsive promoter elements control expression of FOX1 in Chlamydomonas reinhardtii. Eukaryot Cell **6:** 2163-2167.

DENT, R. M., C. M. HAGLUND, B. L. CHIN, M. C. KOBAYASHI and K. K. NIYOGI, 2005 Functional genomics of eukaryotic photosynthesis using insertional mutagenesis of Chlamydomonas reinhardtii. Plant Physiol **137:** 545-556.

DI FONZO, A., D. RONCHI, T. LODI, E. FASSONE, M. TIGANO *et al.*, 2009 The mitochondrial disulfide relay system protein GFER is mutated in autosomal-recessive myopathy with cataract and combined respiratory-chain deficiency. Am J Hum Genet **84:** 594-604.

DORTHU, M. P., S. REMY, M. R. MICHEL-WOLWERTZ, L. COLLEAUX, D. BREYER *et al.*, 1992 Biochemical, genetic and molecular characterization of new respiratory-deficient mutants in Chlamydomonas reinhardtii. Plant Mol Biol **18:** 759-772.

DOUCE, R., J. BOURGUIGNON, M. NEUBURGER and F. REBEILLE, 2001 The glycine decarboxylase system: a fascinating complex. Trends Plant Sci **6:** 167-176.

DUARTE, M., N. MOTA, L. PINTO and A. VIDEIRA, 1998 Inactivation of the gene coding for the 30.4-kDa subunit of respiratory chain NADH dehydrogenase: is the enzyme essential for Neurospora? Mol Gen Genet **257:** 368-375.

DUARTE, M., R. SOUSA and A. VIDEIRA, 1995 Inactivation of genes encoding subunits of the peripheral and membrane arms of neurospora mitochondrial complex I and effects on enzyme assembly. Genetics **139:** 1211-1221.

DUARTE, M., and A. VIDEIRA, 2000 Respiratory Chain Complex I Is Essential for Sexual Development in Neurospora and Binding of Iron Sulfur Clusters Are Required for Enzyme Assembly. Genetics **156:** 607-615.

DUDKINA, N. V., H. EUBEL, W. KEEGSTRA, E. J. BOEKEMA and H. P. BRAUN, 2005 Structure of a mitochondrial supercomplex formed by respiratory-chain complexes I and III. Proc Natl Acad Sci U S A **102:** 3225-3229.

DUNNING, C. J., M. MCKENZIE, C. SUGIANA, M. LAZAROU, J. SILKE *et al.*, 2007 Human CIA30 is involved in the early assembly of mitochondrial complex I and mutations in its gene cause disease. Embo J **26:** 3227-3237.

DURFEE, T., K. BECHERER, P. L. CHEN, S. H. YEH, Y. YANG *et al.*, 1993 The retinoblastoma protein associates with the protein phosphatase type 1 catalytic subunit. Genes Dev **7:** 555-569.

DUROC, Y., C. GAILLARD, S. HIARD, M. C. DEFRANCE, G. PELLETIER *et al.*, 2005 Biochemical and functional characterization of ORF138, a mitochondrial protein responsible for Ogura cytoplasmic male sterility in Brassiceae. Biochimie **87:** 1089-1100.

DUROC, Y., S. HIARD, N. VRIELYNCK, S. RAGU and F. BUDAR, 2009 The Ogura sterility-inducing protein forms a large complex without interfering with the oxidative phosphorylation components in rapeseed mitochondria. Plant Mol Biol **70:** 123-137.

DUTILLEUL, C., S. DRISCOLL, G. CORNIC, R. DE PAEPE, C. H. FOYER *et al.*, 2003 Functional mitochondrial complex I is required by tobacco leaves for optimal photosynthetic performance in photorespiratory conditions and during transients. Plant Physiol **131:** 264-275.

DUTILLEUL, C., C. LELARGE, J. L. PRIOUL, R. DE PAEPE, C. H. FOYER *et al.*, 2005 Mitochondria-driven changes in leaf NAD status exert a crucial influence on the control of nitrate assimilation and the integration of carbon and nitrogen metabolism. Plant Physiol **139:** 64-78.

ELORZA, A., H. ROSCHZTTARDTZ, I. GOMEZ, A. MOURAS, L. HOLUIGUE *et al.*, 2006 A nuclear gene for the iron-sulfur subunit of mitochondrial complex II is specifically expressed during Arabidopsis seed development and germination. Plant Cell Physiol **47:** 14-21.

ERMILOVA, E. V., Z. M. ZALUTSKAYA, B. V. GROMOV, D. P. HADER and S. PURTON, 2000 Isolation and characterisation of chemotactic mutants of Chlamydomonas reinhardtii obtained by insertional mutagenesis. Protist **151:** 127-137.

FATO, R., C. BERGAMINI, M. BORTOLUS, A. L. MANIERO, S. LEONI *et al.*, 2009 Differential effects of mitochondrial Complex I inhibitors on production of reactive oxygen species. Biochim Biophys Acta **1787:** 384-392.

FATO, R., E. ESTORNELL, S. DI BERNARDO, F. PALLOTTI, G. PARENTI CASTELLI *et al.*, 1996 Steady-state kinetics of the reduction of coenzyme Q analogs by complex I (NADH:ubiquinone oxidoreductase) in bovine heart mitochondria and submitochondrial particles. Biochemistry **35:** 2705-2716.

FEARNLEY, I. M., J. CARROLL and J. E. WALKER, 2007 Proteomic analysis of the subunit composition of complex I (NADH:ubiquinone oxidoreductase) from bovine heart mitochondria. Methods Mol Biol **357:** 103-125.

FECKE, W., V. D. SLED, T. OHNISHI and H. WEISS, 1994 Disruption of the gene encoding the NADH-binding subunit of NADH: ubiquinone oxidoreductase in Neurospora crassa. Formation of a partially assembled enzyme without FMN and the iron-sulphur cluster N-3. Eur J Biochem **220:** 551-558.

FIGUEROA-MARTINEZ, F., S. FUNES, L. G. FRANZEN and D. GONZALEZ-HALPHEN, 2008 Reconstructing the mitochondrial protein import machinery of Chlamydomonas reinhardtii. Genetics **179:** 149-155.

FIUMERA, H. L., S. A. BROADLEY and T. D. FOX, 2007 Translocation of mitochondrially synthesized Cox2 domains from the matrix to the intermembrane space. Mol Cell Biol **27:** 4664-4673.

FRISO, G., L. GIACOMELLI, A. J. YTTERBERG, J. B. PELTIER, A. RUDELLA *et al.*, 2004 In-depth analysis of the thylakoid membrane proteome of Arabidopsis thaliana chloroplasts: new proteins, new functions, and a plastid proteome database. Plant Cell **16:** 478-499.

GALKIN, A., S. DROSE and U. BRANDT, 2006 The proton pumping stoichiometry of purified mitochondrial complex I reconstituted into proteoliposomes. Biochim Biophys Acta **1757:** 1575-1581.

GALVAN, A., D. GONZALEZ-BALLESTER and E. FERNANDEZ, 2007 Insertional mutagenesis as a tool to study genes/functions in Chlamydomonas. Adv Exp Med Biol **616:** 77-89.

GARMIER, M., A. J. CARROLL, E. DELANNOY, C. VALLET, D. A. DAY *et al.*, 2008 Complex I dysfunction redirects cellular and mitochondrial metabolism in Arabidopsis. Plant Physiol **148:** 1324-1341.

GERARDS, M., W. SLUITER, B. J. VAN DEN BOSCH, E. DE WIT, C. M. CALIS *et al.*, 2009 Defective complex I assembly due to C20orf7 mutations as a new cause of Leigh syndrome. J Med Genet.

GOHRE, V., F. OSSENBUHL, M. CREVECOEUR, L. A. EICHACKER and J. D. ROCHAIX, 2006 One of two alb3 proteins is essential for the assembly of the photosystems and for cell survival in Chlamydomonas. Plant Cell **18:** 1454-1466.

GOLDSCHMIDT-CLERMONT, M., 1986 The two genes for the small subunit of RuBP Carboxylase/oxygenase are closely linked in *Chlamydomonas reinhardtii*. Plant Molecular Biology **6:** 13-21.

GRAD, L. I., and B. D. LEMIRE, 2004 Mitochondrial complex I mutations in Caenorhabditis elegans produce cytochrome c oxidase deficiency, oxidative stress and vitamin-responsive lactic acidosis. Hum Mol Genet **13:** 303-314.

GRAY, M. W., G. BURGER and B. F. LANG, 2001 The origin and early evolution of mitochondria. Genome Biol **2:** REVIEWS1018.

GREEN, D. E., and A. TZAGOLOFF, 1966 The mitochondrial electron transfer chain. Arch Biochem Biophys **116:** 293-304.

GU, J., S. DEMPSEY and K. J. NEWTON, 1994 Rescue of a maize mitochondrial cytochrome oxidase mutant by tissue culture. Plant J **6:** 787-794.

GUMPEL, N. J., L. RALLEY, J. GIRARD-BASCOU, F.-A. WOLLMAN, J. H. A. NUGENT *et al.*, 1995 Nuclear mutants of *Chlamydomonas reinhardtii* defective in the biogenesis of the cytochrome b_6f complex. Plant Mol. Biol. **29:** 921-932.

GUTIERRES, S., M. SABAR, C. LELANDAIS, P. CHETRIT, P. DIOLEZ *et al.*, 1997 Lack of mitochondrial and nuclear-encoded subunits of complex I and alteration of the respiratory chain in Nicotiana sylvestris mitochondrial deletion mutants. Proc Natl Acad Sci U S A **94:** 3436-3441.

HAMEL, P., W. SAKAMOTO, H. WINTZ and G. DUJARDIN, 1997 Functional complementation of an oxa1- yeast mutation identifies an Arabidopsis thaliana cDNA involved in the assembly of respiratory complexes. Plant J **12:** 1319-1327.

HANSON, M. R., and S. BENTOLILA, 2004 Interactions of mitochondrial and nuclear genes that affect male gametophyte development. Plant Cell **16 Suppl:** S154-169.

HARRIS, E. H., 1989 *The Chlamydomonas Sourcebook: A comprehensive guide to biology and laboratory use*. Academic Press, San Diego, CA.

HATEFI, Y., 1985 The mitochondrial electron transport and oxidative phosphorylation system. Annu Rev Biochem **54:** 1015-1069.

HAWLEY, R. S., and W. D. GILLILAND, 2006 Sometimes the result is not the answer: the truths and the lies that come from using the complementation test. Genetics **174:** 5-15.

HE, S., and T. D. FOX, 1997 Membrane translocation of mitochondrially coded Cox2p: distinct requirements for export of N and C termini and dependence on the conserved protein Oxa1p. Mol Biol Cell **8:** 1449-1460.

HEAZLEWOOD, J. L., K. A. HOWELL and A. H. MILLAR, 2003 Mitochondrial complex I from Arabidopsis and rice: orthologs of mammalian and fungal components coupled with plant-specific subunits. Biochim Biophys Acta **1604:** 159-169.

HEAZLEWOOD, J. L., J. S. TONTI-FILIPPINI, A. M. GOUT, D. A. DAY, J. WHELAN *et al.*, 2004 Experimental analysis of the Arabidopsis mitochondrial proteome highlights signaling and regulatory components, provides assessment of targeting prediction programs, and indicates plant-specific mitochondrial proteins. Plant Cell **16:** 241-256.

HEIDARI, M. M., M. HOUSHMAND, S. HOSSEINKHANI, S. NAFISSI and M. KHATAMI, 2009 Complex I and ATP content deficiency in lymphocytes from Friedreich's ataxia. Can J Neurol Sci **36:** 26-31.

HELL, K., 2007 The Erv1-Mia40 disulfide relay system in the intermembrane space of mitochondria. Biochim Biophys Acta.

HELL, K., J. M. HERRMANN, E. PRATJE, W. NEUPERT and R. A. STUART, 1998 Oxa1p, an essential component of the N-tail protein export machinery in mitochondria. Proc Natl Acad Sci U S A **95:** 2250-2255.

HERRMANN, J. M., W. NEUPERT and R. A. STUART, 1997 Insertion into the mitochondrial inner membrane of a polytopic protein, the nuclear-encoded Oxa1p. Embo J **16:** 2217-2226.

HERZ, U., W. SCHRODER, A. LIDDELL, C. J. LEAVER, A. BRENNICKE *et al.*, 1994 Purification of the NADH:ubiquinone oxidoreductase (complex I) of the respiratory chain from the inner mitochondrial membrane of Solanum tuberosum. J Biol Chem **269:** 2263-2269.

HIKKEL, I., Y. GBELSKA, Q. J. VAN DER AART, G. LUBECU and J. SUBIK, 1997 Cloning and characterization of KlCOX18, a gene required for activity of cytochrome oxidase in Kluyveromyces lactis. Curr Genet **32:** 267-272.

HILL, K. L., H. H. LI, J. SINGER and S. MERCHANT, 1991 Isolation and structural characterization of the Chlamydomonas reinhardtii gene for cytochrome c6. Analysis of the kinetics and metal specificity of its copper-responsive expression. J Biol Chem **266:** 15060-15067.

HIRST, J., J. CARROLL, I. M. FEARNLEY, R. J. SHANNON and J. E. WALKER, 2003 The nuclear encoded subunits of complex I from bovine heart mitochondria. Biochim Biophys Acta **1604:** 135-150.

HOEFNAGEL, M. H. N., O. K. ATKIN and J. T. WISKICH, 1998 Interdependence between chloroplasts and mitochondria in the light and the dark. Biochimica et Biophysica Acta (BBA) - Bioenergetics **1366:** 235-255.

HOWE, G., and S. MERCHANT, 1992 The biosynthesis of membrane and soluble plastidic *c*-type cytochromes of *Chlamydomonas reinhardtii* is dependent on multiple common gene products. EMBO J. **11:** 2789-2801.

HOWE, G., J. QUINN, K. HILL and S. MERCHANT, 1992 Control of the biosynthesis of cytochrome c6 in *Chlamydomonas reinhardtii*. Plant Physiol. Biochem. **30:** 299-307.

IRSHAD, M., H. CANUT, G. BORDERIES, R. PONT-LEZICA and E. JAMET, 2008 A new picture of cell wall protein dynamics in elongating cells of Arabidopsis thaliana: confirmed actors and newcomers. BMC Plant Biol **8:** 94.

JAMES, P., J. HALLADAY and E. A. CRAIG, 1996 Genomic libraries and a host strain designed for highly efficient two-hybrid selection in yeast. Genetics **144:** 1425-1436.

JIA, L., M. DIENHART, M. SCHRAMP, M. MCCAULEY, K. HELL *et al.*, 2003 Yeast Oxa1 interacts with mitochondrial ribosomes: the importance of the C-terminal region of Oxa1. Embo J **22:** 6438-6447.

JIA, L., J. KAUR and R. A. STUART, 2009 Mapping of the Saccharomyces cerevisiae Oxa1-mitochondrial ribosome interface and identification of MrpL40, a ribosomal protein in close proximity to Oxa1 and critical for oxidative phosphorylation complex assembly. Eukaryot Cell **8:** 1792-1802.

KAO, M. C., E. NAKAMARU-OGISO, A. MATSUNO-YAGI and T. YAGI, 2005 Characterization of the membrane domain subunit NuoK (ND4L) of the NADH-quinone oxidoreductase from Escherichia coli. Biochemistry **44:** 9545-9554.

KERSCHER, S., L. GRGIC, A. GAROFANO and U. BRANDT, 2004 Application of the yeast Yarrowia lipolytica as a model to analyse human pathogenic mutations in mitochondrial complex I (NADH:ubiquinone oxidoreductase). Biochim Biophys Acta **1659:** 197-205.

KLEFFMANN, T., D. RUSSENBERGER, A. VON ZYCHLINSKI, W. CHRISTOPHER, K. SJOLANDER *et al.*, 2004 The Arabidopsis thaliana chloroplast proteome reveals pathway abundance and novel protein functions. Curr Biol **14:** 354-362.

KOEHLER, C. M., and H. L. TIENSON, 2009 Redox regulation of protein folding in the mitochondrial intermembrane space. Biochim Biophys Acta **1793:** 139-145.

KROPAT, J., S. TOTTEY, R. P. BIRKENBIHL, N. DEPEGE, P. HUIJSER *et al.*, 2005 A regulator of nutritional copper signaling in Chlamydomonas is an SBP domain protein that recognizes the GTAC core of copper response element. Proc Natl Acad Sci U S A **102:** 18730-18735.

KRUFT, V., H. EUBEL, L. JANSCH, W. WERHAHN and H. P. BRAUN, 2001 Proteomic approach to identify novel mitochondrial proteins in Arabidopsis. Plant Physiol **127:** 1694-1710.

KUFFNER, R., A. ROHR, A. SCHMIEDE, C. KRULL and U. SCHULTE, 1998 Involvement of two novel chaperones in the assembly of mitochondrial NADH:Ubiquinone oxidoreductase (complex I). J Mol Biol **283:** 409-417.

KUHN, A., R. STUART, R. HENRY and R. E. DALBEY, 2003 The Alb3/Oxa1/YidC protein family: membrane-localized chaperones facilitating membrane protein insertion? Trends Cell Biol **13:** 510-516.

KWAN, A. L., L. LI, D. C. KULP, S. K. DUTCHER and G. D. STORMO, 2009 Improving gene-finding in Chlamydomonas reinhardtii:GreenGenie2. BMC Genomics **10:** 210.

LAUER, M., C. KNUDSEN, K. J. NEWTON, S. GABAY-LAUGHNAN and J. R. LAUGHNAN, 1990 A partially deleted mitochondrial cytochrome oxidase gene in the NCS6 abnormal growth mutant of maize. New Biol **2:** 179-186.

LAZAROU, M., M. MCKENZIE, A. OHTAKE, D. R. THORBURN and M. T. RYAN, 2007 Analysis of the assembly profiles for mitochondrial- and nuclear-DNA-encoded subunits into complex I. Mol Cell Biol **27:** 4228-4237.

LAZAROU, M., D. R. THORBURN, M. T. RYAN and M. MCKENZIE, 2009 Assembly of mitochondrial complex I and defects in disease. Biochim Biophys Acta **1793:** 78-88.

LEE, B. H., H. LEE, L. XIONG and J. K. ZHU, 2002 A mitochondrial complex I defect impairs cold-regulated nuclear gene expression. Plant Cell **14:** 1235-1251.

LEE, S. Y., C. HUNTE, S. MALANEY and B. H. ROBINSON, 2001 The N-terminus of the Qcr7 protein of the cytochrome bc(1) complex in S. cerevisiae may be involved in facilitating stability of the subcomplex with the Qcr8 protein and cytochrome b. Arch Biochem Biophys **393:** 215-221.

LELANDAIS, C., B. ALBERT, S. GUTIERRES, R. DE PAEPE, B. GODELLE *et al.*, 1998 Organization and expression of the mitochondrial genome in the Nicotiana sylvestris CMSII mutant. Genetics **150:** 873-882.

LENAZ, G., and M. L. GENOVA, 2009 Structural and functional organization of the mitochondrial respiratory chain: a dynamic super-assembly. Int J Biochem Cell Biol **41:** 1750-1772.

LEON, G., L. HOLUIGUE and X. JORDANA, 2007 Mitochondrial complex II Is essential for gametophyte development in Arabidopsis. Plant Physiol **143:** 1534-1546.

LETERME, S., and M. BOUTRY, 1993 Purification and preliminary characterization of mitochondrial complex I (NADH: ubiquinone reductase) from broad bean (Vicia faba L.). Plant Physiol **102:** 435-443.

LISTER, R., O. CHEW, M. N. LEE, J. L. HEAZLEWOOD, R. CLIFTON *et al.*, 2004 A transcriptomic and proteomic characterization of the Arabidopsis mitochondrial protein import apparatus and its response to mitochondrial dysfunction. Plant Physiol **134:** 777-789.

LIU, Y. G., N. MITSUKAWA, T. OOSUMI and R. F. WHITTIER, 1995 Efficient isolation and mapping of *Arabidopsis thaliana* T-DNA insert junctions by thermal asymmetric interlaced PCR. Plant J. **8:** 457-463.

LOEFFEN, J. L., J. A. SMEITINK, J. M. TRIJBELS, A. J. JANSSEN, R. H. TRIEPELS *et al.*, 2000 Isolated complex I deficiency in children: clinical, biochemical and genetic aspects. Hum Mutat **15:** 123-134.

MALANEY, S., B. L. TRUMPOWER, C. M. DEBER and B. H. ROBINSON, 1997 The N terminus of the Qcr7 protein of the cytochrome bc1 complex is not essential for import into mitochondria in Saccharomyces cerevisiae but is essential for assembly of the complex. J Biol Chem **272:** 17495-17501.

MARIENFELD, J. R., and K. J. NEWTON, 1994 The maize NCS2 abnormal growth mutant has a chimeric nad4-nad7 mitochondrial gene and is associated with reduced complex I function. Genetics **138:** 855-863.

MARMAGNE, A., M. FERRO, T. MEINNEL, C. BRULEY, L. KUHN *et al.*, 2007 A high content in lipid-modified peripheral proteins and integral receptor kinases features in the arabidopsis plasma membrane proteome. Mol Cell Proteomics **6:** 1980-1996.

MARTIN, V., F. VILLARREAL, I. MIRAS, A. NAVAZA, A. HAOUZ *et al.*, 2009 Recombinant plant gamma carbonic anhydrase homotrimers bind inorganic carbon. FEBS Lett **583:** 3425-3430.

MELO, A. M. P., T. H. ROBERTS and I. M. MOLLER, 1996 Evidence for the presence of two rotenone-insensitive NAD(P)H dehydrogenases on the inner surface of the inner membrane of potato tuber mitochondria. Biochimica Et Biophysica Acta-Bioenergetics **1276:** 133-139.

MERCHANT, S. S., S. E. PROCHNIK, O. VALLON, E. H. HARRIS, S. J. KARPOWICZ *et al.*, 2007 The Chlamydomonas genome reveals the evolution of key animal and plant functions. Science **318:** 245-250.

MEYER, E. H., N. L. TAYLOR and A. H. MILLAR, 2008 Resolving and identifying protein components of plant mitochondrial respiratory complexes using three dimensions of gel electrophoresis. J Proteome Res **7:** 786-794.

MEYER, E. H., T. TOMAZ, A. J. CARROLL, G. ESTAVILLO, E. DELANNOY *et al.*, 2009 Remodeled respiration in ndufs4 with low phosphorylation efficiency suppresses Arabidopsis germination and growth and alters control of metabolism at night. Plant Physiol **151:** 603-619.

MOLNAR, A., A. BASSETT, E. THUENEMANN, F. SCHWACH, S. KARKARE *et al.*, 2009 Highly specific gene silencing by artificial microRNAs in the unicellular alga Chlamydomonas reinhardtii. Plant J.

MOUSTAKAS, A., and C. H. HELDIN, 2003 Ecsit-ement on the crossroads of Toll and BMP signal transduction. Genes Dev **17:** 2855-2859.

NARGANG, F. E., M. PREUSS, W. NEUPERT and J. M. HERRMANN, 2002 The Oxa1 protein forms a homooligomeric complex and is an essential part of the mitochondrial export translocase in Neurospora crassa. J Biol Chem **277:** 12846-12853.

NEHLS, U., T. FRIEDRICH, A. SCHMIEDE, T. OHNISHI and H. WEISS, 1992 Characterization of assembly intermediates of NADH:ubiquinone oxidoreductase (complex I) accumulated in Neurospora mitochondria by gene disruption. J Mol Biol **227:** 1032-1042.

NEWTON, K. J., C. KNUDSEN, S. GABAY-LAUGHNAN and J. R. LAUGHNAN, 1990 An abnormal growth mutant in maize has a defective mitochondrial cytochrome oxidase gene. Plant Cell **2:** 107-113.

OGILVIE, I., N. G. KENNAWAY and E. A. SHOUBRIDGE, 2005 A molecular chaperone for mitochondrial complex I assembly is mutated in a progressive encephalopathy. J Clin Invest **115:** 2784-2792.

OHNISHI, T., 1998 Iron-sulfur clusters/semiquinones in complex I. Biochim Biophys Acta **1364:** 186-206.

OHNISHI, T., and J. C. SALERNO, 2005 Conformation-driven and semiquinone-gated proton-pump mechanism in the NADH-ubiquinone oxidoreductase (complex I). FEBS Lett **579:** 4555-4561.

OSSENBUHL, F., V. GOHRE, J. MEURER, A. KRIEGER-LISZKAY, J. D. ROCHAIX *et al.*, 2004 Efficient assembly of photosystem II in Chlamydomonas reinhardtii requires Alb3.1p, a homolog of Arabidopsis ALBINO3. Plant Cell **16:** 1790-1800.

PAGLIARINI, D. J., S. E. CALVO, B. CHANG, S. A. SHETH, S. B. VAFAI *et al.*, 2008 A mitochondrial protein compendium elucidates complex I disease biology. Cell **134:** 112-123.

PARISI, G., M. PERALES, M. S. FORNASARI, A. COLANERI, N. GONZALEZ-SCHAIN *et al.*, 2004 Gamma carbonic anhydrases in plant mitochondria. Plant Mol Biol **55:** 193-207.

PELLNY, T. K., O. VAN AKEN, C. DUTILLEUL, T. WOLFF, K. GROTEN *et al.*, 2008 Mitochondrial respiratory pathways modulate nitrate sensing and nitrogen-dependent regulation of plant architecture in Nicotiana sylvestris. Plant J **54:** 976-992.

PELTIER, J. B., Y. CAI, Q. SUN, V. ZABROUSKOV, L. GIACOMELLI *et al.*, 2006 The oligomeric stromal proteome of Arabidopsis thaliana chloroplasts. Mol Cell Proteomics **5:** 114-133.

PELTIER, J. B., A. J. YTTERBERG, Q. SUN and K. J. VAN WIJK, 2004 New functions of the thylakoid membrane proteome of Arabidopsis thaliana revealed by a simple, fast, and versatile fractionation strategy. J Biol Chem **279:** 49367-49383.

PENDLE, A. F., G. P. CLARK, R. BOON, D. LEWANDOWSKA, Y. W. LAM *et al.*, 2005 Proteomic analysis of the Arabidopsis nucleolus suggests novel nucleolar functions. Mol Biol Cell **16:** 260-269.

PERALES, M., H. EUBEL, J. HEINEMEYER, A. COLANERI, E. ZABALETA *et al.*, 2005 Disruption of a nuclear gene encoding a mitochondrial gamma carbonic anhydrase reduces complex I and supercomplex I + III2 levels and alters mitochondrial physiology in Arabidopsis. J Mol Biol **350:** 263-277.

PERALES, M., G. PARISI, M. S. FORNASARI, A. COLANERI, F. VILLARREAL *et al.*, 2004 Gamma carbonic anhydrase like complex interact with plant mitochondrial complex I. Plant Mol Biol **56:** 947-957.

PEREZ-MARTINEZ, X., A. ANTARAMIAN, M. VAZQUEZ-ACEVEDO, S. FUNES, E. TOLKUNOVA *et al.*, 2001 Subunit II of cytochrome c oxidase in Chlamydomonad algae is a heterodimer encoded by two independent nuclear genes. J Biol Chem **276:** 11302-11309.

PEREZ-MARTINEZ, X., M. VAZQUEZ-ACEVEDO, E. TOLKUNOVA, S. FUNES, M. G. CLAROS *et al.*, 2000 Unusual location of a mitochondrial gene. Subunit III of cytochrome C oxidase is encoded in the nucleus of Chlamydomonad algae. J Biol Chem **275:** 30144-30152.

PINEAU, B., O. LAYOUNE, A. DANON and R. DE PAEPE, 2008 L-galactono-1,4-lactone dehydrogenase is required for the accumulation of plant respiratory complex I. J Biol Chem **283:** 32500-32505.

PLA, M., C. MATHIEU, R. DE PAEPE, P. CHETRIT and F. VEDEL, 1995 Deletion of the last two exons of the mitochondrial nad7 gene results in lack of the NAD7 polypeptide in a Nicotiana sylvestris CMS mutant. Mol Gen Genet **248:** 79-88.

POLLOCK, S. V., S. L. COLOMBO, D. L. PROUT, JR., A. C. GODFREY and J. V. MORONEY, 2003 Rubisco activase is required for optimal photosynthesis in the green alga Chlamydomonas reinhardtii in a low-CO(2) atmosphere. Plant Physiol **133:** 1854-1861.

POTLURI, P., N. YADAVA and I. E. SCHEFFLER, 2004 The role of the ESSS protein in the assembly of a functional and stable mammalian mitochondrial complex I (NADH-ubiquinone oxidoreductase). Eur J Biochem **271:** 3265-3273.

PRIAULT, P., C. FRESNEAU, G. NOCTOR, R. DE PAEPE, G. CORNIC *et al.*, 2006a The mitochondrial CMSII mutation of Nicotiana sylvestris impairs adjustment of photosynthetic carbon assimilation to higher growth irradiance. J Exp Bot **57:** 2075-2085.

PRIAULT, P., G. TCHERKEZ, G. CORNIC, R. DE PAEPE, R. NAIK *et al.*, 2006b The lack of mitochondrial complex I in a CMSII mutant of Nicotiana sylvestris increases photorespiration through an increased internal resistance to CO2 diffusion. J Exp Bot **57:** 3195-3207.

PRICE, C. E., and A. J. DRIESSEN, 2008 YidC is involved in the biogenesis of anaerobic respiratory complexes in the inner membrane of Escherichia coli. J Biol Chem **283:** 26921-26927.

PRICE, C. E., and A. J. DRIESSEN, 2010 Conserved negative charges in the transmembrane segments of subunit K of the NADH:ubiquinone oxidoreductase determine its dependence on YidC for membrane insertion. J Biol Chem **285:** 3575-3581.

QUILES, M. J., M. E. ALBACETE, B. SABATER and J. CUELLO, 1996 Isolation and Partial Characterization of the NADH Dehydrogenase Complex from Barley Chloroplast Thylakoids. Plant Cell Physiol. **37:** 1134-1142.

RAGONE, G., R. CAIZZI, R. MOSCHETTI, P. BARSANTI, V. DE PINTO *et al.*, 1999 The Drosophila melanogaster gene for the NADH:ubiquinone oxidoreductase acyl carrier protein: developmental expression analysis and evidence for alternatively spliced forms. Mol Gen Genet **261:** 690-697.

REEVES, M. B., A. A. DAVIES, B. P. MCSHARRY, G. W. WILKINSON and J. H. SINCLAIR, 2007 Complex I binding by a virally encoded RNA regulates mitochondria-induced cell death. Science **316:** 1345-1348.

REMACLE, C., M. R. BARBIERI, P. CARDOL and P. P. HAMEL, 2008 Eukaryotic complex I: functional diversity and experimental systems to unravel the assembly process. Mol Genet Genomics **280:** 93-110.

REMACLE, C., D. BAURAIN, P. CARDOL and R. F. MATAGNE, 2001a Mutants of Chlamydomonas reinhardtii deficient in mitochondrial complex I: characterization of two mutations affecting the nd1 coding sequence. Genetics **158:** 1051-1060.

REMACLE, C., P. CARDOL, N. COOSEMANS, M. GAISNE and N. BONNEFOY, 2006 High-efficiency biolistic transformation of Chlamydomonas mitochondria can be used to insert mutations in complex I genes. Proc Natl Acad Sci U S A **103:** 4771-4776.

REMACLE, C., F. DUBY, P. CARDOL and R. F. MATAGNE, 2001b Mutations inactivating mitochondrial genes in Chlamydomonas reinhardtii. Biochem Soc Trans **29:** 442-446.

REMACLE, C., G. GLOIRE, P. CARDOL and R. F. MATAGNE, 2004 Impact of a mutation in the mitochondrial LSU rRNA gene from Chlamydomonas reinhardtii on the activity and the assembly of respiratory-chain complexes. Curr Genet **45:** 323-330.

REUMANN, S., S. QUAN, K. AUNG, P. YANG, K. MANANDHAR-SHRESTHA *et al.*, 2009 In-depth proteome analysis of Arabidopsis leaf peroxisomes combined with in vivo subcellular targeting verification indicates novel metabolic and regulatory functions of peroxisomes. Plant Physiol **150:** 125-143.

RHOADS, D. M., C. S. LEVINGS, 3RD and J. N. SIEDOW, 1995 URF13, a ligand-gated, pore-forming receptor for T-toxin in the inner membrane of cms-T mitochondria. J Bioenerg Biomembr **27:** 437-445.

ROHR, J., N. SARKAR, S. BALENGER, B. R. JEONG and H. CERUTTI, 2004 Tandem inverted repeat system for selection of effective transgenic RNAi strains in Chlamydomonas. Plant J **40:** 611-621.

ROSCHZTTARDTZ, H., I. FUENTES, M. VASQUEZ, C. CORVALAN, G. LEON *et al.*, 2009 A nuclear gene encoding the iron-sulfur subunit of mitochondrial complex II is regulated by B3 domain transcription factors during seed development in Arabidopsis. Plant Physiol **150:** 84-95.

RYMARQUIS, L. A., J. M. HANDLEY, M. THOMAS and D. B. STERN, 2005 Beyond complementation. Map-based cloning in Chlamydomonas reinhardtii. Plant Physiol **137:** 557-566.

SAADA, A., S. EDVARDSON, M. RAPOPORT, A. SHAAG, K. AMRY *et al.*, 2008 C6ORF66 is an assembly factor of mitochondrial complex I. Am J Hum Genet **82:** 32-38.

SAADA, A., R. O. VOGEL, S. J. HOEFS, M. A. VAN DEN BRAND, H. J. WESSELS *et al.*, 2009 Mutations in NDUFAF3 (C3ORF60), encoding an NDUFAF4 (C6ORF66)-interacting complex I assembly protein, cause fatal neonatal mitochondrial disease. Am J Hum Genet **84:** 718-727.

SABAR, M., R. DE PAEPE and Y. DE KOUCHKOVSKY, 2000 Complex I impairment, respiratory compensations, and photosynthetic decrease in nuclear and mitochondrial male sterile mutants of Nicotiana sylvestris. Plant Physiol **124:** 1239-1250.

SACCONI, S., L. SALVIATI and E. TREVISSON, 2009 Mutation analysis of COX18 in 29 patients with isolated cytochrome c oxidase deficiency. J Hum Genet **54:** 419-421.

SAMBROOK, J., E. F. FRITSCH and T. MANIATIS, 1989 *Molecular Cloning A Laboratory Manual*. Cold Spring Harbor Laboratory Press, New York.

SARACCO, S. A., and T. D. FOX, 2002 Cox18p is required for export of the mitochondrially encoded Saccharomyces cerevisiae Cox2p C-tail and interacts with Pnt1p and Mss2p in the inner membrane. Mol Biol Cell **13:** 1122-1131.

SARZI, E., M. D. BROWN, S. LEBON, D. CHRETIEN, A. MUNNICH *et al.*, 2007 A novel recurrent mitochondrial DNA mutation in ND3 gene is associated with isolated complex I deficiency causing Leigh syndrome and dystonia. Am J Med Genet A **143:** 33-41.

SATO, T., and K. MIHARA, 2009 Topogenesis of mammalian Oxa1, a component of the mitochondrial inner membrane protein export machinery. J Biol Chem **284:** 14819-14827.

SAZANOV, L. A., 2007 Respiratory complex I: mechanistic and structural insights provided by the crystal structure of the hydrophilic domain. Biochemistry **46:** 2275-2288.

SAZANOV, L. A., and P. HINCHLIFFE, 2006 Structure of the hydrophilic domain of respiratory complex I from Thermus thermophilus. Science **311:** 1430-1436.

SCAGLIA, F., J. A. TOWBIN, W. J. CRAIGEN, J. W. BELMONT, E. O. SMITH *et al.*, 2004 Clinical spectrum, morbidity, and mortality in 113 pediatric patients with mitochondrial disease. Pediatrics **114:** 925-931.

SCHÄGGER, H., and G. VON JAGOW, 1991 Blue native electrophoresis for isolation of membrane protein complexes in enzymatically active form. Anal. Biochem. **199:** 223-231.

SCHULTE, U., 2001 Biogenesis of respiratory complex I. J Bioenerg Biomembr **33:** 205-212.

SCHWAB, R., S. OSSOWSKI, M. RIESTER, N. WARTHMANN and D. WEIGEL, 2006 Highly specific gene silencing by artificial microRNAs in Arabidopsis. Plant Cell **18:** 1121-1133.

SELLEM, C. H., C. LEMAIRE, S. LORIN, G. DUJARDIN and A. SAINSARD-CHANET, 2005 Interaction between the oxa1 and rmp1 genes modulates respiratory complex assembly and life span in Podospora anserina. Genetics **169:** 1379-1389.

SHEFTEL, A. D., O. STEHLING, A. J. PIERIK, D. J. NETZ, S. KERSCHER *et al.*, 2009 Human ind1, an iron-sulfur cluster assembly factor for respiratory complex I. Mol Cell Biol **29:** 6059-6073.

SHIMIZU, H., L. PENG, F. MYOUGA, R. MOTOHASHI, K. SHINOZAKI *et al.*, 2008 CRR23/NdhL is a subunit of the chloroplast NAD(P)H dehydrogenase complex in Arabidopsis. Plant Cell Physiol.**:** pcn058.

SHIMOGAWARA, K., S. FUJIWARA, A. GROSSMAN and H. USUDA, 1998 High-efficiency transformation of Chlamydomonas reinhardtii by electroporation. Genetics **148:** 1821-1828.

SHUMWAY, L. K., and L. F. BAUMAN, 1967 NONCHROMOSOMAL STRIPE OF MAIZE. Genetics **55:** 33-38.

SKLADAL, D., J. HALLIDAY and D. R. THORBURN, 2003 Minimum birth prevalence of mitochondrial respiratory chain disorders in children. Brain **126:** 1905-1912.

SMEITINK, J., L. VAN DEN HEUVEL and S. DIMAURO, 2001 The genetics and pathology of oxidative phosphorylation. Nat Rev Genet **2:** 342-352.

SOMANCHI, A., and J. V. MORONEY, 1999 As Chlamydomonas reinhardtii acclimates to low-CO2 conditions there is an increase in cyclophilin expression Plant Molecular Biology **40:** 1055-1062.

SOUZA, R. L., N. S. GREEN-WILLMS, T. D. FOX, A. TZAGOLOFF and F. G. NOBREGA, 2000 Cloning and characterization of COX18, a Saccharomyces cerevisiae PET gene required for the assembly of cytochrome oxidase. J Biol Chem **275:** 14898-14902.

SPENCE, E., S. BAILEY, A. NENNINGER, S. G. MOLLER and C. ROBINSON, 2004 A homolog of Albino3/OxaI is essential for thylakoid biogenesis in the cyanobacterium Synechocystis sp. PCC6803. J Biol Chem **279:** 55792-55800.

STIBUREK, L., D. FORNUSKOVA, L. WENCHICH, M. PEJZNOCHOVA, H. HANSIKOVA *et al.*, 2007 Knockdown of human Oxa1l impairs the biogenesis of F1Fo-ATP synthase and NADH:ubiquinone oxidoreductase. J Mol Biol **374:** 506-516.

STRAUSS, C., J. H. MUSSGNUG and O. KRUSE, 2001 Ligation-mediated suppression-PCR as a powerful tool to analyse nuclear gene sequences in the green alga Chlamydomonas reinhardtii. Photosynth Res **70:** 311-320.

SUGIANA, C., D. J. PAGLIARINI, M. MCKENZIE, D. M. KIRBY, R. SALEMI *et al.*, 2008 Mutation of C20orf7 disrupts complex I assembly and causes lethal neonatal mitochondrial disease. Am J Hum Genet **83:** 468-478.

SUNDBERG, E., J. G. SLAGTER, I. FRIDBORG, S. P. CLEARY, C. ROBINSON *et al.*, 1997 *ALBINO3*, an Arabidopsis nuclear gene essential for chloroplast differentiation, encodes a chloroplast protein that shows homology to proteins present in bacterial membranes and yeast mitochondria. Plant Cell **9:** 717-730.

SUNDERHAUS, S., N. V. DUDKINA, L. JANSCH, J. KLODMANN, J. HEINEMEYER *et al.*, 2006 Carbonic anhydrase subunits form a matrix-exposed domain attached to the membrane arm of mitochondrial complex I in plants. J Biol Chem **281:** 6482-6488.

SZYRACH, G., M. OTT, N. BONNEFOY, W. NEUPERT and J. M. HERRMANN, 2003 Ribosome binding to the Oxa1 complex facilitates co-translational protein insertion in mitochondria. Embo J **22:** 6448-6457.

THORBURN, D. R., 2004 Mitochondrial disorders: prevalence, myths and advances. J Inherit Metab Dis **27:** 349-362.

TRIEPELS, R., J. SMEITINK, J. LOEFFEN, R. SMEETS, F. TRIJBELS *et al.*, 2000 Characterization of the human complex I NDUFB7 and 17.2-kDa cDNAs and mutational analysis of 19 genes of the HP fraction in complex I-deficient-patients. Hum Genet **106:** 385-391.

TSANG, W. Y., L. C. SAYLES, L. I. GRAD, D. B. PILGRIM and B. D. LEMIRE, 2001 Mitochondrial respiratory chain deficiency in Caenorhabditis elegans results in developmental arrest and increased life span. J Biol Chem **276:** 32240-32246.

VAHSEN, N., C. CANDE, J. J. BRIERE, P. BENIT, N. JOZA *et al.*, 2004 AIF deficiency compromises oxidative phosphorylation. Embo J **23:** 4679-4689.

VALLON, O., 2005 Chlamydomonas immunophilins and parvulins: survey and critical assessment of gene models. Eukaryot Cell **4:** 230-241.

VALLON, O., L. BULTE, P. DAINESE, J. OLIVE, R. BASSI *et al.*, 1991 Lateral redistribution of cytochrome b6/f complexes along thylakoid membranes upon state transitions. Proc Natl Acad Sci U S A **88:** 8262-8266.

VAN DER LAAN, M., M. L. URBANUS, C. M. TEN HAGEN-JONGMAN, N. NOUWEN, B. OUDEGA *et al.*, 2003 A conserved function of YidC in the biogenesis of respiratory chain complexes. Proc Natl Acad Sci U S A **100:** 5801-5806.

VERKHOVSKAYA, M. L., N. BELEVICH, L. EURO, M. WIKSTROM and M. I. VERKHOVSKY, 2008 Real-time electron transfer in respiratory complex I. Proc Natl Acad Sci U S A **105:** 3763-3767.

VIDEIRA, A., J. E. AZEVEDO, S. WERNER and P. CABRAL, 1993 The 12.3 kDa subunit of complex I (respiratory-chain NADH dehydrogenase) from Neurospora crassa: cDNA cloning and chromosomal mapping of the gene. Biochem J **291 (Pt 3):** 729-732.

VIDEIRA, A., and M. DUARTE, 2002 From NADH to ubiquinone in Neurospora mitochondria. Biochimica et Biophysica Acta (BBA) - Bioenergetics **1555:** 187-191.

VIDEIRA, A., and S. WERNER, 1989 Assembly kinetics and identification of precursor proteins of complex I from Neurospora crassa. Eur J Biochem **181:** 493-502.

VILLARREAL, F., V. MARTIN, A. COLANERI, N. GONZALEZ-SCHAIN, M. PERALES *et al.*, 2009 Ectopic expression of mitochondrial gamma carbonic anhydrase 2 causes male sterility by anther indehiscence. Plant Mol Biol **70:** 471-485.

VOGEL, R., L. NIJTMANS, C. UGALDE, L. VAN DEN HEUVEL and J. SMEITINK, 2004 Complex I assembly: a puzzling problem. Curr Opin Neurol **17:** 179-186.

VOGEL, R. O., C. E. DIETEREN, L. P. VAN DEN HEUVEL, P. H. WILLEMS, J. A. SMEITINK *et al.*, 2007a Identification of mitochondrial complex I assembly intermediates by tracing tagged NDUFS3 demonstrates the entry point of mitochondrial subunits. J Biol Chem **282:** 7582-7590.

VOGEL, R. O., R. J. JANSSEN, C. UGALDE, M. GROVENSTEIN, R. J. HUIJBENS *et al.*, 2005 Human mitochondrial complex I assembly is mediated by NDUFAF1. Febs J **272:** 5317-5326.

VOGEL, R. O., R. J. JANSSEN, M. A. VAN DEN BRAND, C. E. DIETEREN, S. VERKAART *et al.*, 2007b Cytosolic signaling protein Ecsit also localizes to mitochondria where it interacts with chaperone NDUFAF1 and functions in complex I assembly. Genes Dev **21:** 615-624.

VOGEL, R. O., J. A. SMEITINK and L. G. NIJTMANS, 2007c Human mitochondrial complex I assembly: a dynamic and versatile process. Biochim Biophys Acta **1767:** 1215-1227.

VOGEL, R. O., M. A. VAN DEN BRAND, R. J. RODENBURG, L. P. VAN DEN HEUVEL, M. TSUNEOKA *et al.*, 2007d Investigation of the complex I assembly chaperones B17.2L and NDUFAF1 in a cohort of CI deficient patients. Mol Genet Metab **91:** 176-182.

WERNER, R. M., D., 1998 Mating Type Determination of Chlamydomonas reinhardtii by PCR. Plant Molecular Biology Reporter **16:** 295-299.

WOLLMAN, F. A., 2001 State transitions reveal the dynamics and flexibility of the photosynthetic apparatus. Embo J **20:** 3623-3630.

WOOLHEAD, C. A., S. J. THOMPSON, M. MOORE, C. TISSIER, A. MANT *et al.*, 2001 Distinct Albino3-dependent and -independent pathways for thylakoid membrane protein insertion. J Biol Chem **276:** 40841-40846.

YAMATO, K. T., and K. J. NEWTON, 1999 Heteroplasmy and homoplasmy for maize mitochondrial mutants: a rare homoplasmic nad4 deletion mutant plant. J Hered **90:** 369-373.

YANO, T., W. R. DUNHAM and T. OHNISHI, 2005 Characterization of the delta muH+-sensitive ubisemiquinone species (SQ(Nf)) and the interaction with cluster N2: new insight into the energy-coupled electron transfer in complex I. Biochemistry **44:** 1744-1754.

YANO, T., S. MAGNITSKY and T. OHNISHI, 2000 Characterization of the complex I-associated ubisemiquinone species: toward the understanding of their functional roles in the electron/proton transfer reaction. Biochim Biophys Acta **1459:** 299-304.

YI, L., F. JIANG, M. CHEN, B. CAIN, A. BOLHUIS *et al.*, 2003 YidC is strictly required for membrane insertion of subunits a and c of the F(1)F(0)ATP synthase and SecE of the SecYEG translocase. Biochemistry **42:** 10537-10544.

ZARA, V., I. PALMISANO, L. CONTE and B. L. TRUMPOWER, 2004 Further insights into the assembly of the yeast cytochrome bc1 complex based on analysis of single and double deletion mutants lacking supernumerary subunits and cytochrome b. Eur J Biochem **271:** 1209-1218.

ZICKERMANN, V., M. BOSTINA, C. HUNTE, T. RUIZ, M. RADERMACHER *et al.*, 2003 Functional implications from an unexpected position of the 49-kDa subunit of NADH:ubiquinone oxidoreductase. J Biol Chem **278:** 29072-29078.

ZICKERMANN, V., S. KERSCHER, K. ZWICKER, M. A. TOCILESCU, M. RADERMACHER *et al.*, 2009 Architecture of complex I and its implications for electron transfer and proton pumping. Biochim Biophys Acta **1787:** 574-583.

ZYBAILOV, B., H. RUTSCHOW, G. FRISO, A. RUDELLA, O. EMANUELSSON *et al.*, 2008 Sorting signals, N-terminal modifications and abundance of the chloroplast proteome. PLoS One **3:** e1994.